E.O. Paton Electric Welding Institute of the National Academy of Sciences of Ukraine

International Scientific-Technical and Production Journal

The Paton WELDING JOURNAL

February 2016
No. 2

Published since 2000

English translation of the monthly «Avtomaticheskaya Svarka» (Automatic Welding) journal published in Russian since 1948

Founders
E.O. Paton Electric Welding Institute, NASU
International Association «Welding»

Publisher
International Association «Welding»

Translators
A.A. Fomin, O.S. Kurochko, I.N. Kutianova
Editor
N.A. Dmitrieva
Electron galley
D.I. Sereda, T.Yu. Snegiryova

Address
E.O. Paton Electric Welding Institute,
International Association «Welding»
11 Kazimir Malevich Str. (former Bozhenko Str.),
03680, Kiev, Ukraine
Tel.: (38044) 200 60 16, 200 82 77
Fax: (38044) 200 82 77, 200 81 45
E-mail: journal@paton.kiev.ua
www.patonpublishinghouse.com

State Registration Certificate
KV 4790 of 09.01.2001
ISSN 0957-798X

Subscriptions
$348, 12 issues per year,
air postage and packaging included.
Back issues available.

CONTENTS

doi.org/10.15407/tpwj2016.02.01

CALCULATION AND EXPERIMENTAL RESEARCH OF STATIC AND DYNAMIC VOLT-AMPERE CHARACTERISTICS OF ARGON ARC WITH REFRACTORY CATHODE*

V.N. SYDORETS, I.V. KRIVTSUN, V.F. DEMCHENKO, I.V. KRIKENT, D.V. KOVALENKO, I.V. KOVALENKO and **A.G. PAVLOV**
E.O. Paton Electric Welding Institute, NASU
11 Kazimir Malevich Str., 03680, Kiev, Ukraine. E-mail: office@paton.kiev.ua

Well-grounded selection of optimum modes of non-consumable pulse-arc welding requires investigation of dynamics of pulsed arc burning. Proposed earlier model of nonstationary arc with distributed parameters, due to large computing expenses, allows considering effect on arc of only single current pulse. Whereas, investigation of dynamic characteristics of the arc in supply of batches of high-frequency pulses of welding current is of practical interest. In this connection, it is interesting to develop an arc dynamic model with lumped parameters, which does not have limitations from point of view of amount of computations and allows high accuracy tracing of the dynamics of change of characteristics in arc with refractory cathode at high-frequency current modulation. The same data were received for comparison using calculation method based on the model with distributed parameters. Arc column time constant was determined based on calculation data of dynamics of arc voltage change, received employing the model with distributed parameters. In total complex of carried research and experimental investigations allowed working out an algorithms of application of the model with lumped parameters and identifying them. The results are given on expemental investigations of dynamics of change of current and arc voltage in high-frequency non-consumable pulse-arc welding, which are matched with the results of calculations using the model with lumped parameters. 14 Ref., 1 Table, 8 Figures.

Keywords: *pulse-arc welding, non-consumable electrode welding, high-frequency pulses, dynamic characteristics of arc, nonstationary arc, arc column, argon arc, refractory cathode*

Non-consumable inert gas arc (TIG) welding is widely used in manufacture of critical structures in nuclear and chemical machine building, aircraft and rocket construction, food and other branches of industry. The disadvantage of TIG welding is low efficiency promoted by insufficient penetration capability of the arc. In order to eliminate this disadvantage different methods of activation of processes of energy transfer in arc plasma and weld pool, namely welding over activating flux layer (A-TIG process) and hybrid welding (TIG + laser) etc., are currently used [1–4]. Work [5], employing the methods of mathematical modelling of arc with refractory cathode, states an effect of significant increase of current density at pulse leading edge and density of heat flow at anode in supply of welding current pulse with high rate of its change in comparison with corresponding characteristics of stationary arc. A technological consequence, which can be expected as a result of intensification of heat and dynamic impact of pulsed arc on melt, can be an increase of penetration depth and rise of molten metal volume in comparison with direct current welding.

Indicated peculiarity of dynamics of arc burning in the pulse mode indicate that high-frequency modulation of welding current can be used as one more method for activation of processes of energy transfer in arc plasma and metal being welded at corresponding selection of mode parameters. This promotes for an interest in further investigations of dynamic characteristics of the arc with refractory cathode in pulse mode. The primary instrument, which is widely used in welding arc analysis, is its volt-ampere characteristic (VAC). Investigation of relationship between current and voltage in non-consumable electrode welding is of interest in the case of direct current welding as well as in the case of high-frequency current pulse modulation, at which described above dynamic processes are observed. Present work is dedicated to experimental and theoretical investigation of static and

*Based on materials presented on at VII International Conference «Mathematical Modelling and Information Technologies in Welding and Related Processes», September 15–19, 2014, Odessa, Ukraine.

dynamic VAC of the argon arc with refractory cathode.

The model of nonstationary arc, proposed in work [6] and realized in work [5], is based on description of processes of energy-, mass- and electric transfer in column plasma and anode area of the nonstationary arc with refractory cathode (model with distributed parameters). Such an approach requires significant computation resources for calculation of heat, electromagnetic and gas-dynamic characteristics of the arc plasma, that limits the field of model application by consideration of only single current pulses. At the same time, researching the effect of batches of pulses of different shape and frequency is of practical interest.

Main definitions. Relationship between current I and arc voltage U is set by determination of electric arc VAC. It is known fact that arc voltage is the sum of three constituents, namely cathode potential drop U_c, arc column voltage U_p and anode potential drop U_a, which is negative [7] for most of electric atmospheric pressure arcs, including for welding arcs. Since the potentials on the surface of metallic cathode and anode can be considered constant with sufficient accuracy (due to high electric conductivity of metals), a total arc voltage U can be determined (measured) as a difference of potentials of anode and cathode surface, i.e. it is assumed that $U = \varphi_a - \varphi_c$, where φ_a, φ_c are the potentials of working surfaces of anode and cathode, respectively. However, such generally accepted determination of voltage as integral electric characteristic of arc discharge is not acceptable for determination of its constituents, namely cathode U_c and anode U_a potential drop as well as arc column voltage U_p. It is caused by the fact that according to calculations of characteristics of plasma of argon arc with refractory cathode and water-cooled [8] or evaporating [9] anode, particularly, arc in hybrid (TIG + CO_2-laser) welding [10], plasma potential in the anode layer interface φ_{ap}, the same as plasma potential in the cathode layer interface φ_{cp}, vary along Γ_{ap} and Γ_{cp} interfaces, dividing the anode and cathode areas with arc column, i.e. specified conditions are not equipotential.

The following is done for determination of effective (integral) values of anode drop $<U_a>$, which in sum with correspondingly determined values of cathode drop $<U_c>$ and column voltage $<U_p>$ shall provide the total arc voltage $U = <U_c> + <U_p> + <U_a>$. The following integral relationship arises from equation of continuity div $\vec{j} = 0$, since density of electric current in the arc column is determined by expression $\vec{j} = -\sigma$ grad φ, where σ is the electric conductivity, and φ is the potential of electric field in arc column plasma:

$$\int_{\Omega} \frac{|\vec{j}|^2}{\sigma} dV = -\int_{\Gamma} \varphi j_n dS, \qquad (1)$$

where Ω is the area covered by arc column; Γ is its boundary; j_n is the projection of vector of current density to the external normal $\vec{n}$ to boundary Γ. Boundary Γ is presented as $\Gamma = \Gamma_{ap} + \Gamma_{cp} + \Gamma_{bp}$, where Γ_{bp} is the part of boundary Γ without current ($j_n|\Gamma_{bp} = 0$). Then, the following is received from (1):

$$\int_{\Omega} \frac{|\vec{j}|^2}{\sigma} dV = \int_{\Gamma_{ap}} \varphi j_{n'} \quad d\Gamma_{ap} - \int_{\Gamma_{cp}} \varphi j_n \, d\Gamma_{cp}, \qquad (2)$$

where $\vec{n}' = -\vec{n}$. Expression in the left part of (2) is the thermal power, emitted in the arc column.

The following is written in accordance with Joule–Lenz's law:

$$\int_{\Omega} \frac{|\vec{j}|^2}{\sigma} dV = I \left\langle U_p \right\rangle,$$

where under

$$\left\langle U_p \right\rangle = \frac{1}{I} \int_{\Omega} \frac{|\vec{j}|^2}{\sigma} dV$$

the effective arc column voltage drop should be realized. Since Γ_{ap} and Γ_{cp} surfaces are not equipotential, let's introduce for them the concepts of the effective values of potentials Φ_{ap} and Φ_{cp} in the following way

$$\Phi_{ap} = \frac{1}{I} \int_{\Gamma_{ap}} \varphi j_{n'} \, d\Gamma_{ap}; \quad \Phi_{cp} = \frac{1}{I} \int_{\Gamma cp} \varphi j_n \, d\Gamma_{cp}. \qquad (3)$$

Then proceeding from (2) the arc column voltage drop can be determined as a difference of the effective values of potentials Φ_{ap} and Φ_{cp}, i.e. assuming $<U_p> = \Phi_{ap} - \Phi_{cp}$. Using (3), the effective anode $<U_a>$ and cathode $<U_c>$ drops are determined in form of

$$\left\langle U_a \right\rangle = \varphi_a - \Phi_{ap}; \quad \left\langle U_c \right\rangle = \Phi_{cp} - \varphi_c.$$

Standard expression for arc voltage in form of sum of voltage drops in separate segments of the arc discharge can be obtained in scope of given definitions:

$$U = \left\langle U_c \right\rangle + \left\langle U_p \right\rangle + \left\langle U_a \right\rangle = \varphi_a - \varphi_c, \qquad (4)$$

where it should be taken into account that the effective anode voltage drop is negative.

Static VAC of argon arc with refractory cathode. Let's consider the results of experimental measurements of static VAC of arcs with l = 1.5 and 3.0 mm lengths, burning on water-cooled anode. Figure 1 provides for experimental data in form of separate markers, the hatches show approximation of these data by Laurent series, coefficients of which are presented in the Table:

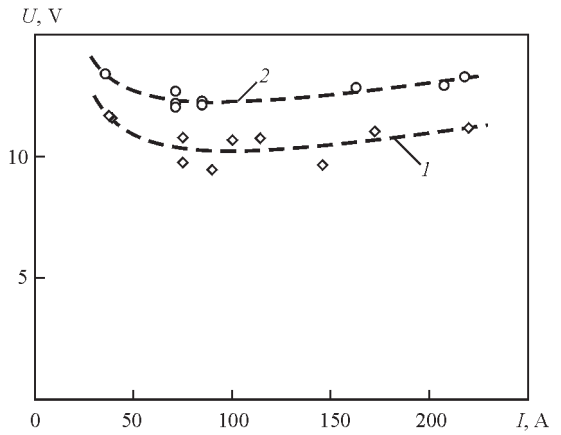

Figure 1. Experimental data and approximations of static VAC of 1.5 (*1*) and 3.0 mm (*2*) length argon arc with refractory cathode and copper water-cooled anode

$$U(I) = \sum_{j=-1}^{j=1} a_j \left(\frac{I}{100}\right)^j. \qquad (5)$$

Results of calculations in [8] for distributed characteristics of 3 mm length stationary arc, carried in I = 50–250 A current range, based on model of work [6], are used for theoretical evaluation of arc voltage constituents, being included in formula (4). Curves with markers from Figure 2 show dependence on arc current of anode potential drop $<U_a>$ and total voltage on column and anode area of the arc $<U_{pa}> = <U_p> + <U_a>$, calculated by difference of effective (integral) values of potentials on corresponding surfaces. The same Figure curves without markers show voltage drop U_{a0}, $U_{pa0} = U_{p0} + U_{a0}$ determined as difference of axial values of corresponding potentials. As follows from presented curves, an error in determination of the arc column voltage and potential drop in the anode layer, using two studied methods, is around 10 %. However, the effective values, introduced in the first chapter of this work, will be used for further analysis and averaging sign < > is eliminated for their writing.

Model [6] does not consider cathode area of the arc in explicit form, therefore theoretical evaluation of values of the cathode potential drop using data of calculations, made in work [8], is not possible.

Coefficients of approximation

Arc length l, mm		1.5	3.0
Coefficient of approximation	a_{-1}	1.394283	1.113619
	a_0	7.343352	9.765307
	a_1	1.443792	1.333032

In order to find U_c let's use experimental data (see Figure 1) and calculate the cathode voltage drop as a difference between experimentally determined value U and calculated effective voltage on column and anode area of arc $U_{pa} = U_p + U_a$, given in Figure 3. Figure 4 shows determined in such a way change of the effective cathode drop U_c depending on arc current. The same Figure represents calculation data on value of the cathode voltage drop, from presentation [8], based on approximated model of cathode layer. Comparison of these results indicates qualitatively similar nature of dependence of cathode drop on current, however it is around 1.3 V variation of data. Obtained in such a way calculation-experimental data on $U_c(I)$ dependences (see curve *2* in Figure 4) will be used for determination of dynamic VAC of the pulsed arc.

Dynamic model of arc with lumped parameters. Equations of dynamic model of arc with lumped parameters, allowing analytical solution which is not related with intricate calculations, is developed as an alternative to nonstationary arc model with distributed parameters [5, 6].

The arc column in scope of given model is considered as some object following energy conservation law [12]

$$\frac{dQ}{dt} = P - P_\theta, \qquad (6)$$

where Q is the arc column internal energy; P, P_θ are the input and output power, respectively. Application of the arc column VAC $I_p^{st}(I)$ and corresponding time constant θ as initial data allows this model to describe the arc dynamics at any current change $I(t)$:

$$U_p(t) = \frac{U_p^{st}\left(i_\theta(t)\right)}{i_\theta(t)} I(t). \qquad (7)$$

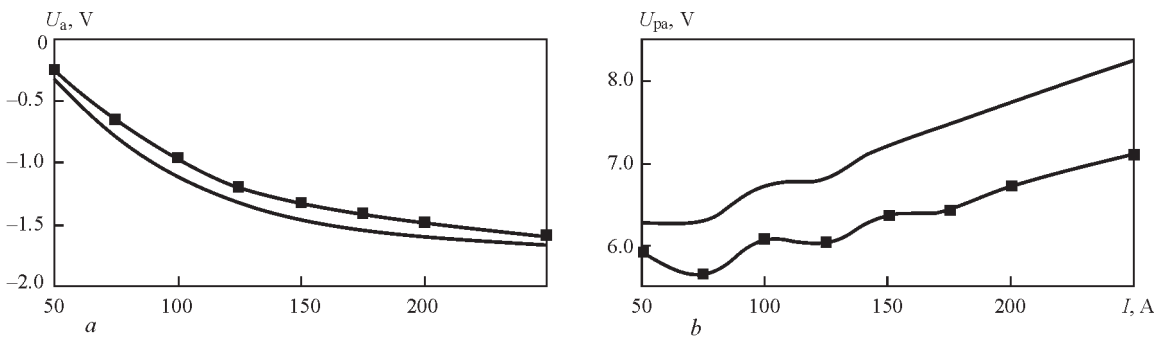

Figure 2. Calculation dependencies of anode potential drop (*a*) and total voltage on column and anode area (*b*) on arc current received using model of stationary arc with distributed parameters

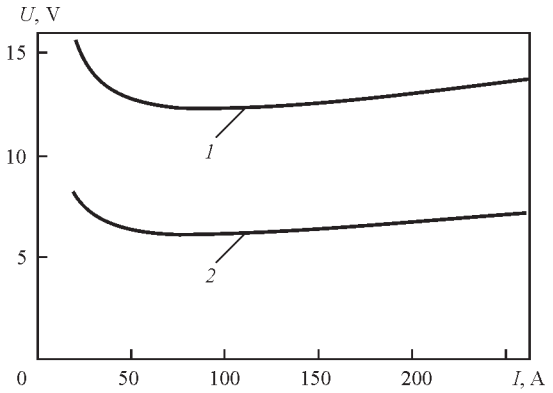

Figure 3. Dependence of arc total voltage (*1*) (experiment) and sum of effective voltage on column and anode area of arc (*2*) (calculation) on current

Formula (7) uses a state current concept i_θ which is illustrated employing Figure 5. Only one point of static VAC of ($U_p^{st}(i_\theta)$, i_θ) coordinates corresponds to each point of dynamic VAC of the arc column with (U_p, I) coordinates. At that, internal energy Q (and resistance R) of the arc column is equal in static and dynamic states.

Formula (7) follows from the equations, which correspond to Kirchhoff laws, describing electric circuit. These equations are complimented by equation of the arc column dynamic model, which is an electro-technical analogue [12] of equation (6):

$$\theta \frac{di_\theta^2}{dt} + i_\theta^2 = I^2. \qquad (8)$$

It should be noted that static VAC of arc column can be measured experimentally as well as calculated theoretically using the distributed parameters model.

Total arc voltage was determined by formula

$$U(I) = \frac{U_p^{st}(i_\theta)}{i_\theta} I + U_c(I) + U_a(I), \qquad (9)$$

where $U_a(I)$ is the effective anode potential drop, which can be determined employing the distributed parameters model; $U_c(I)$ is the effective cathode

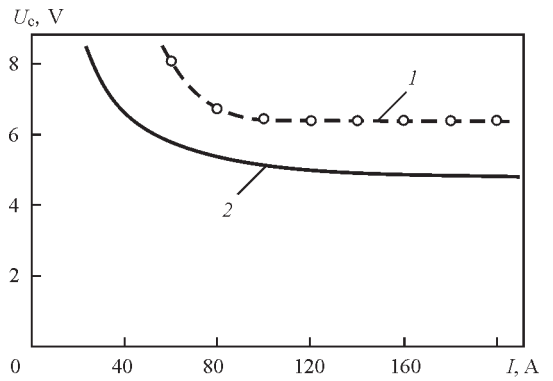

Figure 4. Dependence of cathode voltage drop on arc current: *1* — on data of work [11]; *2* — calculation in accordance with data given in Figure 3

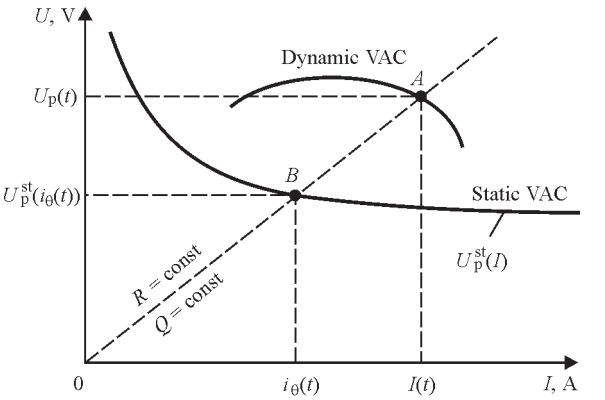

Figure 5. Determination of dynamic arc column voltage drop using concept of arc state current i_θ

potential drop, which can be determined using the proposed calculation-experimental procedure.

Thus, nonstationary arc voltage drop in scope of the dynamic model is calculated as a function of instandeneous value of current in pulse. At that, data on dependence of anode and cathode potential drop on current, which were obtained experimentally or using distributed parameter model, are employed as priori set parameters of the dynamic arc model.

Dynamic VAC of argon arc with refractory cathode. Application algorithm for model with lumped parameters requires its preliminary calibra-

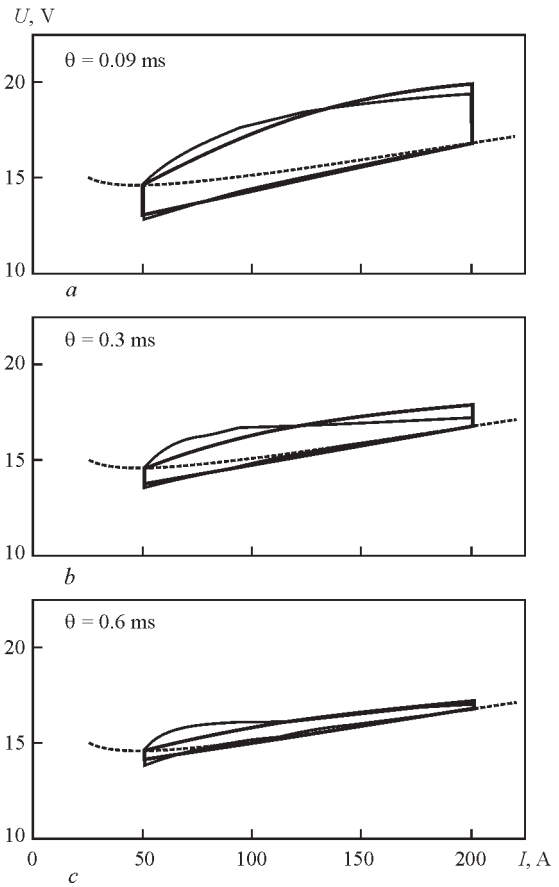

Figure 6. Static (*dotted lines*) and dynamic VAC of arc ащк model with distributed (*solid*) and lumped (*solid thick*) parameters at durations of pulse edges of 20 (*a*), 100 (*b*) and 200 (*c*) μs

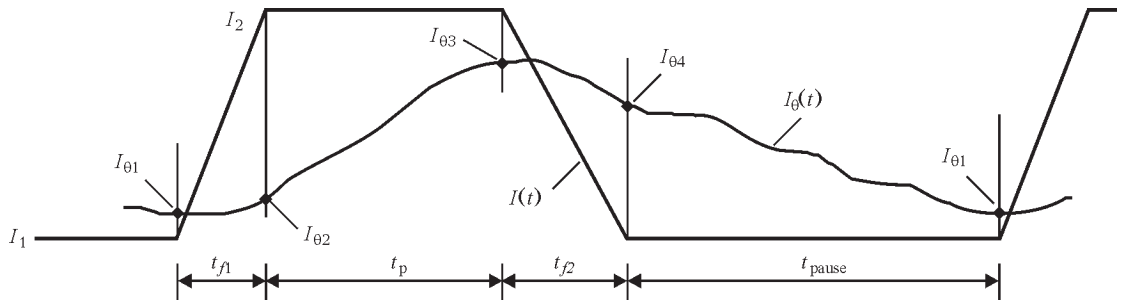

Figure 7. Investigation of influence of trapezoid current pulse on arc using fitting method

tion, namely, determination of time constant θ. For this it is necessary to choose some dynamic mode of arcing, being described by both models and compare their results. Value of the time constant θ can be determined when reaching maximum matching of the results by means of its fitting.

This work studies impact on the arc of trapezoidal pulses of current with different duration of edges. The calculations were carried out for argon arc of 3 mm length with refractory cathode and water-cooled anode. Pulse parameters were varied in the following way: duration of leading and trailing edges of pulse were 20, 100 and 200 μs. It is assumed that after current increase (drop) the arc burns at direct current, corresponding to the end of transition process up to setting of stationary state. The cathode and anode potential drops depending on instandeneous current value were selected in correspondence with data of Figures 2 and 4. The results of calculation of dynamic VAC for the models with distributed parameters are presented in Figure 6.

Below is given a brief description on calculation of the dynamic VAC employing arc model with lumped parameters in supply of trapezoid current pulse (Figure 7).

Such an impact can be studied stepwise, as a sequential effect of pulse edges (of t_{f1} and t_{f2} durations) and direct current (of t_p and t_{pause} pulse durations). General solutions of differential equation (8) for these steps are as follows:

$$i^2_{\theta C}(t, I_\theta, I_1) = I_1^2 + \left(I_\theta^2 - I_1^2\right)e^{-t/\theta}; \tag{10}$$

$$i^2_{\theta f}(t, I_\theta, I_1, I_2, t_f) = I_\theta^2 e^{-t/\theta} + I_1^2\left(1 - e^{-t/\theta}\right) - 2\frac{\theta}{t_f} I_1\left(I_2 - I_1\right)\left(1 - \frac{t}{\theta} - e^{-t/\theta}\right) + 2\left(\frac{\theta}{t_f}\right)^2\left(1 - \frac{t}{\theta} + \frac{t^2}{2\theta^2} - e^{-t/\theta}\right), \tag{11}$$

where t_f is the edge duration; I_θ is the initial value of state current at each step.

Stationary solutions were found by fitting method, which allowed determining conditions on edge boundaries:

$$\begin{aligned} i_{\theta f}\left(t_{f1}, I_{\theta 1}, I_1, I_2, t_{f1}\right) &= I_{\theta 2};\\ i_{\theta C}\left(t_p, I_{\theta 2}, I_2\right) &= I_{\theta 3};\\ i_{\theta f}\left(t_{f2}, I_{\theta 3}, I_2, I_1, t_{f2}\right) &= I_{\theta 4};\\ i_{\theta C}\left(t_{pause}, I_{\theta 4}, I_1\right) &= I_{\theta 1}. \end{aligned} \tag{12}$$

Solutions of equations (12) become compact due to matrix recording form:

$$\begin{pmatrix} I^2_{\theta 1}\\ I^2_{\theta 2}\\ I^2_{\theta 3}\\ I^2_{\theta 4} \end{pmatrix} = \begin{pmatrix} -e^{-t_{f1}/\theta} & 1 & 0 & 0\\ 0 & -e^{-t_i/\theta} & 1 & 0\\ 0 & 0 & -e^{-t_{f2}/\theta} & 0\\ 1 & 0 & 0 & -e^{-t_p/\theta} \end{pmatrix}^{-1} \times \begin{pmatrix} i^2_{\theta f}(t_{f1}, 0, I_1, I_2, t_{f1})\\ i^2_{\theta C}(t_p, 0, I_2)\\ i^2_{\theta f}(t_{f2}, 0, I_2, I_1, t_{f2})\\ i^2_{\theta C}(t_{pause}, 0, I_1) \end{pmatrix}. \tag{13}$$

Substitution of values of state currents on the boundaries of these stages from formula (13) in expressions (10) and (11) allows receiving a dependence of change of state current on time under effect of trapezoid pulse on arc.

If duration of pulse and pause are taken sufficiently large (for arc to reach stationary state), the results received employing lumped parameters can be compared with the results obtained for single edges (see Figure 6) using the model with distributed parameters.

Values of time constant θ in the model with lumped parameters, received by comparison of two models, are indicated in this Figure. It should be noted that the time constant decreases with reduction of the pulse edge duration. Typical feature of VAC of the dynamic arc is the fact that it is presented in form of hysteresis loop, in which upper and lower curves correspond to leading and trailing pulse edge, and vertical pieces — to transfer in arc stationary state (static VAC is plotted in this Figures for comparison). Dynamic VAC in form of hysteresis loop was experimentally received

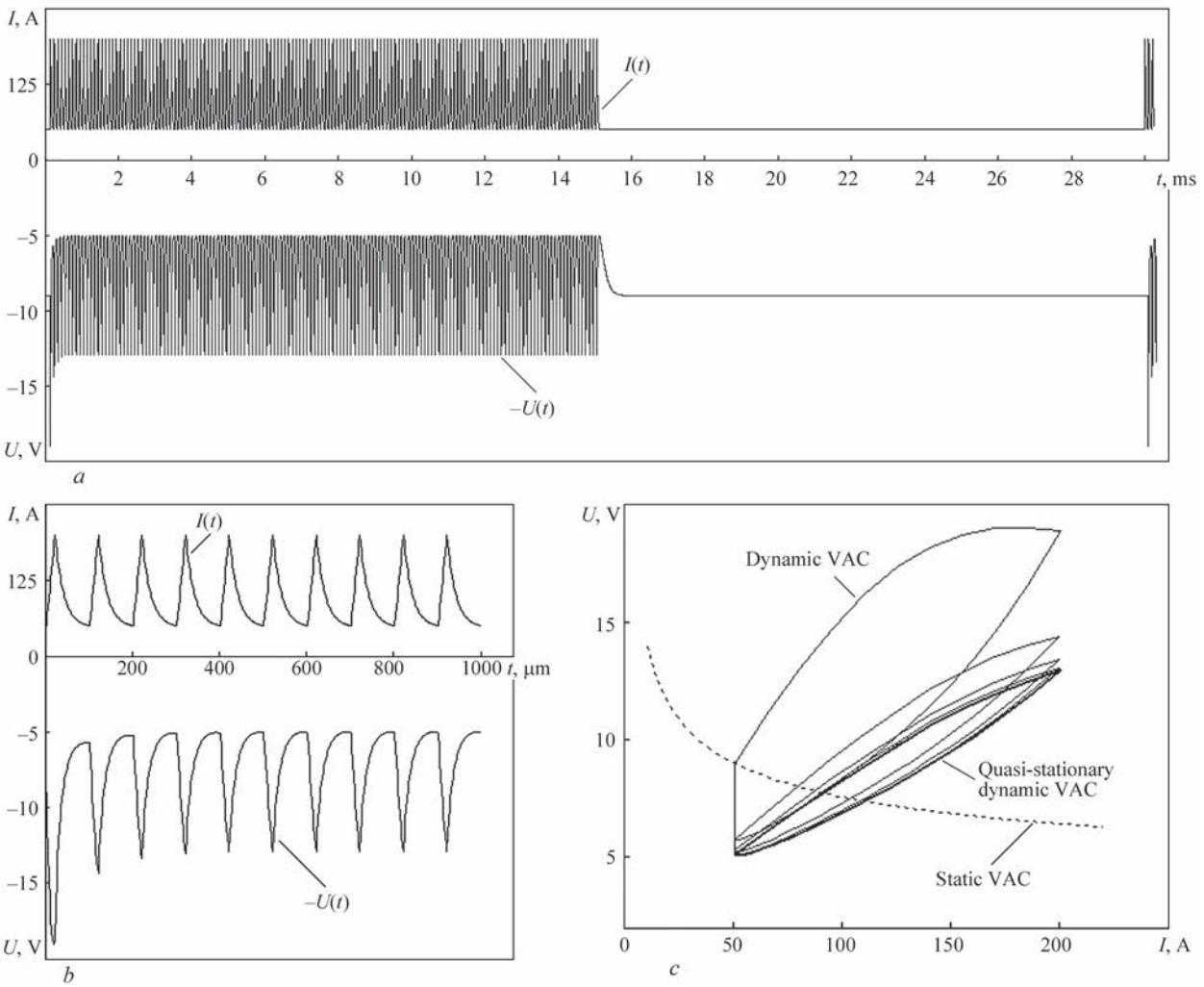

Figure 8. Impact of batches of high-frequency current pulses on arc: *a* — time dependence of arc current and voltage; *b* — influence of several initial pulses of batch (enlarged scale); *c* — calculation dynamic VAC of arc at such an influence

in works [10, 11]. Physical reason of appearance of such a loop is different level of inertia of processes of energy, pulse and charge transfer at current rise or drop [5]. It should be noted that increase of pulse duration promotes for reduction of spread of hysteresis loop and VAC of the dynamic arc is approached to VAC of the static arc.

After finalizing the model of dynamic arc with lumped parameters, above described, and calibrating the time constant, this model was used for calculation of the dynamic VAC in supply of batches of HF pulses. In experimental way pulses were generated using a device, developed in the PWI Department. This device generates batches of HF pulses in 5–25 kHz frequency range of close to triangular form. Frequency of sequence of pulse batches is 1–75 Hz, filling of batch by HF pulses makes from 1 to 99 %.

Experimental researches of impact of batches of HF pulses on arc were carried out, and oscillograms of change of current and arc voltage in time were received. Theoretical study of the same impact using the lumped parameters model showed (Figure 8) good matching of the results with the experimental data, that indicates adequacy of the proposed description of transfer processes in the arc at welding current HF modulation. Data of Figure 8, *c* indicate that reaction of the arc for six-eight initial pulses of the batch differ from reaction for the rest of pulses. Quasi-stationary dynamic VAC of the arc is formed only after this transfer process is finished.

Conclusions

A concept of effective values of arc voltage componets was implemented, namely the cathode and anode potential drop as well as column voltage, taking into account non-equipotentiality of interfaces of the electric arc column with its near-electrode areas. The effective values of voltage drop on column and anode layer of argon arc with refractory cathode and water-cooled anode were calculated based on the model with distributed parameters. The effective cathode potential drop in such an arc is determined by calculation-experimental method.

It is shown that corresponding selection of the time constant allows sufficiently accurate conformity of the results of calculations of transfer processes in the pulsed arc with refractory cathode, based on the model with lumped parameters, to the calculation data received using the distributed parameters model. The dynamic model of arc with lumped parameters does not require large calculation resources, that make it perspective for investigation of transfer processes in supply of batches of high-frequency pulses.

Volt-ampere characteristics of the arc were received based on comparative analysis of the models with lumped and distributed parameters, describing transfer processes in the pulse arc with refractory cathode. It is shown that increase of slopes of edges of current pulses provides for rise of spread of hysteresis loop of arc dynamic VAC.

Adjustment of quasi-stationary VAC of the pulsed arc with refractory cathode at HF current modulation of arc current is achieved after passing 6–8 pulses.

1. Gurevich, S.M., Zamkov, V.N., Kushnirenko, N.A. (1965) Increase of penetration efficiency of titanium alloys in argon arc welding. *Avtomatich. Svarka*, **9**, 1–4.
2. Yushchenko, K.A., Kovalenko, D.V., Kovalenko, I.V. (2001) Application of activators for TIG welding of steels and alloys. *The Paton Welding J.*, **7**, 37–43.
3. Steen, W.M., Eboo, M. (1979) Arc augmented laser welding. *Metal Construction*, 11(**7**), 332–335.
4. Lu, S., Fujii, H., Nogi, K. (2004) Marangoni convection and weld shape variations in Ar–O_2 and Ar–CO_2 shielded GTA welding. *Materials Sci. and Eng. A*, 380(**1**/**2**), 290–297.
5. Krivtsun, I.V., Krikent, I.V., Demchenko, V.F. (2013) Modelling of dynamic characteristics of a pulsed arc with refractory cathode. *The Paton Welding J.*, **7**, 13–23.
6. Krivtsun, I.V., Demchenko, V.F., Krikent, I.V. (2010) Model of the processes of heat-, mass- and charge transfer in the anode region and column of the welding arc with refractory cathode. *Ibid*., **6**, 2–9.
7. Sanders, N.A., Pfender, E. (1984) Measurement of anode falls and anode heat transfer in atmospheric pressure high intensity arcs. *J. Appl. Phys*., 55(**3**), 714–722.
8. Krikent, I.V., Krivtsun, I.V., Demchenko, V.F. (2012) Modelling of processes of heat-, mass- and electric transfer in column and anode region of arc with refractory cathode. *The Paton Welding J.*, **3**, 2–6.
9. Krikent, I.V., Krivtsun, I.V., Demchenko, V.F. (2014) Simulation of electric arc with refractory cathode and evaporating anode. *Ibid*., **9**, 17–24.
10. Krivtsun, I.V., Krikent, I.V., Demchenko, V.F. et al. (2015) Interaction of CO_2-laser radiation beam with electric arc plasma in hybrid (laser + TIG) welding. *Ibid*., **3**/**4**, 6–15.
11. Uhrlandt, D., Baeva, M., Kozakov, R. et al. (2013) Cathode fall voltage of TIG arcs from a non-equilibrium arc model. In: *IIW Doc. 2500*. SG 212 on Physics of Welding.
12. Sidorets, V.N., Pentegov, I.V. (2013) *Deterministic chaos in nonlinear circuits with electric arc*. Kiev: IAW.
13. Trofimov, N.M., Sinitsky, R.V. (1967) Dynamic characteristics of pulsed arc in argon arc welding. *Svarochn. Proizvodstvo*, **8**, 18–19.
14. Sokolov, O.I., Gladkov, E.A. (1977) Dynamic characteristics of free-burning and constricted welding arcs of direct current with nonconsumable electrode. *Ibid*., **4**, 3–5.

Received 26.10.2015

doi.org/10.15407/tpwj2016.02.02

MICROSTRUCTURAL FEATURES OF MULTILAYER WELDS WITH DIFFERENT HOT CRACKING SENSITIVITY*

K.A. YUSHCHENKO, L.I. MARKASHOVA, A.V. ZVYAGINTSEVA, Yu.A. KHOKHLOVA, O.S. KUSHNARYOVA and **N.O. CHERVYAKOV**
E.O. Paton Electric Welding Institute, NASU
11 Kazimir Malevich Str., 03680, Kiev, Ukraine. E-mail: office@paton.kiev.ua

The work deals with multilayer welds made with Inconel 52 wire, which have a high sensitivity to formation of hot ductility dip cracks in the heat-affected zone, and welds made with 52MSS wire, which turned out to be insensitive to formation of this type of cracks at a certain level of strain rates. Changes of structural characteristics of welds made with the above wires were studied by the methods of transmission microscopy, X-ray microprobe analysis, microhardness measurement, as well as electron backscatter diffraction. 9 Ref., 2 Tables, 8 Figures.

Keywords: *multilayer surfacing, ductility dip cracks, nickel alloys, dislocation density, stacking fault energy, microhardness*

Prediction and control of structure and properties of metallic materials and welded structures from them require multilevel hierarchic approach to the solid body, as a totality of interrelated subsystems, such as electron subsystem; crystalline lattice, the structure of which is determined by electron subsystem; subsystem of crystalline lattice defects; surface layers; all inner interfaces; individual phase subsystems in complex heterogeneous media [1].

At present, plotting of multilevel model of deformed solid is in the active stage of its development. Main characteristics of individual subsystems, their functional relationships, regularities of their self-consistent change in different fields of external impact (mechanical, thermal, electric, radiation, etc.) are experimentally studied.

This work deals with structural changes under the impact of welding cycle for multilayer deposits, made with wires with different sensitivity to hot cracking.

Known is the high sensitivity to formation of ductility dip cracks (DDC) in welded joints of nickel alloys of Inconel 690 type, when cracks form in the temperature range of about 700–1000 °C along high-angle migration boundaries of austenite grains predominantly in multipass welds [2–4]. Mechanical testing in Ala-Too unit (Greeble type) showed differences in susceptibility to ductility dip formation. Welded joints performed with Inconel 52 wire have lower values of relative elongation in temperature range of 600–1000 °C, unlike welded joints made with Inconel 52MSS wire, in which ductility dip in the respective temperature range is small [3].

In connection with problems, arising at assessment of welded joint properties, it was proposed to perform work on modeling the welding conditions for multipass welds in welded structures, which were made as six-pass deposits on Inconel 690 alloy plates of (6–8)×40×200 mm size into pre-planed grooves.

Table 1 gives chemical composition of welding wires and base metal.

The process of automatic groove welding proper with application of 0.9 mm diameter wire was performed with non-consumable electrode in argon in the following modes: U_a = 10.5 V; $v_{w.f}$ = 75 m/h;

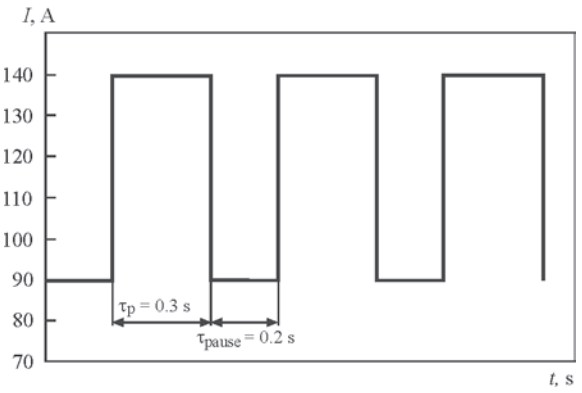

Figure 1. Automatic welding modes

*Based on materials of the work performed under purpose-oriented integrated program of the NAS of Ukraine «Problems of life and safe operation of structures, constructions and machines» (2013–2015).

Table 1. Chemical composition of base metal and welding wires, wt.%

Alloy grade	C	Mn	Ni	Cr	Fe	Nb	Mo	Ti	S	P	Al	Si
In 690	0.025	0.24	Base	29.72	10.3	–	–	0.28	0.002	0.005	0.87	0.32
In 52	0.026	0.31	Same	28.80	8.5	0.03	0.03	0.51	0.001	0.004	0.72	0.12
In 52MSS	0.024	0.29	»	30.30	7.2	2.52	3.51	0.25	0.0008	0.0006	0.22	0.15

f_{osc} = 60 osc/min; A_{osc} = 25 mm; v_w = 6 m/h, shown in Figure 1.

Under these conditions, selected welding modes provided optimum formation of each bead of multilayer weld without undercuts or lacks-of-penetration between the beads and minimum penetration of the previous weld.

Samples were prepared from surfaced plates (gauging and grinding to 340×180×3 mm dimensions) for respective testing in PVR-Test unit with variable straining rate during welding in the range of 0–12 mm/min. Testing procedure and results are described in [5].

As regards subsequent analysis of the conditions of development and nature of propagation of DDC in the weld made with Inconel 52MSS and Inconel 52 wires, experimental studies of grain structure in the HAZ were performed in the first stage, using scanning electron microscope with application of EDX and CCD-detector. EDX methods were used to study the chemical inhomogeneity of cellular structure of Inconel 52MSS weld metal and of Inconel 52 weld metal, unalloyed with molybdenum and niobium, for comparison (Figures 2 and 3).

Investigations showed that chemical inhomogeneity is much smaller in Inconel 52 welds, in which molybdenum and niobium content is minimum (their total content is ~0.7 %), that promotes DDC formation. At the same time, in individual sections of Inconel 52MSS wire weld, niobium and molybdenum content rises ~2–4 times, compared to total content (of the order of 6 %).

At the next stage of investigations, TEM method was used to study fine (dislocation) structure of metal in different zones of welded joint, in particular substructure nature, details of intergranular, subgranular boundaries and other structural parameters. Direct transmission studies of fine structure were conducted in JEM-200CX unit (JEOL) at accelerating voltage of 200 kV. In this case, assessment of scalar density and nature of dislocation distribution (Figure 4) was performed with secant method. Here, specific values of dislocation density were found from the dependence

$$\rho = \frac{M}{t}\left(\frac{n_1}{L_1} \div \frac{n_2}{L_2}\right), \qquad (1)$$

where M, t are the foil magnification and thickness; n_1, n_2 is the number of intersections with horizontal and vertical lines, respectively; L_1, L_2 is the total length of horizontal and vertical lines. All the results on evaluation of dislocation density in weld metal (both at application of Inconel 52MSS and Inconel 52 wires) in different sections of the structure, namely in inner grain volumes, along intergranular, as well as subgrain boundaries, are given in Table 2.

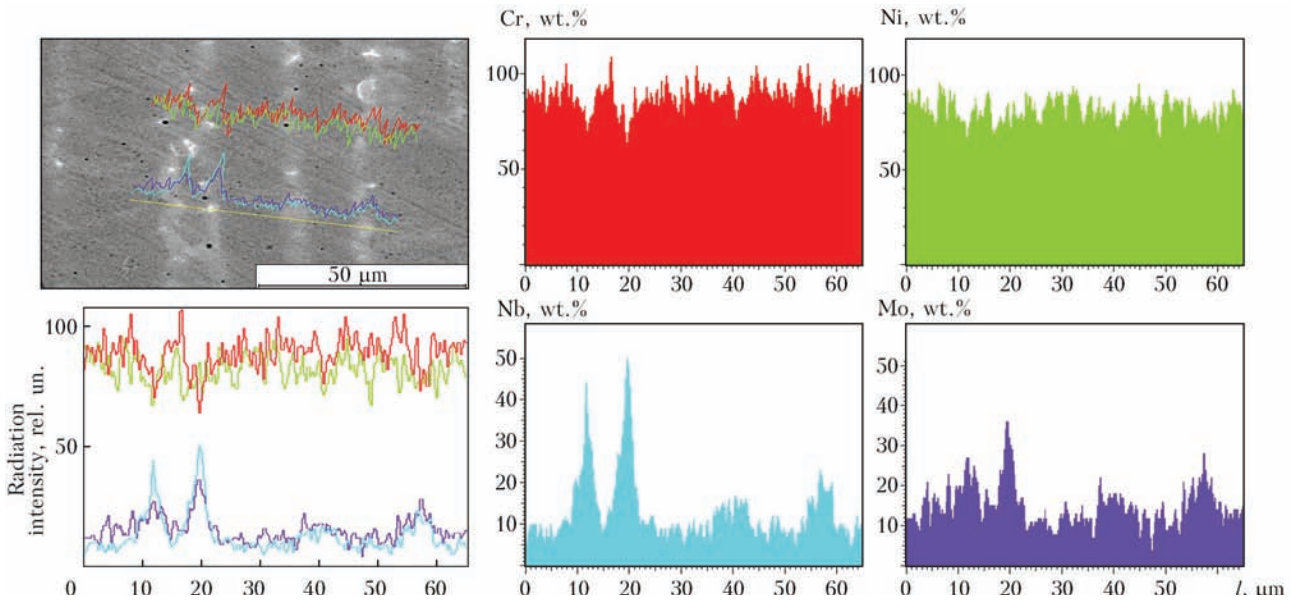

Figure 2. Concentrational changes of chemical elements in studied regions of metal of welds, made with Inconel 52MSS wire in argon, in which chemical inhomogeneity by niobium and molybdenum is observed

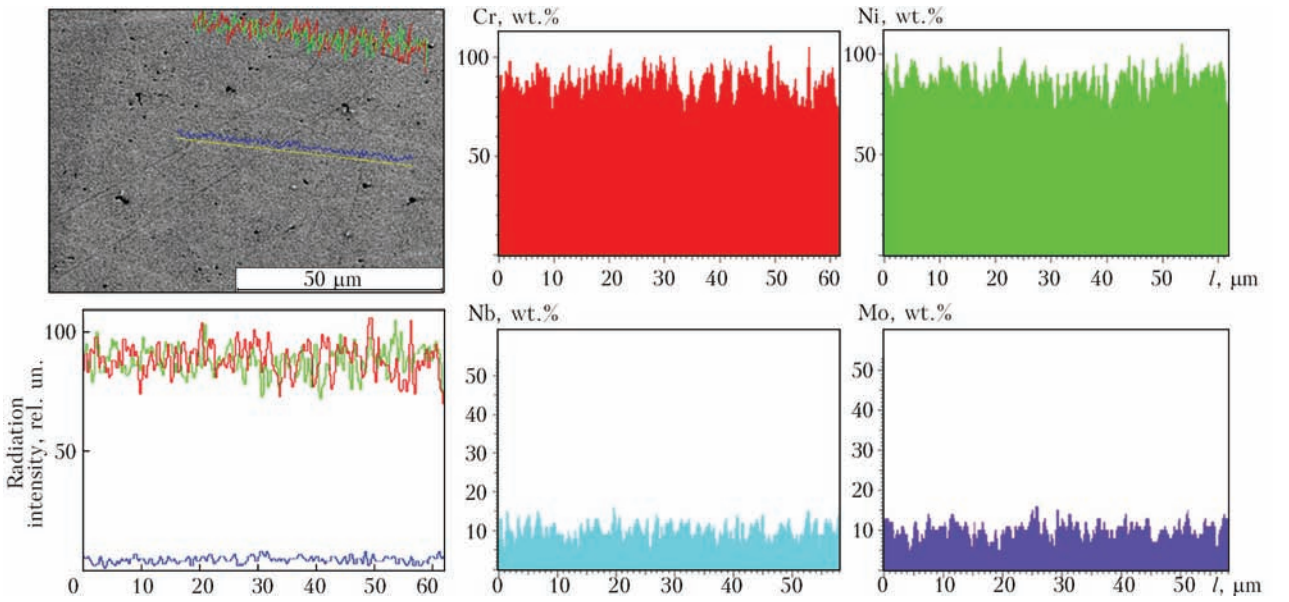

Figure 3. Concentrational changes of chemical elements in studied regions of metal of welds made, with Inconel 52 wire in argon, in which chemical inhomogeneity is not observed

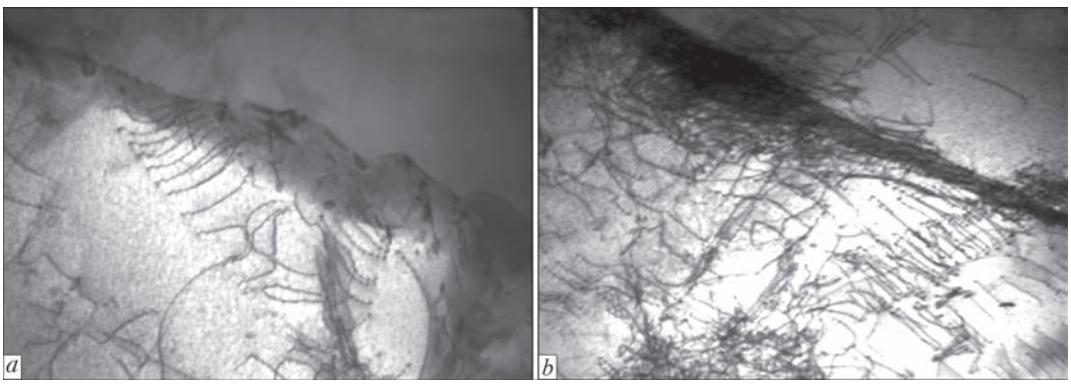

Figure 4. Nature of dislocation distribution in weld metal (×30,000): *a* — uniform distribution with low density in Inconel 52MSS alloy; *b* — greater dislocation density at its graded distribution in Inconel 52 alloy

Phase composition of precipitates forming in welding zone was determined by the methods of microdiffraction analysis.

Detailed studies of the nature of dislocation structure also allowed assessment of such defect formation parameters as stacking fault energy (SFE), which is the characteristic of the conditions of structural defect formation and can characterize hot cracking susceptibility of the studied material.

Values of SFE were determined in this case by the width of dislocation splitting, and stacking fault width was determined by direct measurement on structural images obtained at transmission studies of fine structure. Specific SFE values were given by the dependence [6–8]

$$\gamma = \frac{\mu b^2 (2-\nu)}{8\pi d_0 (1-\nu)}, \qquad (2)$$

where ν is the Poisson's ratio; b is the Burgers vector; γ is the SFE; μ is the shear modulus; d_0 is the width of dislocation splitting (distance between partial dislocations).

As a result of investigations in this direction, it was established that in weld metal the width of dislocation splitting (both in the volume of grains, and at intergranular boundaries) is equal to 0.045–0.070 μm at application of Inconel 52MSS wire (see Figure 4, *a*), that corresponds to γ_{SFE} ~0.091 J/m^2 (Figure 5). It should be noted here that in this weld metal increased content of Mo = 3.51 % and Nb = 2.51 % lowers the

Table 2. Dislocation density in inner grain volumes and along intergranular and subgranular boundaries of weld metal at application of wire with different alloying

Structure regions	ρ, cm^{-2}	
	Inconel 52MSS	Inconel 52
Grain volume	10^8–10^9	$2\cdot10^9$–$8\cdot10^{10}$
Grain subboundary	10^9	$9\cdot10^{10}$
Grain boundary	(6–7)·(10^9–10^{10})	10^{11}–$2.2\cdot10^{11}$ (rare $3\cdot10^{11}$)

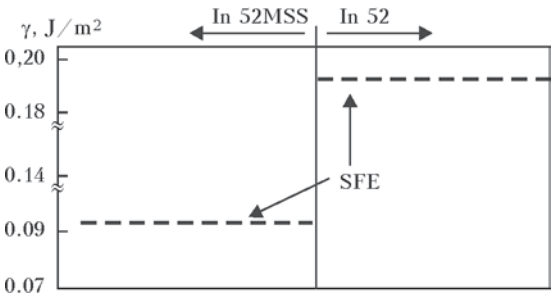

Figure 5. Change of SFE for welds at application of Inconel 52MSS and Inconel 52 wires

SFE value, which is exactly what leads to increase of crack resistance of the studied metal.

For a more detailed analysis of the nature of DDC propagation in the weld, made with Inconel 52MSS and Inconel 52 wires, experimental studies of grain structure near the crack in the HAZ were performed in the Zeiss scanning electron microscope EVO-50, with application of CCD-detector. Maps of crystallographic orientation of grains (Figure 6) for each of the studied samples are indicative of the fact that DDC in welded joint HAZ propagate along high-angle boundaries (Figure 7) that is also confirmed in [9].

As regards samples made with Inconel 52MSS wire, no cracks were found in the HAZ of this type of samples. Additional studies of the substructure showed presence of a large number of low-angle boundaries with 2–4° fragment disorientation in the grain body. The low-angle boundaries are practically absent in Inconel 52 welds. Statistical studies of the sites of DDC propagation in the HAZ showed that defects of this type propagated, mainly, along grain boundaries predominantly with <111> and <101> orientation, or along grain boundaries with <100> orientation.

Then, moduli of elasticity and microhardness were measured in grain structures with known crystallographic directions. The objective of experiment was to study the mechanical and crystallographic changes during plastic deformation

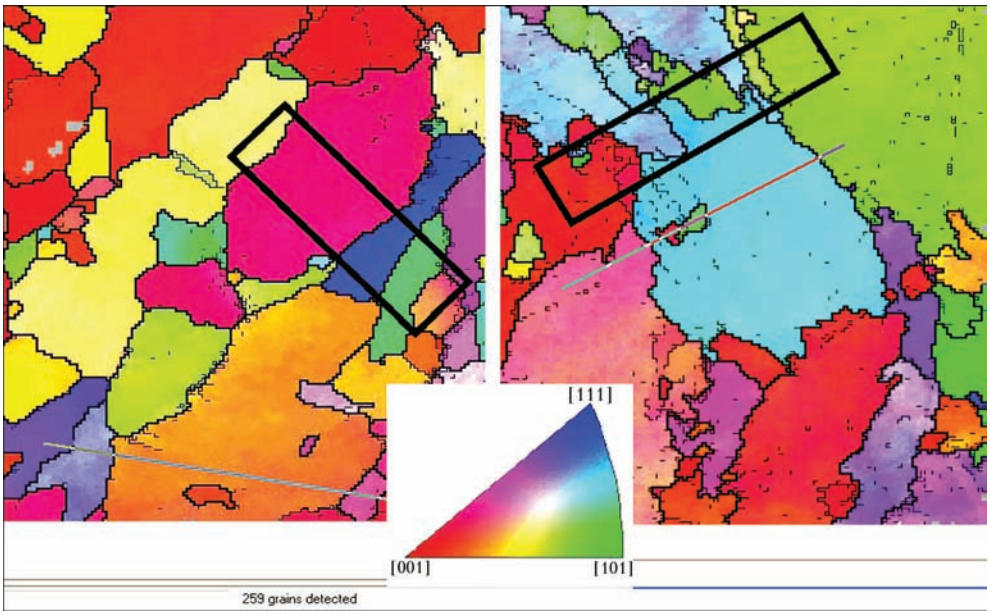

Figure 6. Fragments of crystallite orientation (inverse pole figure) of HAZ metal of welds, made with Inconel 52 (*a*) and Inconel 52MSS (*b*) wires (rectangles mark points where microhardness measurement was performed)

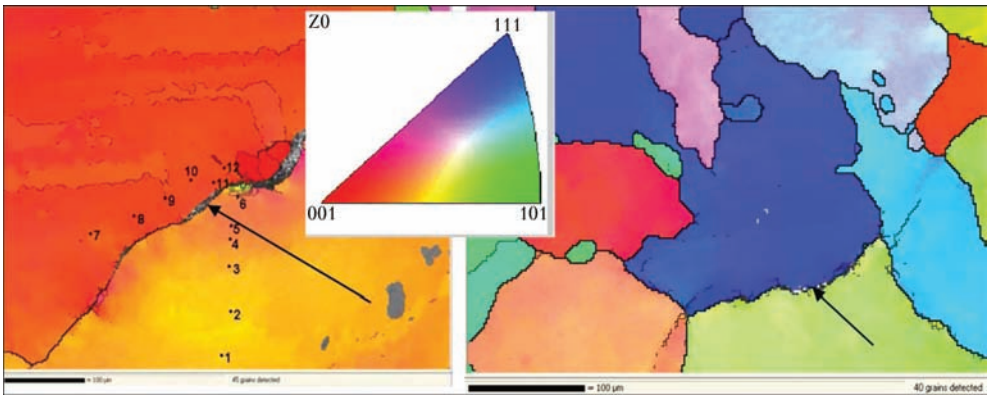

Figure 7. Crystallographic pattern of crack location in HAZ metal of Inconel 52 welded joint (arrows indicate cracks along grain boundaries)

of polycrystalline nickel alloy and to assess plastic deformation localizing within several grains by microindentation method. Here, microhardness measurements were conducted in Micron-gamma microindentometer using 5 and 10 g load.

Measurement results showed microhardness values for Inconel 52 within 2.8–5.5 GPa, while microhardness for a sample made with Inconel 52MSS wire show a greater scatter of values from 2.9 to 7.0 GPa (Figure 8).

Conclusions

Results of investigations of multilayer deposits, made with wires with different sensitivity to hot cracking, allowed showing that microstructural components and their change under the impact of welding thermal cycle significantly influence hot cracking resistance of welded joints.

In Inconel 52 welds, in which molybdenum and niobium content is minimum (total Mo + Nb = 0.7 %), chemical inhomogeneity decreases significantly, that promotes DDC development. At the same time, cracks are absent in welds of this type in individual regions of Inconel 52MSS weld, where niobium and molybdenum content rises 2 to 4 times, compared to total content (Mo + Nb = 6 %).

It is established that the fine structure of weld metal at application of Inconel 52 wire is characterized by higher dislocation density, particularly at grain boundaries (of up to $\rho \sim 10^{11}$–$2.2 \cdot 10^{11}$ cm^{-2}).

Absence of cracks in weld metal in the case of application of Inconel 52MSS wire is associated with uniform (without gradients) distribution of dislocation density, as well as lowering of SFE values (to $\gamma_{SFE} \sim 0.091$ J/cm^2).

DDC in welded joint HAZ propagate, as a rule, along high-angle grain boundaries.

Results of microhardness measurements in welds made with Inconel 52 wire showed values within 2.8–5.5 GPa, while that of a sample made with Inconel 52MSS wire have greater scatter of 2.9 to 7.0 GPa.

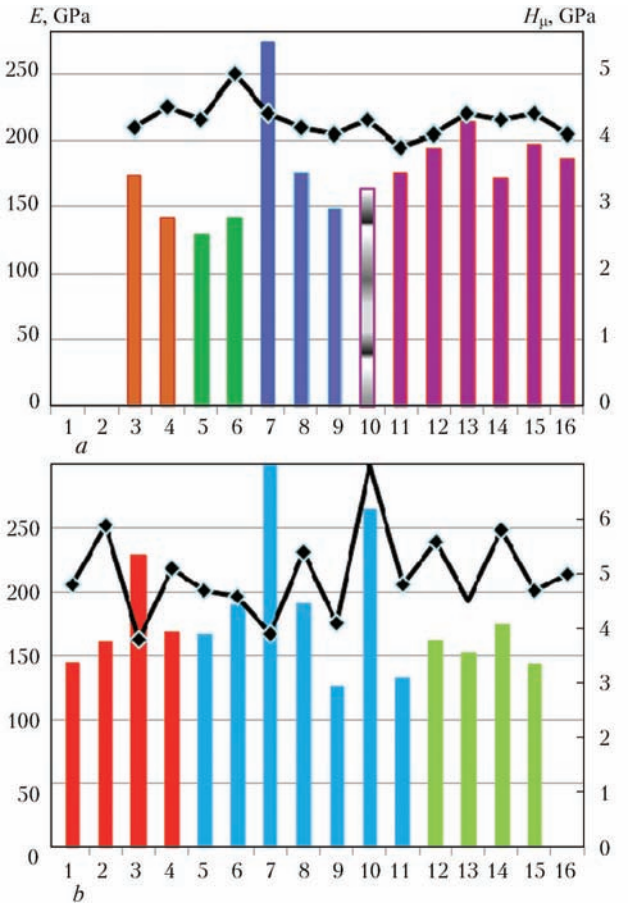

Figure 8. Microhardness and modulus of elasticity for HAZ of welded joints made with Inconel 52 (*a*) and Inconel 52MSS (*b*) wire

1. Panin, V.E., Egorushkin, V.E. (2008) Nonequilibrium thermodynamics of deformed solid as a multilevel system. Wave-corpuscle dualism of plastic shear. *Fizich. Mezomekhanika*, **11**, 9–30.
2. Torres, E.A., Peternella, F.G., Caram, R. et al. (2010) In situ scanning electron microscopy high temperature deformation experiments to study ductility dip cracking of Ni–Cr–Fe alloys. In: *In-situ studies with phonons, neutrons and electrons scattering*, 28. Berlin; Heidelberg: Springer.
3. Yushchenko, K., Savchenko, V., Chervyakov, N. et al. (2011) Comparative hot cracking evaluation of welded joints of alloy 690 using filler metals Inconel® 52 and 52MSS. *Welding in the World*, 55(**9/10**), 28–35.
4. Lippold, J.C., Kotecki, D.J. (2005) *Welding metallurgy and weldability of stainless steels*. John Wiley & Sons.
5. Yushchenko, K.A., Savchenko, V.S., Chervyakov, N.O. et al. (2014) Investigation of cracking susceptibility of austenitic material using PVR-test procedure. *The Paton Welding J.*, **6/7**, 10–13.
6. Hirsch, P., Howie, A., Nickolson, R. et al. (1968) *Electron microscopy of thin crystals*. Moscow: Mir.
7. Thomas, G. (1963) *Electron microscopy of metals*. Moscow: IL.
8. Gorelik, S.S., Rostarguev, L.N., Skakov, Yu.A. (1970) *X-ray and electrooptic analyses*. Moscow: Metallurgiya.
9. Collins, M.G., Ramirez, A.I., Lippold, J.C. (2004) An investigation of ductility-dip cracking in nickel-based weld metals. Pt 3. *Welding J.*, **2**, 39–49.

Received 22.12.2015

doi.org/10.15407/tpwj2016.02.03

RESEARCH PROGRESS OF SUPERSONIC LASER DEPOSITION TECHNOLOGY

JIANHUA YAO[1, 2] and **V. KOVALENKO**[1, 2, 3]
[1]Research Center of Laser Processing Technology and Engineering,
Zhejiang University of Technology, Hangzhou, China
[2]Zhejiang Provincial Collaborative Innovation Center
of High-end Laser Manufacturing Equipment, Hangzhou, China
[3]Laser Technology Research Institute, NTUU «Kiev Polytechnic Institute», Kiev, Ukraine

Supersonic laser deposition is a new coating and fabrication process, in which a supersonic powder stream generated in cold spray impinges onto a substrate which is simultaneously irradiated with a laser. It will be increasingly employed for depositing coatings and metal additive manufacturing because of its unique advantages: solid-state deposition of dense, homogeneous and pore-free coatings onto a range of substrate, high build rate at reduced operating costs without the use of expensive gas heating and large volumes of helium, and opening up a new opportunity for efficiently depositing high hardness metallic powders which are usually difficult to be deposited solely by cold spray. Based on the current research results in our group, this paper systematically reviews state-of-the-art of supersonic laser deposition technique at home and abroad, from the viewpoints of materials selection, process optimization, properties characterization, equipment design and so on. The existing issues in these aspects are deeply analyzed, and the corresponding solutions are tentatively proposed. Meanwhile, the potential industrial applications of supersonic laser deposition in various fields are elaborated in detail, as well as the future perspectives and challenges facing this technology, in order to provide insight for further investigations and innovation in supersonic laser deposition as an emerging combination additive re-manufacturing technology with high efficiency, low cost and high quality. 16 Ref., 18 Figures.

Keywords: *supersonic laser deposition, materials, process parameters, performances, applications*

Supersonic laser deposition (SLD) is a newly developed technology in the field of laser material processing, which can be used for surface modification and coating of engineering components for increased functionality [1–3]. This technology combines the supersonic powder beam found in cold spray (CS) with laser heating of the deposition site. In SLD, a laser heats both the spraying particles and the substrate to 30–80 % of their melting point, thus significantly reducing the strength of the particles and substrate, and allowing the particles to plastically deform and build up a coating at an impact velocity about half of that in CS.

SLD technology has been increasingly employed for coating deposition because of its technological and economic advantages over conventional coating methods, namely solid-state deposition of dense, homogeneous and pore-free coatings onto a range of substrates; high deposition rate at reduced operating costs without the use of expensive heating and process inert gases; less sensitivity to feedstock materials characteristics; consolidation of difficult-to-deposit powders; and significant improvements in the properties of coating materials. More importantly, lower processing temperatures and shorter processing time of SLD technique will enable the coating, and fabrication of near-net shape components with little or no melting, thus avoiding the deleterious effects of high-temperature processes such as laser cladding and traditional thermal spray processes include deposit-substrate dilution, high thermally induced residual stresses, and as-solidified microstructures, which lead to component distortion and poor mechanical properties.

As compared to CS, the inclusion of laser heating into SLD can considerably softened the spraying particles and the substrate, which would reduce the critical deposition velocity and allow bonding to occur on impact at velocities around half those found in CS, even when depositing materials that are difficult to process solely using CS. Eliminating the need for high impacting velocities permits cold or slightly heated nitrogen to be used instead of high-temperature helium as the process gas, thus reducing operating costs by over an order of magnitude. This reduction in capital and operating costs means that SLD may be viable in many applications, for which CS has proved too costly allowing the fully solid process route found in CS to find a use in a wider range of applications. A variety of material coatings such as Cu, Ti, Stellite 6, Ni60, Al–Cu and Al–Si alloys, have been successfully prepared with SLD technique [4–16].

In order to provide insight for further investigations and innovation in SLD as an emerging combination additive re-manufacturing technology with high efficiency, low cost and high quality, this paper presents a systematical overview about state-of-the-art of SLD technology based on the current research

results in our group, from the viewpoints of equipment design, materials selection, process optimization, properties characterization, and so on. The existing issues in these aspects are deeply analyzed and the corresponding solutions are tentatively proposed. Meanwhile, the potential industrial applications of SLD in various fields are elaborated in detail as well as the future perspectives and challenges facing this technology.

Supersonic laser deposition system. Schematic diagram of the SLD system is illustrated in Figure 1, *a*. The laser energy and powder distribution are schematically illustrated in Figure 1, *b*. High-pressure gas was supplied to a converging-diverging nozzle in two different imports: one was through the gas heater, the other was via a powder feeder, where feedstock powders were held. The feedstock powder stream and high-pressure gas were mixed and passed through the nozzle, where the particles were accelerated to supersonic speed. The gas heating temperature, gas pressure and powder feeding rate were monitored and adjusted by the control unit of the CS equipment (Figure 2, *a*). The high-velocity particles impacted a region of the substrate, which was synchronously heated by a diode laser (Figure 2, *b*). Combined lenses were used to focus the laser beam onto the substrate surface. A high-speed infrared pyrometer was used to obtain real-time temperature measurements and control the temperature of the deposition zone during the SLD process. Data from the pyrometer was fed through a closed-loop feedback system, which altered laser power as necessary to maintain the desired temperature. The nozzle, laser head and pyrometer were assembled on a robot (Figure 2, *c*). The spraying nozzle was perpendicular to the substrate surface. The laser beam was at 30° angle to the surface normal. In deposition process, the substrate was stationary and the nozzle, laser head and pyrometer were moveable, controlled by the robot. The process gas can be compressed air (or high-pressure nitrogen), which can be provided by an air compressor (or a manifolded cylinder palette) (Figure 2, *d*).

Coating fabrication and characterization. *Single material coatings*. This section focuses on the comparison of the single material coatings prepared by SLD and other conventional coating technologies such as CS and laser cladding, in regard to deposition efficiency (DE), coating density, microstructure evolution, interfacial bonding, properties, etc.

Comparison of single material coatings prepared by SLD and CS. Shown in Figure 3 is the comparison of thickness of CS-Cu and SLD-Cu coatings. It is evident that the SLD-Cu coating is thicker than the CS-Cu coating. The peak thickness of CS-Cu coating is around 1.3 mm while that of SLD-Cu coating is about 2.2 mm, i.e laser irradiation increased the peak

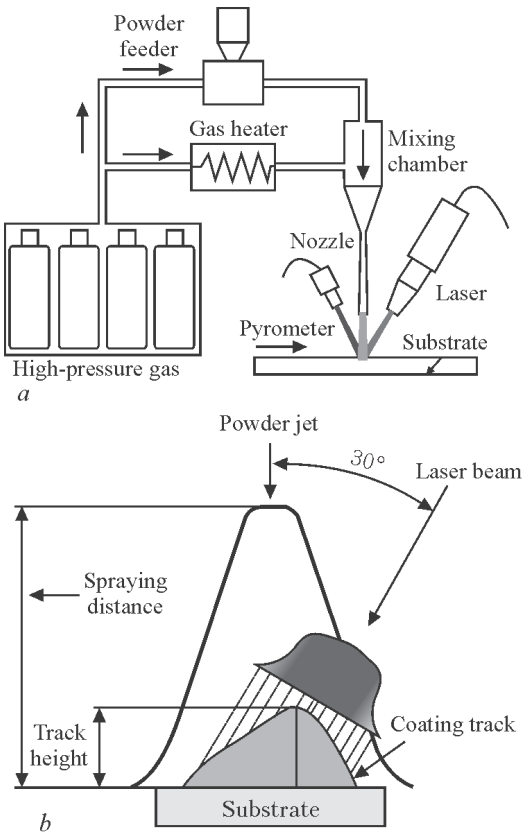

Figure 1. Schematic illustration of SLD system (*a*), and laser energy and powder distribution in SLD process (*b*)

coating thickness by 70 %. In other words, laser heating considerably improved the DE.

Figure 4 shows the comparison of density of CS-Cu and SLD-Cu coatings. It is observed that CS-Cu coating has lots of gaps and pores between the deformed copper particles, while the SLD one has a much denser microstructure, with gaps and pores hardly observed. Porosity measurements using image analysis software indicated that the porosity of the

Figure 2. SLD system: *a* — control unit of SC equipment; *b* — diode laser; *c* — robot; *d* — air compressor

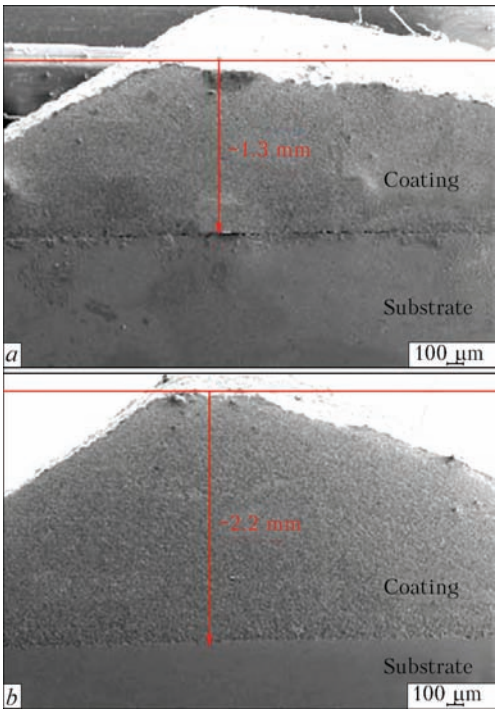

Figure 3. Comparison of the CS-Cu (*a*) and SLD-Cu (*b*) coating thickness

CS-Cu coating was 3.367 % in area, while it was only 0.08 % in area for the SLD-Cu coating. This confirms the beneficial effect of laser irradiation on the coating density.

Figure 5 presents the coating–substrate interfacial bonding of the CS-Cu and SLD-Cu coatings. As can be seen from Figure 5, *a*, there is an obvious crack observed at the interface between coating layer and substrate of the CS-Cu coating specimen, but this is not found in the SLD-Cu coating, instead, material penetration has occurred at the interface of this coating

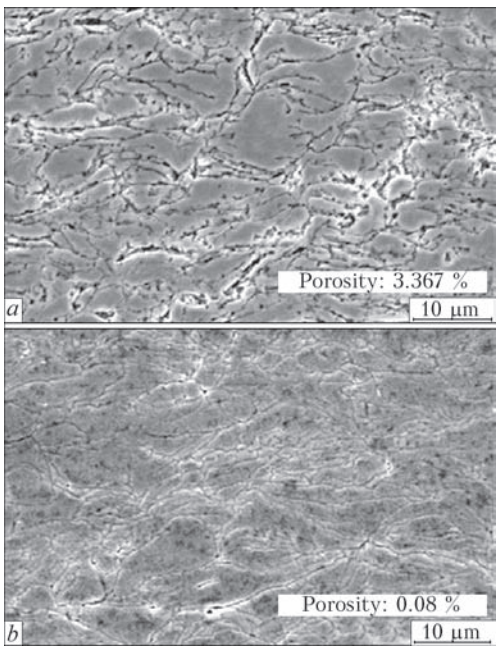

Figure 4. Comparison of density of the CS-Cu (*a*) and SLD-Cu (*b*) coatings

(Figure 5, *b*), which would enhance the coating bonding to the substrate. Adhesion strength test according to ASTM Standard C633 was performed on the CS-Cu and SLD-Cu coatings in order to quantify the real bonding force for each coating. The comparison of adhesion strength of coatings is shown in Figure 5, *c*. It can be seen that the adhesion strength of the CS-Cu coating is very weak but it increased significantly with the assistance of laser irradiation.

From the above-mentioned results it can be concluded that DE, coating density and interfacial bonding of CS coating can be improved by the assistance of laser irradiation. The improvement of DE should be ascribed to the reduction of critical deposition velocity due to the softening of spraying particles by laser heating. One of the most important parameter in CS process is the critical deposition velocity. For a given material, there exists a critical deposition velocity that must be achieved. Only

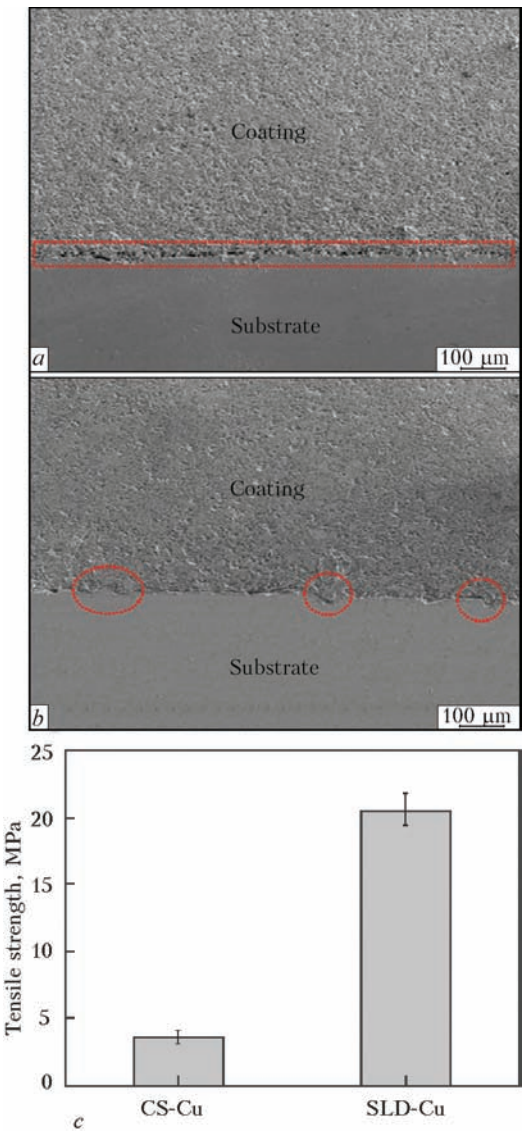

Figure 5. Coating substrate interfacial bonding of the CS-Cu (*a*) and SLD-Cu (*b*) coating, and comparison of their adhesion strength (*c*)

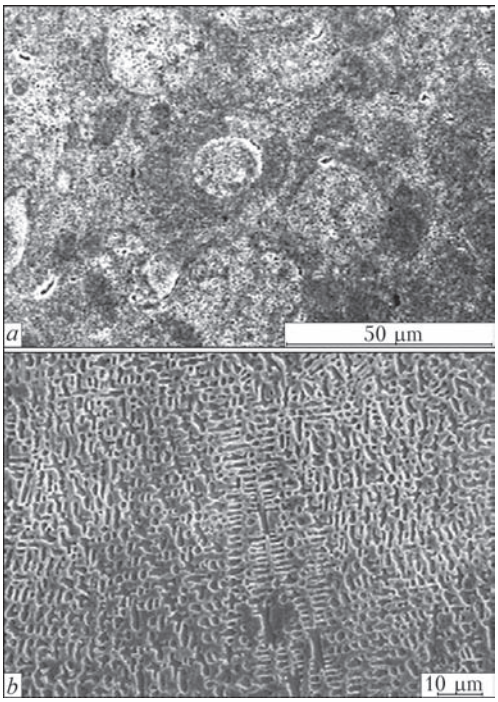

Figure 6. Comparison of microstructure of the SLD-Ni60 (*a*) and LC-Ni60 (*b*) coatings

particles, whose velocities exceed this value, can be effectively deposited, in turn producing the desired coating. Conversely, particles that have not reached this threshold velocity contribute to the erosion of the substrate. Theoretical modelling of critical deposition velocity v_{cr}, m/s, proposed by Assadi et al. can be expressed as

$$v_{cr} = 667 - 14\rho + 0.08T_m + 0.1\sigma_u - 0.4T_i, \quad (1)$$

where ρ is the material density (g/cm^3); T_m is the melting temperature (°C); σ_u is the ultimate strength (MPa); and T_i is the initial particle temperature (°C). According to formula (1), particle preheating will decrease the critical deposition velocity because as T_i is increased, σ_u of materials is reduced. Both the increase of T_i and reduction of σ_u would contribute to decrease of v_{cr}.

In SLD, the powder jet and laser beam partially overlapped with each other. Although the spraying particles were travelling at high velocities and had limited time of exposure to the laser, it is expected that the particles would be significantly heated in flight by laser prior to hitting the substrate because of the high laser power density and small particle size, which could bring down the critical deposition velocity of spraying particles. As a consequence, the proportion of particles exceeding this velocity would increase, leading to the DE improvement. In CS process, the initially deposited particles are hammered by successive high-speed impacting particles. The softened particles by laser heating get easily deformed by the impact of particles at a high velocity, leading to tight bonding of deposited particles (high coating density). In the case of synchronous laser irradiation on the deposition

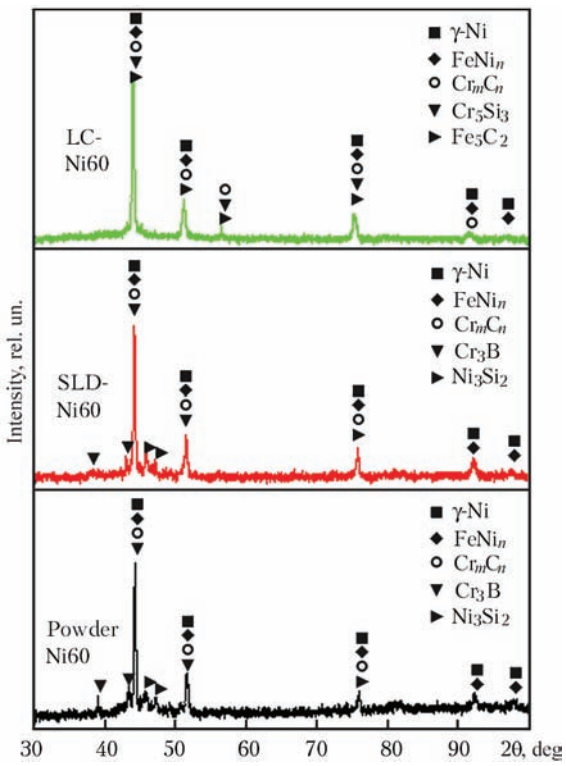

Figure 7. XRD patterns of the LS-Ni60 and SLD-coatings and Ni60 powder

site, the substrate temperature is increased and it is thereby softened. The softened substrate easily lodges the particles to form mechanical interlocking. Moreover, the increased substrate temperature can promote the atomic diffusion between the coating and the substrate, which greatly increases the possibility of metallurgical bonding. All these contribute to the good interfacial bonding of the SLD coating.

Comparison of the single material SLD and laser clad coatings. Figure 6 shows the SEM microstructure of the Ni60 coating specimens prepared with SLD and LC. As can be seen, the microstructure of the SLD-Ni60 coating shows accumulated plastic deformation of the Ni60 particles with the similar fine as-cast structure to original powder particles (solid-state deposition), while the microstructure of the LC-Ni60

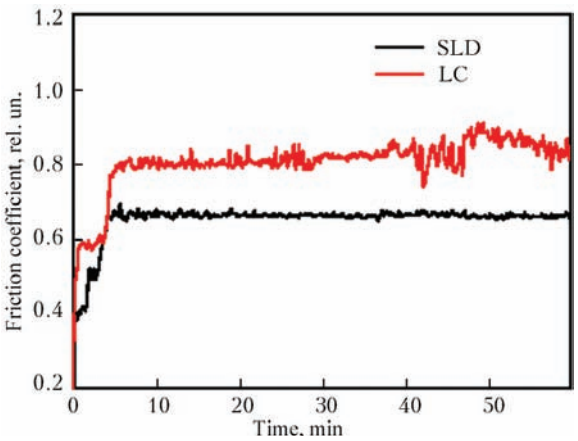

Figure 8. Friction coefficient versus sliding time for SLD-Ni60 and LC-Ni60 coatings

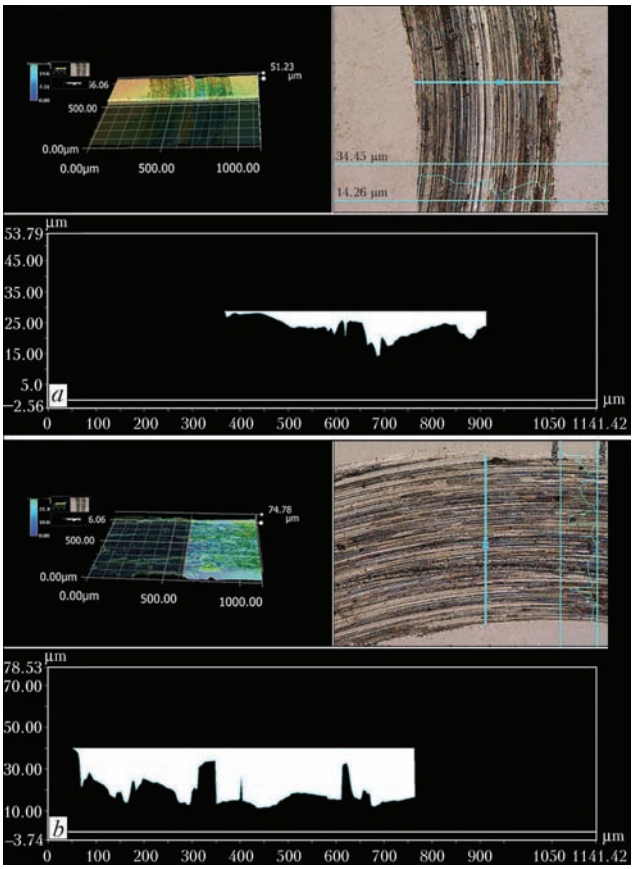

Figure 9. Cross-sectional profile of wear track for SLD-Ni60 (*a*) and LC-Ni60 (*b*) coatings

coating exhibits a typical coarse cladding dendritic structure.

Further XRD analysis (Figure 7) shows that the SLD-Ni60 coating has identical phases to that of the original powder particles. However, the phases in XRD pattern of the LC-Ni60 coating differ from those of the SLD-Ni60 coating and Ni60 powder, in that LC process generated a new phase Fe_5C_2 due to dilution effect. Shown in Figure 8 are the evolutions of friction coefficient of the coating specimens that recorded during the wear test. As illustrated, the friction coefficient of the SLD specimen is much smaller and more stable than that of the LC specimen. Deep plough scars can be observed obviously in the wear track of the LC specimen, while the SLD specimen looks smoother (Figure 9). Also, the wear track width of the LC specimen is wider than that of the SLD one. It is clear that the SLD coating has better wear resistance than the LC one.

Laser irradiation in SLD provides heat, which can synchronously soften the high-speed particles and substrate, while the heat in LC process melts the particles. Since SLD process has less laser energy input than LC one, the coating–substrate interface and HAZ of the SLD specimen are smoother and smaller. Moreover, due to the relatively low temperature in SLD, the as-deposited Ni60 coating still remains the same microstructure and phases as that of the feedstock powder materials. The superior wear resistance property of the SLD-Ni60 coating to the LC one should be attributed to the finer structures in the SLD coating, that is, the carbides and borides are more homogeneously distributed in the nickel matrix. It should be noted that hard Ni60 powder particles can be successfully deposited by SLD while it is impossible to be deposited by CS, indicating the SLD technique broadens the materials range that can be processed with CS. Furthermore, this novel deposition technique surpasses conventional LC technique, when used to deposition of hard materials such as Ni60 alloy, in that it can suppress the dilution of the steel substrate.

Metal-matrix composite material coatings. Comparisons of metal-matrix composite (MMC) material prepared by SLD and other conventional coating technologies are focused on the heat sensitive materials such as tungsten carbide (WC) and diamond.

Comparison of the SLD- and CS-MMC coatings. Shown in Figure 10 are the SEM images of cross-section of the WC/SS316L composite coating specimens. As observed, the central peak height strongly depends on the laser heating temperature. The peak height of the WC/SS316L coating deposited without laser assistant is 869.5 μm, and it is gradually increased to 1.153 mm with the increase of deposition temperature from 500 to 900 ºC. This result indicates that laser heating can also improve the DE of MMC coatings as similar to the single material coatings, which is ascribed to the reduction of critical deposition velocity by laser irradiation. It can be found in Figure 11 that WC particles are evenly distributed in all the specimens, and the concentration of WC particles in the coatings is increased with deposition temperature. SEM images at high magnification show (Figure 12) that WC particles are not effectively embedded into the SS316L matrix in the case without laser heating. With less laser heating or at low deposition temperature,

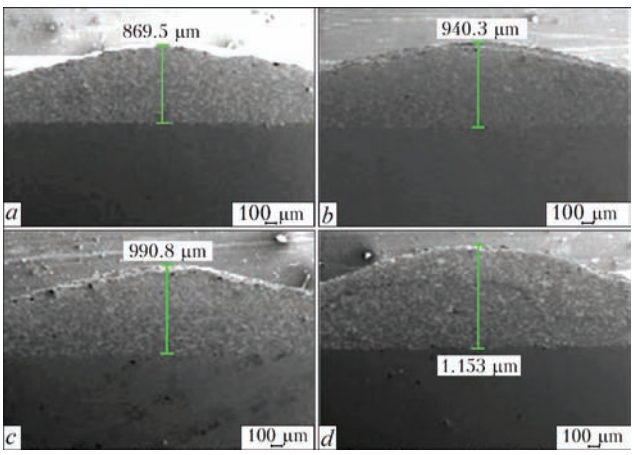

Figure 10. Thickness of the WC/SS316L composite coating deposited without laser heating (*a*), at 500 (*b*), 700 (*c*) and 900 (*d*) ºC deposition temperature

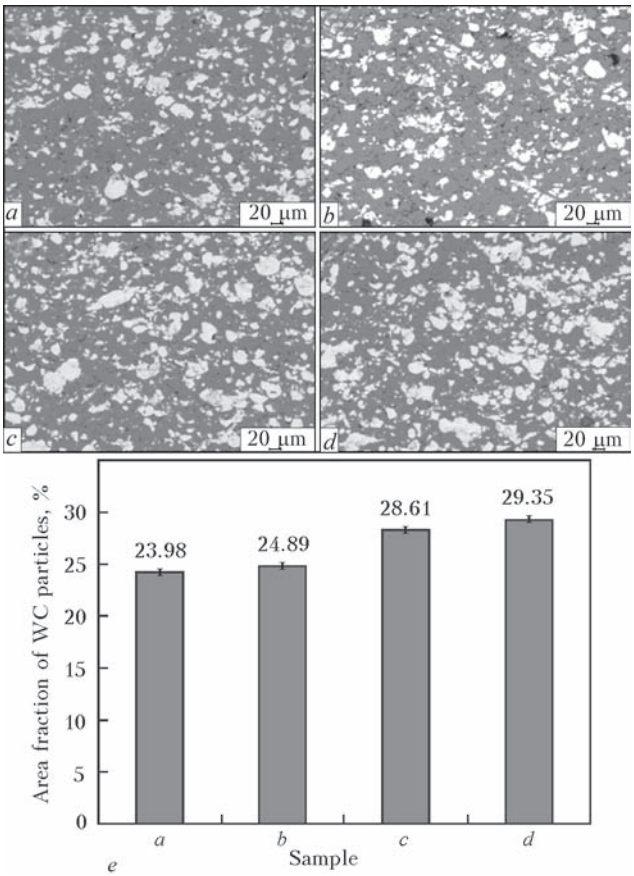

Figure 11. Distribution and concentration of WC particles in the composite coatings produced without laser heating (*a*), at 500 (*b*), 700 (*c*) and 900 (*d*) °C deposition temperature; *e* — area fractions

although the WC particles can be embedded in the coating, obvious gaps can still be found at the interface between WC particles and SS316L matrix. Further increasing deposition temperature enhances the interface bonding strength. The WC particles are well embedded in the SS316L matrix with little gaps.

The beneficial effects of laser irradiation on the concentration of WC particles in the WC/SS316L composite coatings can be attributed to the softening of SS316L powder. During SLD process, the WC

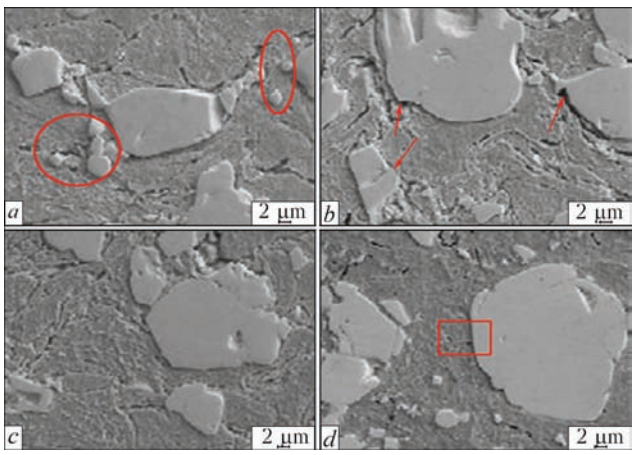

Figure 12. Interface bonding between SS316L matrix and WC particles in coatings deposited without laser heating (*a*), at 500 (*b*), 700 (*c*) and 900 (*d*) °C deposition temperature

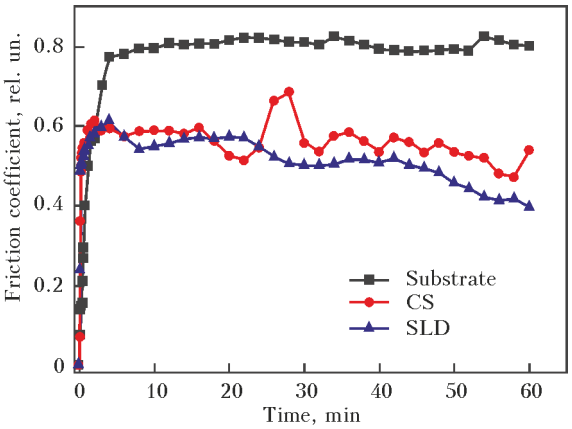

Figure 13. Friction coefficient versus sliding time for SLD- and CS-WC/SS316L composite coatings

particles may not deform due to high hardness and they are embedded in the deformable SS316L matrix. Without laser assistance or with less laser heating, SS316L powder may not be softened enough to accommodate the hard particles, resulting in relatively low WC concentration. In the case of more laser heating, SS316L powder easily deforms to take in WC particles owing to sufficient softening, leading to higher WC particle concentration. Furthermore, due to softening effect by laser irradiation in SLD, SS316L powder particles are easier to deform, which also favours lodging the impacting WC particles to form intimate bonding, therefore showing improved bonding strength than the CS coating. The relatively high content of WC particles in the composite coating and the strong interfacial bonding between WC particles and SS316L matrix results in better

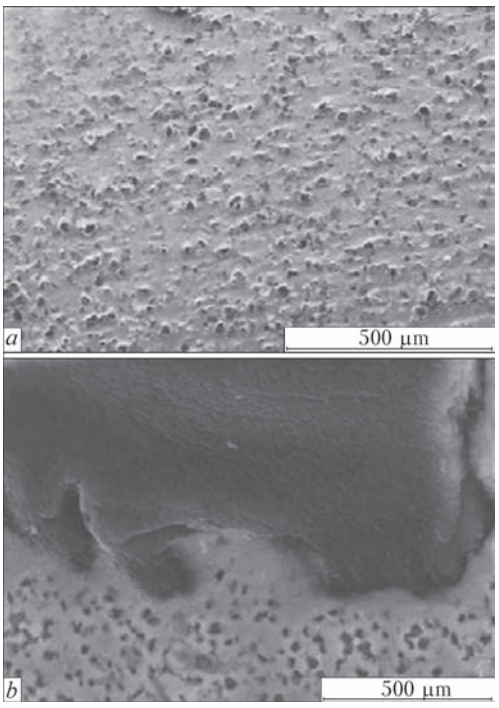

Figure 14. Microstructure of the SLD-diamond/Ni60 composite coating

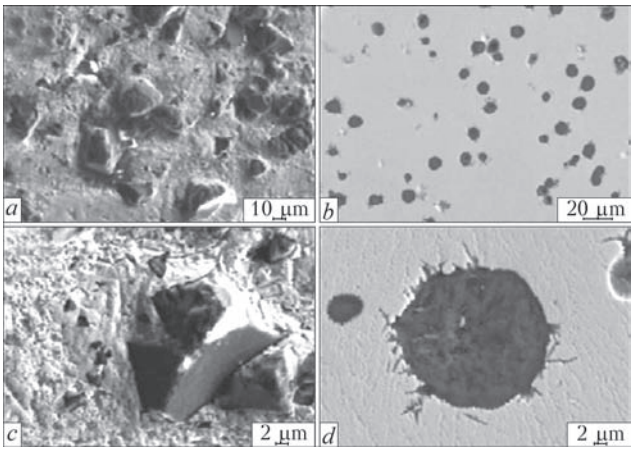

Figure 15. Graphitization of diamond in the SLD- (*a*, *c*) and LC-diamond/Ni60 coatings (*b*, *d*)

tribological properties of the WC/SS316L coating produced by SLD than with CS, as shown in Figure 13.

Comparison of SLD- and LC-MMC coatings. Figure 14 presents the microstructure of the diamond/Ni60 composite coating produced with SLD. It shown that the diamond particles are uniformly distributed within the Ni60 matrix (Figure 14, *a*), and the diamond particles are firmly embedded in the Ni60 matrix with good interface bonding (Figure 14, *b*). Most of the diamond particles in the composite coatings were fully retained. This may be due to the softened Ni60 matrix by laser heating. In this case, Ni60 particles were more prone to deform by adiabatic shear instability. The softened Ni60 particles are beneficial for wrapping and holding the diamond particles.

Figure 15 provides some information on diamond graphitization between the SLD-diamond/Ni60 and the LC-diamond/Ni60 coatings. In LC process, the high temperature and oxidation environment of molten pool, produced by laser irradiation, make the diamond particles easier to graphitize, compared with SLD process. In Figure 15, *b* and *d*, the black regions indicate serious graphitization of the diamond particles; carbon diffusion occurred at the interface between the diamond particle and Ni60 matrix. It is

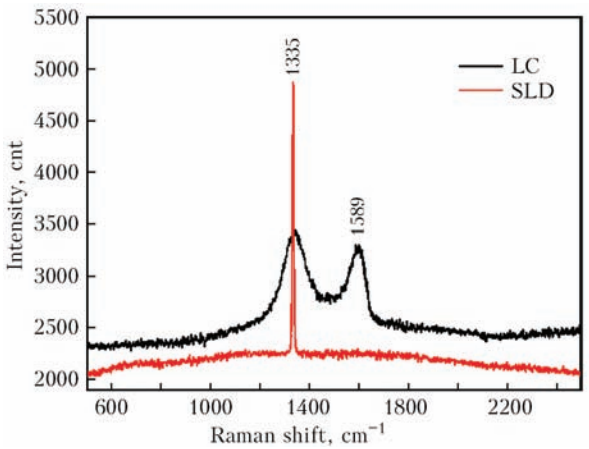

Figure 16. Raman spectra of the SLD- and LC-diamond/Ni60 coatings

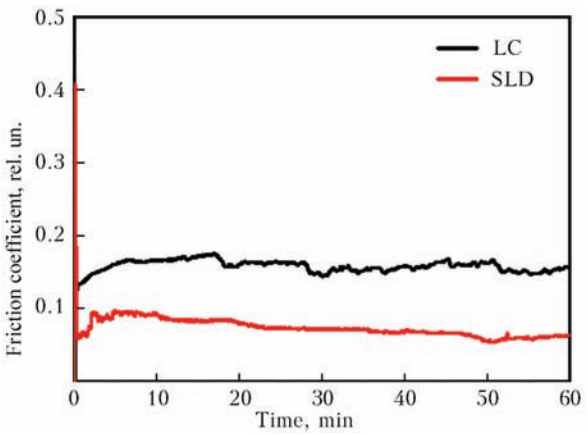

Figure 17. Friction coefficient versus sliding time for LC- and SLD-diamond/Ni60 coatings

also found that the irregular shape of the diamond particles was changed to spherical shape during LC. However, graphitization is not as severe in the SLD coating specimen as in the LC one.

From the Raman spectra in Figure 16 it can be seen that not only a typical diamond peak at 1335 cm^{-1} but also an obvious non-diamond component peak at 1589 cm^{-1} are presented in the LC coating, while only a single and sharp diamond peak is observed at 1335 cm^{-1} in the SLD coating. The Raman spectra analysis results demonstrate that part of the diamond particles have been graphitized in the LC coating but no graphitization occurred in the SLD coating. All these findings suggest that the relatively high impact pressure, low deposition temperature and inert N_2 atmosphere are beneficial for preventing diamond particles from graphitizing during SLD process.

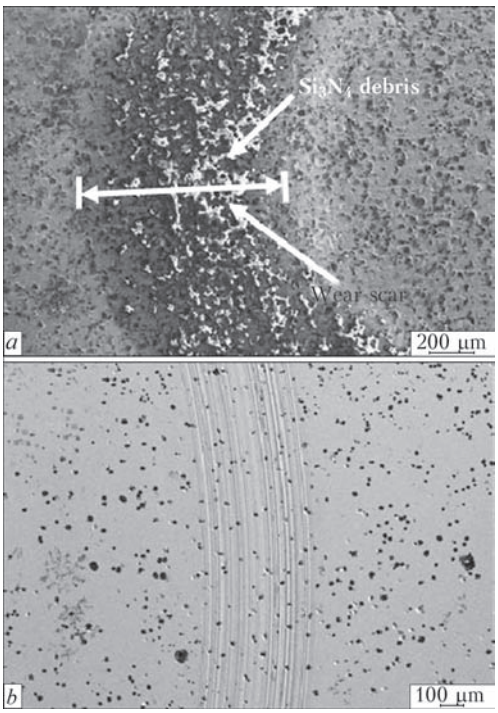

Figure 18. SEM images of worn surfaces: *a* — wear track of SLD specimen; *b* — LC specimen

According to the results of wear test (Figures 17 and 18), the diamond/Ni60 composite coating has excellent tribological properties. Under the cyclic load in the wear process and the cutting of irregular diamond particles, the surface of the Si_3N_4 grinding ball was seriously abrased. It is believed that friction between the contact surfaces was reduced due to abrasion resistance of hard irregular diamond particles. The low friction and high abrasion resistance of the diamond/Ni60 composite alleviate the damage of wear surface. Since the sliding wear mechanism of diamond is abrasion, the wear surface of pin is damaged by groove ploughing. The wear track is characterized by numerous discontinuous, short and shallow grooves. These imply that wear resistance of the SLD specimen is better than that of the LC specimen, because the interface bonding between the diamond and Ni60 particles is strong enough to sustain the mechanical attack under the wear.

Future perspective and challenges. On the basis of the results from the reviewed studies, it can be concluded that SLD has great potential for rapid transfer of laboratory-developed technology to various industrial fields such as automotive, marine, biomedical, aeronautical/aerospace, power generation, petrochemical, and mining. Furthermore, the need to reduce high cost of preparing coatings, reduce fabrication stages into a single step, and improve coating's functional properties are among the reasons that SLD technique will continue to gain attention both in academic and industrial research. Some application-oriented challenges such as specific tribology, severe abrasive wear, high-temperature creep, fatigue, and severe erosion need to be investigated for successful utilization of SLD technology in the industry.

The focus of further work should be on improving the efficiency and capability of SLD technology. The efficiency in current study was limited due to the mismatching of laser spot and the powder footprint and the non-uniform heat distribution (Gaussian heating profile) across the deposition site. Using a more powerful laser would enable the laser spot to be increased to the size of powder footprint, and the effects of deposition at higher traverse rates and build rates to be investigated. If a top-hat laser beam profile is used, a more uniform temperature distribution could be expected, which would increase consistency of deposition conditions across the tracks, thus improve process control. The use of higher particle velocities should be investigated through the use of gas heating or improved nozzle designs, as well as improved deposition efficiency, density and mechanical properties of coatings should be expected.

Acknowledgements. *The authors would like to appreciate financial supports from the National Natural Science Foundation of China (51475429), the Zhejiang Provincial Commonweal Technology Applied Research Project (2014C31122) and the Postdoctoral Scientific Research Project of Zhejiang Province (Z42102002).*

1. Bray, M., Cockburn, A., O'Neill, W. (2011) The laser-assisted cold spray process and deposit characterization. *Surface and Coating Techn.*, **203**, 2851–2857.
2. Lupoi, R., Sparkes, M., Cockburn, A. et al. (2011) High speed titanium coating by supersonic laser deposition. *Materials Letter*, **65**, 3205–3207.
3. Jones, M., Cockburn, A., Lupoi, R. et al. (2014) Solid-state manufacturing of tungsten deposits onto molybdenum substrates with supersonic laser deposition. *Ibid*., **134**, 295–297.
4. Olakanmi, E.O., Doyoyo, M. (2014) Laser assisted cold-spray corrosion- and wear-resistant coatings: A review. *J. Thermal Spray Techn.*, **23**, 765–785.
5. Kulmala, M., Vuoristo, P. (2008) Influence of process conditions in laser-assisted low pressure cold spraying. *Surface and Coatings Techn.*, **202**, 4503–4508.
6. Li, B., Yang, L.J., Li, Z.H. et al. (2015) Beneficial effects of synchronous laser irradiation on the characteristics of cold-sprayed copper coatings. *J. Thermal Spray Techn.*, **24**, 836–847.
7. Luo, F., Cockburn, A., Lupoi, R. et al. (2012) Performance comparison of Stellite 6 deposited on steel using supersonic laser deposition and laser cladding. *Surface and Coatings Techn.*, **212**, 119–127.
8. Yao, J.H., Yang, L.J., Li, B. et al. (2015) Beneficial effects of laser irradiation on the deposition process of diamond/Ni60 composite coating with cold spray. *Appl. Surface Sci.*, **330**, 300–308.
9. Li, B., Yao, J.H., Zhang, Q.L. et al. (2015) Microstructure and tribological performance of tungsten carbide reinforced stainless steel composite coatings by supersonic laser deposition. *Surface and Coatings Techn.*, **275**, 58–68.
10. Yao, J.H., Yang, L.J., Li, B. et al. (2015) Characteristics of performance of hard Ni60 alloy coating produced with supersonic laser deposition technique. *Materials and Design*, **83**, 26–35.
11. Olakanmi, E.O., Tlotleng, M., Meacock, C. et al. (2013) Deposition mechanism and microstructure of laser-assisted cold-sprayed (LACS) Al–12 wt.% Si coatings: Effect of laser power. *JOM*, **65**, 776–783.
12. Riveiro, A., Lusquinos, F., Comesana, R. et al. (2007) Supersonic laser spray of aluminum alloy on a ceramic substrate. *Appl. Surface Sci.*, **254**, 926–929.
13. Yuan, L.J., Luo, F., Yao, J.H. (2013) Deposition behavior at different substrate temperatures by using supersonic laser deposition. *J. Iron and Steel Res. Int*., **20**, 87–93.
14. Tlotleng, M., Akinlabi, E., Shukla, M. et al. (2015) Microstructural and mechanical evaluation of laser-assisted cold sprayed bio-ceramic coatings: Potential use for biomedical applications. *J. Thermal Spray Techn.*, **24**, 423–435.
15. Luo, F., Cockburn, A., Cai, D.B. et al. (2015) Simulation analysis of Stellite 6 particle impact on steel substrate in supersonic laser deposition process. *Ibid*., **24**, 378–393.
16. Yang, L.J., Li, B., Yao, J.H. et al. (2015) Effects of diamond size on the deposition characteristics and tribological behavior of diamond/Ni60 composite coating prepared by supersonic laser deposition. *Diamond and Related Materials* (in press).

Received 23.01.2016

doi.org/10.15407/tpwj2016.02.04

EVALUATION OF SUSCEPTIBILITY TO TEMPER BRITTLENESS OF HEAT-RESISTANT STEELS USING HIGH-TEMPERATURE TESTING

V.Yu. SKULSKY[1], **V.V. ZHUKOV**[1], **M.A. NIMKO**[1], **S.I. MORAVETSKY**[1] and **L.D. MISHCHENKO**[2]
[1]E.O. Paton Electric Welding Institute, NASU
11 Kazimir Malevich Str., 03680, Kiev, Ukraine. E-mail: office@paton.kiev.ua
[2]Company «Turboatom»
199 Moskovsky Ave., 61037, Kharkov, Ukraine. E-mail: office@turboatom.com.ua

Main point of problem of crack formation in tempering is defined. It is shown that low metal ductility during plastic deformation, promoted by stress relaxation is a condition for nucleation of such cracks. Important brittleness factor under these conditions is temporarily developing secondary hardening, related with nucleation and precipitation of secondary phases in matrix. Since alloys with different level of alloying demonstrate different behavior during tempering, then evaluation of their possible tendency to temper brittleness is of interest in each specific case. A procedure is described for high-temperature tensile testing, which allows evaluating ductile properties of metal under different tempering conditions. Susceptibility to temper brittleness was evaluated using a criterion of value of relative reduction in area $\psi \leq 25$ %. Studied was a nature of ductility change in complexly-alloyed heat-resistant steels under different tempering modes resulting in secondary hardening condition and after hardening stage. It is shown that steels in a period of steel hardening development have low ductility with typical for such a state intergranular fracture. Determined are critical tempering modes, under which a high ductility state is achieved, based on which absence of susceptibility to tempering cracks can be predetermined. 9 Ref., 1 Table, 8 Figures.

Keywords: *hardening steels, tempering, cracks, secondary hardening, tempering ductility, high ductility condition*

Crack formation in process of tempering or re-heating in heat-hardenable steels and their welded joints is a result of combination of three factors, i.e. structural (caused by secondary hardening), brittleness (related with precipitation along grain boundary of secondary phases and segregation of additives), and force (in form of stresses promoted by formation of hardening structures, metal shrinkage or applied external loading).

Force factor, which is based on energy of elastic distortions accumulated in a crystal system, promotes development of relaxation plastic deformations in heating. Deformation acquires a local nature, namely concentrates along grain boundaries or in area of more compliant (soft) structural constituents, under conditions of reduced ductility, caused by secondary hardening. Small ductility resource of such areas and additional segregation of additives increase the possibility of nucleation of such mircodefects and formation of cracks.

The cracks having small size and being located inside the metal can remain undetected, if non-destructive testing is carried out before final heat treatment. Therefore, it is important to determine the possibility and conditions for formation of such cracks before production of commercial products in order to apply preventive measures.

Different method are used in research practice for checking steel and their welded joints susceptibility to brittleness and formation of cracks in tempering. Specimens of small size from homogeneous metal as well as cut out from the welded joints can be used. In series of cases special fitting or equipment are necessary. More convenient and less time-consuming are the experimental methods allowing eliminating operations related with welding from preparation cycle, and using simple for production specimens of small size. Such a method can be high-temperature tensile testing [1–3]. At that, value of relative reduction in area ψ = 25 % [3] can be used as brittleness criterion, i.e. metal is susceptible to tempering cracks at lower values. In earlier works [4] Vinkier and Pense determined ψ = 20 % as a threshold value.

The aim of present work lied in investigation of effect of tempering modes of preliminary hardened energy-machine building steels on temper brittleness using the method of high-temperature tensile tests.

Tests were carried out on Gleeble 380 unit. Cylindrical specimens of 10 mm diameter with parts threaded at the ends for their fixing in loading jaws were used. Heating on set mode was performed with the help of current passed through the specimen from connected to it copper grips. In order to guarantee

fracture in operating part (between the grips), the specimens include cavity of smaller diameter (6 mm) in the center.

Cast, forged and hot-worked heat-resistant steels P3 (15Kh2M2FBS), EI415 (20Kh3VMFA) and P91 (X10CrMoVNb91) (10Kh9MFB type) were used as pilot materials. Time-temperature diagrams, limiting secondary hardening areas, were plotted on results of hardness measurement after different tempering modes (different holding at various temperatures) of preliminary quenched specimens. Weld metal specimens of similar alloying system were used in these experiments for steel P91; received experimental hardening diagrams served a marker for choosing the conditions of further tensile tests using specimens from hot-worked pipe steel.

The following approach is used for tensile tests at selected temperatures. It is known fact that the tempering cracks are formed as a result of slowly developing plastic deformation – relaxation creep (based on data of work [2], deformation rate (relative elongation) makes 10^{-4}–10^{-5} %/h). Under such conditions deformation initiates precipitation of carbide phases, promoting brittleness of grain boundaries [5], and, hypothetically, displacement of additive atoms together with moving dislocations to the boundaries becomes possible. In simple static tensile tests the deformation rates are higher and no signs of brittleness can be observed.

As was shown by Dix and Savage using the example of nickel alloy [6], high-temperature brittleness appeared at small deformation rates; in tension with more than 25 mm/min rate the brittleness effect became weaker and metal had increased ductility. Sufficiently low specimen deformation rate was also created for tests carried out in present work, namely grips movement speed made 0.04 mm/min.

The experiment had two heating cycles (Figure 1). The first cycle provided for specimen heating to T_{max} = 1250 °C for 5 s, holding during 15 s and further accelerated cooling to room temperature with $w_{6/5}$ = = 40 °C/s in 600–500 °C interval. This stage was used for reconstruction of the condition of welding heating and HAZ quenching. The second cycle was spent for slow (2 °C/s) heating up to necessary heat treatment temperature, holding at set temperature for preliminary selected time, and then specimen was deformed (at the same temperature). Temperature and holding time were set based on time-temperature boundaries of the secondary hardening areas. In some cases specimens after heat treatment, corresponding to achievement of hardening state and, respectively, low ductility were tested. In other cases they were examined after treatment mode providing coming

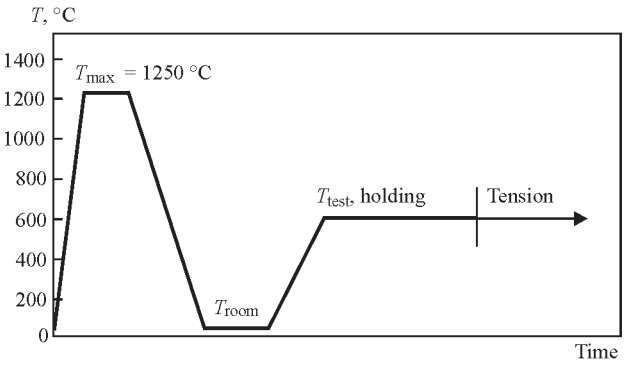

Figure 1. Temperature cycles of experiments

out from the hardening area, when metal should become more ductile. More «rigid» in comparison with work [4] criterion ψ = 25 % was taken. Heat mode of treatment in the experiments was evaluated with the help of Larson–Miller parameter P_{LM} which simultaneously considers absolute temperature T (K) and time of heat effect on metal τ (h) namely P_{LM} = = $T(20 + \lg(\tau))$.

Figure 2 demonstrates preliminary carried investigations on susceptibility to secondary hardening. The registered hardening areas have different time-temperature limits. The general point is their reduction and shifting to small holding durations with temperature increase, that is caused by amplification of thermal activation of atoms diffusion in the crystal system, quick nucleation, precipitation and coarsening of carbide and carbide-nitride phases

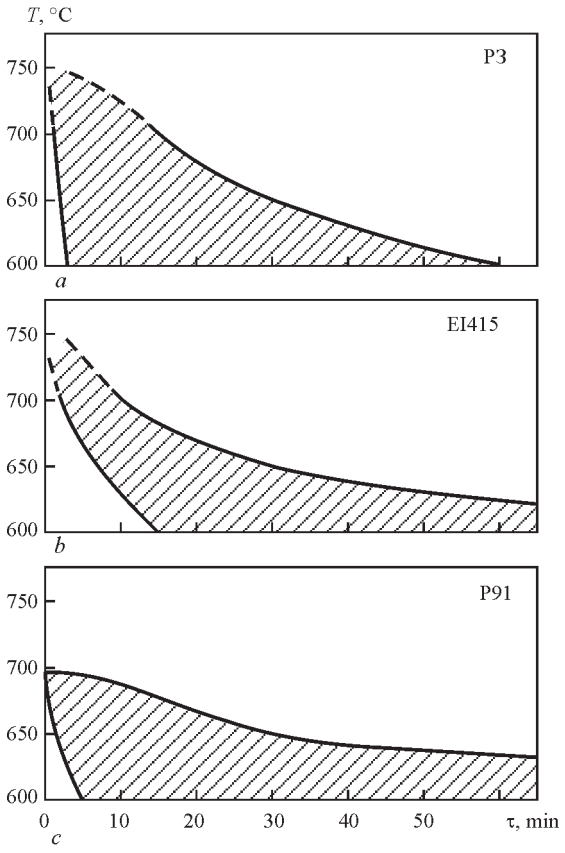

Figure 2. Diagrams of secondary hardening for steels used (*a*–*c*)

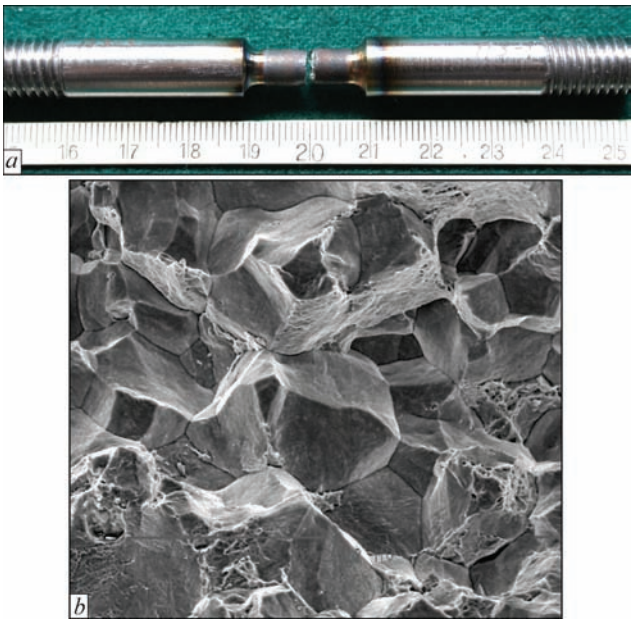

Figure 3. Nature of specimen fracture under conditions of development of secondary hardening in metal: *a* — specimen after testing; *b* — fracture surface (×600)

(depending on steel alloying system), and as a result, quick transfer to solid solution softening stage.

The Table shows the modes of specimen heat treatment. Positions I and II correspond to tests in hardening state and out of hardening areas.

The results showed that metal is susceptible to brittle fracture under secondary hardening condition. Reduction in area values received under these conditions lied at sufficiently low level in ψ = 1.7–6.0 % range. Specimens fractured virtually without thinning with typical for such a condition mainly intergrainular facture* (Figure 3).

As shown in Figure 4, low ductility is preserved in some intervals of time-temperature parameters P_{LM} in the ranges of areas of secondary hardening as well as out of its boundaries. Boundary values P^{B}_{LM} (inclined dashed lines), calculated on hardening diagrams, make $(17.5–18.9)\cdot10^3$ and $(17.7–18.7)\cdot10^3$ for P3 and EI415 steels, respectively, in 700–600 °C range, and $(15.8–16.2)\cdot10^3$ for steel P91 in 550–500 °C range.

In contrast to steels EI415 and P91, in which ψ values start rising out of the hardening area, ductility of steel P3 remains very small in some interval of modes exceeding the maximum tempering. Thus, relative reduction in area of steel P3 specimens remained at initially low level in testing at 700 °C after holding up to 40 min, which is obviously higher than evaluated experimental time for hardening stage finishing (around 15 min). Probably, in this

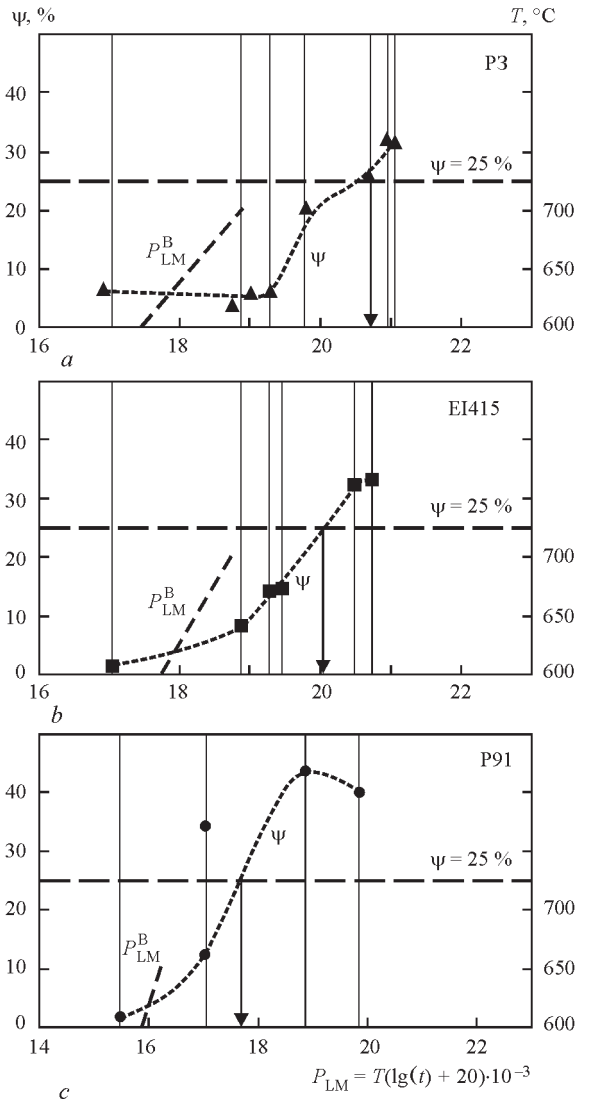

Figure 4. Change of relative reduction in area ψ depending on parameter P_{LM}, and relationship of time-temperature boundaries of hardening P^{B}_{LM} with tempering temperature *T* for steels used (*a*–*c*)

case an additional effect of process of activation of precipitation of plastic deformation carbide phases on hardening development can appear [5]. It could result in a shift of boundaries of the hardening area to the side of longer holding time relatively to their position determined based on hardness measurement. Also, there is a possibility of effect of another type carbide precipitations [5, 7–9] on additional hardening and limitation of plasticity improvement at elevated temperature (and deformation).

In whole, studied steels demonstrate increase of high-temperature ductility (see Figure 4) after hardening stage is finished. Moreover, in steel P91** this transfer takes place more abrupt at lower values and in narrower range of P_{LM} parameter. Under such

*Metallographic examinations were carried out with the participation of T.A. Alekseenko.

**Testing at 600 °C/20 min showed larger spread of ψ values. Lower value was considered in carried analysis as the possible worth variant of ductility.

Modes of specimen heat treatment

Steel	Group of testing	Sample number	Quenching at T, °C/τ, min	$P_{LM}\cdot10^{-3}$
P3 (15Kh2M2FBS)	I	1	600/20	17.04
		2	700/15	18.87
		3	700/15	18.87
	II	4	700/40	19.29
		5	740/20	19.78
		6	760/60	20.66
		7	750/100	20.69
		8	750/180	20.95
		9	780/60	21.06
EI415 (20Kh3MVF)	I	1	600/20	17.04
		2	700/15	18.87
	II	3	700/40	19.29
		4	700/60	19.46
		5	740/100	20.48
		6	740/180	20.74
P91 (X10CrMoVNb9-1)	I	1	520/20	15.48
	II	2	600/20	17.04
		3	600/20	17.04
		4	700/15	18.87
		5	760/10	19.86

conditions ψ increased to higher level (not lower than 40 % at $P_{LM} \approx (18.9–19.9)\cdot10^3$) than in steels P3 and EI415. The latter were more «inert» in process of transfer from high to low ductility. The maximum ψ values achieved lower level also at larger values of P_{LM} parameter, i.e. 32–33 % at $P_{LM} \approx 30\cdot10^3$ in steel P3, and 33–34 % at $P_{LM} = (25–27)\cdot10^3$ in steel EI415. The following critical values of tempering parameter were determined using received experimental curves. They allow reaching criterial relative reduction in area, namely 25 % at $\psi = 20.7\cdot10^3$ for cast steel P3, $20\cdot10^3$ for forged steel EI415, and $17.6\cdot10^3$ for hot-worked pipe steel P91.

Energy characteristic of fracture resistance can be a work of crack propagation, which is nucleated in the specimen after reaching specific loading (stress). A measure of work of crack propagation A_w is an area under the part of fracture diagram after crack appearance. However, determination of such a characteristic on tension diagram is not very accurate, since it is difficult to determine the stress, at which the crack is nucleated. For this reason, the evaluation of metal resistance to crack propagation carried out in the work shall be considered approximate, however,

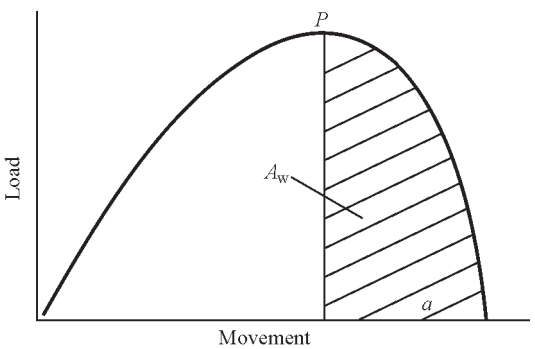

Figure 5. Scheme of tension diagram and calculated area corresponding to work of fracture propagation A_w

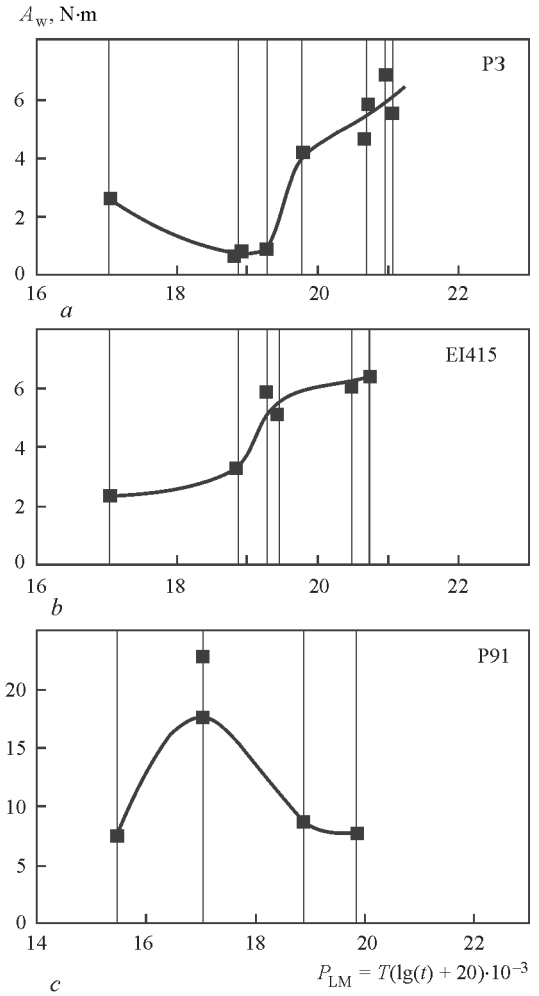

Figure 6. Computation values of fracture work A_w for steels used (*a*–*c*)

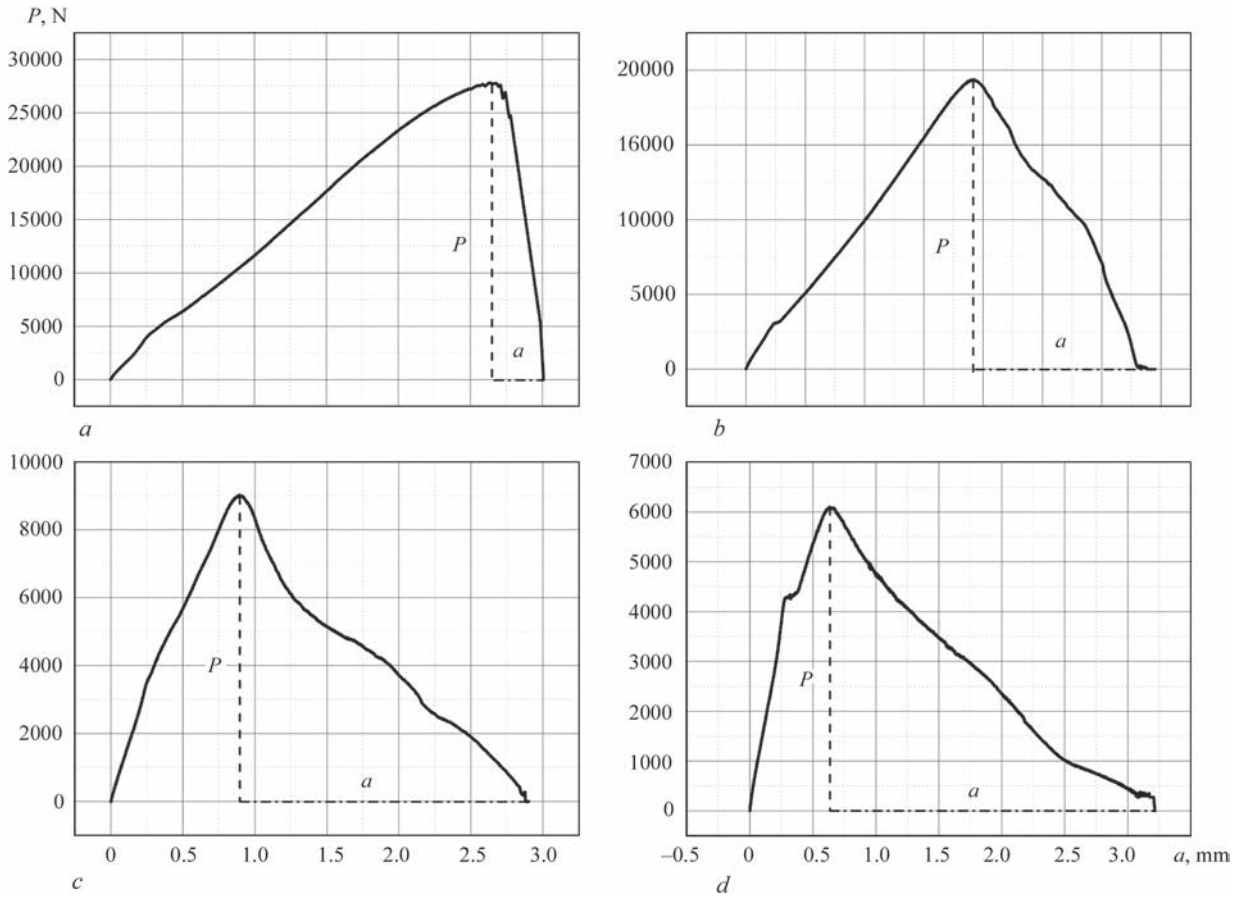

Figure 7. Diagrams of tension of steel P91 specimens for $P_{LM} = 15.48 \cdot 10^3$ (*a*), $17.04 \cdot 10^3$ (*b*), $18.87 \cdot 10^3$ (*c*) and $19.86 \cdot 10^3$ (*d*)

it illustrates the relationship with determined above indices of ductility. In this case the work of crack propagation was evaluated using an area under descending branch of the diagram after reaching maximum loading P in areas corresponding to the movement a of machine grips (Figure 5). At that, it was assumed that specimens have already had fracture centers at this stage. Corresponding calculations of the areas (Figure 6) on diagrams of tension received in tests were carried out by integration method using Origin 7.5 program (Origin Lab Corp., USA) .

Comparing indicated results and data in Figure 4 it can be noted that steels P3 and EI415 have some disagreement in change of fracture work and relative reduction in area at rise of P_{LM} tempering parameter. Nature of change of these characteristics is different in the case of steel P91. The reason of observed differences lies in relationship of values of maximum (fracture) force P and registered movement a at fracture stage (Figure 7). Thus, in the case of initial testing with $P_{LM} = 15.48 \cdot 10^3$ the metal had high strength and sufficiently small movement a, corresponding to brittle fracture susceptibility. Computation fracture work A_w made 7.5 N·m. Maximum A_w value was received in testing at $P_{LM} = 17.04 \cdot 10^3$. Movement in fracture increased in this state, and force was kept at high level. In the last two tests, reduction of fracture force took place regardless the rise of movement values, that resulted in decrease of resultant A_w values. It can be assumed that such steel behavior is determined by the peculiarities of structural changes developing in tempering and high-temperature deformation.

Constituent of fracture work, namely movement of machine grips a at fracture stage (Figure 8), is used as a characteristic of brittle fracture resistance for larger level of agreement with nature of ψ change, instead of the fracture work. It follows from the latter dependencies that high resistance of studied steels to crack formation due to re-heating is achieved at their such condition, under which movement during tensile testing in processes of tempering exceeds a = 1.2–1.5 mm (1.5, 1.2 and 1.5 mm for steels P3, EI415 and P91, respectively, determined for the conditions indicated by arrows of critical values of parameter P_{LM}).

In the conclusion it should be noted that secondary hardening can periodically appear at different stages of tempering. Wavy changes of hardness (increase and decrease) at longer holdings were registered after the first (considered above) stage in given investigations of hardening susceptibility. However, such temporary rises of hardness values were insignificant against a background of already achieved total softening of solid solution. This work paid specific attention to the first stage of hardening found in the process of relatively

short holdings (up to ~ 3 h). An interest to this period is caused by the fact that stress relaxation is developed, in particular at the beginning of tempering, that under conditions of ductility degradation due to hardening results in possibility of microdefect formation.

Conclusions

1. Time-temperature areas of development of secondary hardening were determined under conditions of high-temperature tempering of steels 15Kh2M2FBS, 20Kh3VMFA and X10CrMoVNb9-1, which were preliminary quenched using simulation welding thermal cycle. The external boundaries of hardening areas correspond to the following Larson–Miller parameter: P_{LM} = (17.5–18.9)·10³ and (17.7–18.7)·10³ for steel P3 and E415 in 700–600 °C range, and P_{LM} = (15.8–16.2)·10³ for steel P91 in 550–500 °C temperature range. Nature of change of ductility depending on tempering modes and condition of studied steels can be illustrated with the help of method of high-temperature tensile tests. It is shown that steel has low ductility and susceptible to brittle intergranular fracture under conditions of secondary hardening.

2. Value of relative reduction in area $\psi \leq 25$ % was used as a criterion of susceptibility to high-temperature brittleness for determination of the tempering modes, at which high ductility can be achieved and possibility of secondary heating cracks is eliminated: for steel P3 — $P_{LM} \geq 20.7 \cdot 10^3$, for steel EI415 — $P_{LM} \geq 20 \cdot 10^3$, and for steel P91 — $P_{LM} \geq 17.6 \cdot 10^3$.

1. Prager, M., Sines, G. (1971) Embrittlement of precipitation hardenable nickel-base alloy by oxygen. *Transact. of ASME*, 93(**2**), 112–119.
2. Zemzin, V.N., Shron, R.Z. (1978) *Heat treatment and properties of welded joints*. Leningrad: Mashinostroenie.
3. Titova, T.I., Shulgan, N.A., Borovskoj, A.S. (2012) Current requirements to consumables for welding of petrochemical pressure vessels made from steel of 2.25Cr–1Mo–0.25V type. In: *Proc. of Sci.-Techn. Conf. on Welding Consumables*, 192–201. St.-Petersburg: PI.
4. Vinkier, A.G., Pense, A.W. (1974) A review of underclad cracking in pressure-vessel components. *WRC Bulletin*, 197(**August**).

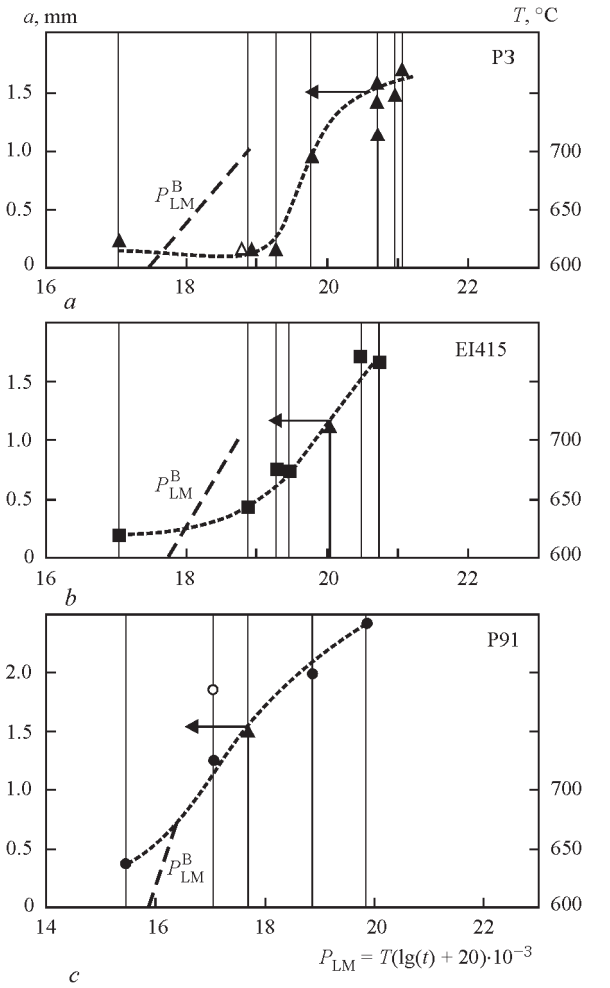

Figure 8. Effect of tempering modes on value of movement *a* at fracture stage for steels used (*a*–*c*)

5. Nawrocki, J.G., DuPont, J.N., Robin, C.V. et al. (2003) The mechanism of stress-relief cracking in a ferritic alloy steel. *Welding J*., 82(**2**), 25–35.
6. Dix, A.W., Savage, W.F. (1971) Factors influencing strain-age cracking in Inconel X-750. *Ibid*., 50(**6**), 247–252.
7. Olenin, M.I., Gorynin, V.I., Timofeev, B.T. et al. (2014) Nature of thermal brittleness of steels of NPP equipment and methods of its decrease. *Voprosy Materialoved.,* **3**, 167–173.
8. Lundin, C.D., Khan, K.K. (1996) Fundamental studies of metallurgical causes and mitigation of reheat cracking in 11.4Cr–1.2Mo and 21.4Cr–1Mo steels. *WRC Bulletin*, 409(**February**).
9. Lanskaya, K.A. (1976) *High-chromium heat-resistant steels*. Moscow: Metallurgiya.

Received 05.11.2015

doi.org/10.15407/tpwj2016.02.05

ACTIVITIES OF THE INSTITUTE OF WELDING IN GLIWICE IN THE FIELD OF TRAINING THE PERSONNEL FOR WELDING PRODUCTION

J. PILARCZYK
Institute of Welding
16/18 Bl. Czeslawa Str., 44-100, Gliwice, Poland. E-mail: is@is.gliwice.pl

The Institute of Welding in Gliwice is the largest and very important research center in Poland, which carries out works on research, development and implementation in all the fields and directions of welding production, that is very helpful in the process of education and training the personnel. The research staff members of the Institute, who have been working for decades in many fields of welding production, combine a profound theoretical knowledge with a huge laboratory experience within their specialties, and due to that the valuable results of practical cooperation with industrial enterprises fully meet the requirements specified to the educators of the highest level. 3 Ref., 1 Table.

Keywords: *welding production, training of personnel, harmonization, European and international systems, training and supervision centers, local education centers*

Training activities of the Institute of Welding in Gliwice [1] are carried out in several main areas:

- education and training of welding personal (engineers, technologists and masters of welding as well as welders) in the framework of the harmonized European and international systems;
- maintenance and supervision of the internal system for training welders at the local training centers;
- training of personnel in the field of non-destructive testing methods, covering all of the most important methods and techniques;
- courses on non-destructive testing methods in the field of railway transport;
- different special courses.

Training of welding personnel in the framework of harmonized European and international systems. This training is carried out in a close cooperation with:

- EWF (31 members) (European Federation for Welding, Joining and Cutting, formerly European Welding Federation) [2], founded in 1992 after the establishment of the European Union. The main task of EWF was the development of the Harmonized Education and Training System of personnel for welding production on the highest, medium and professional levels, which would ensure the issue of a single sample of documents, that would be irrevocably recognized in all the Member States without need in testing the knowledge and skills of persons who passed the education;
- IIW (56 members) (International Institute of Welding [3], founded in 1947, and included into the harmonized system of training the welding personnel in 2000, when the decision was taken to establish the IAB (International Authorization Board), comprising two groups: group A on matters of education, training and qualification, and group B on implementation of the systems and its authorization. The international auditors group (Lead and Peer Assessors) was established. In the countries which entered the system, the Authorised National Bodies IIW-ANB and IIW-ANBCC were established, exactly the same as those operating in EWF.

The authorized national bodies examine and certify the persons, who finished the preparatory courses, carried out by the education authorities — ATB (Approved Training Bodies) approved by these organizations.

The harmonized system of education, qualification and certification of personnel responsible for supervision of welding processes is currently based on the IIW recommendations. The basic document IAB 252 of 2007, which determines the principles of system operation, is subjected to systematic revision in the subsequent publications.

At the present time the IIW-ANB status belongs to the institutes and welding organizations in the following countries (in alphabetical order): Australia, Austria, Belgium, Brazil. Bulgaria, Canada, Croatia, Czech Republic, Denmark, Finland, France, Germany, Hungary, India, Indonesia, Iran, Italy, Japan, Nigeria, Norway, China, Poland, Portugal, Republic of Korea, Romania, Russia, Serbia, Singapore, Slovakia, Slovenia, South Africa, Spain, Sweden, Switzerland, Thailand, The Netherlands, Turkey, Ukraine and the United Kingdom.

The International and European system of harmonized training, qualification and certification of personnel includes the following levels.

The personnel responsible for supervision of welding:

- International/European Welding Engineer;
- International/European Welding Technologist;
- International/European Welding Specialist;
- International/European Welding Practicioner.

The rest of the personnel:

- International/European Welder;
- International/European Welding Inspection Personnel: C — comprehensive, S — standard, and B — basic.

The knowledge and diplomas received in the framework of harmonized training system allow finding a job in the open labor market in all the countries of the world. The availability of comprehensively trained welding personnel with the appropriate documents confirming the special knowledge has a fundamental importance in the countries involved into production of steel structures in a large volume. To these countries Poland also belongs, which currently occupies the second place in Europe (after Germany) in the field of production of steel welded structures. In Poland more than a half of steel rolled products is produced, which are then processed into welded structures and products. In total, Poland produces more than 1 million tons of welded structures, about half of which is exported.

As was mentioned above, in Poland the supervision of system of the international harmonized training in the field of welding is carried out by ANB, which is the Institute of Welding in Gliwice, more exactly the Center for Certification Authority founded by the Institute. The training is conducted in the ATBs, approved by ANB. The first ATB in Poland was the Center for welding training and supervision of the Institute of Welding. The Center has the authority to conduct education at all the levels starting from welding engineers, and finishing with welders.

In the boldest forecasts it was not supposed that, since 1997 the activities in the field of education and training of welding personnel would be demanded in such a large volume and carried out for such a wide range of the concerned persons. Due to a growing number of comers, the Institute invited the Polish higher education institutions to cooperation, where education of welding specialties was carried out. Based on the formal agreements between the directors of these institutions and the director of the Institute the ATB status in the field of training the engineers of welding (IWE/EWE) was received by the following institutions:

- Wroclaw University of Technology, Mechanical Faculty; Institute of machine technologies and automation, Welding department;
- Gdansk University of Technology, Mechanical Faculty, Chair of materials technology for machines and welding production;
- West Pomeranian University of Technology in Szczecin, Faculty of mechanical engineering and mechatronics, Welding department;
- Czestochowa University of Technology, Faculty of mechanical engineering and informatics, Welding department;
- University of Technology and Humanities in Bydgoszcz, Faculty of mechanical engineering;
- Warsaw University of Technology, Faculty of production engineering;
- Cracow University of Technology, Mechanical Faculty, Institute of materials engineering

At the same time, several ATB were established for training welders and mid-level personnel in welding at different education centers throughout the whole country.

In total, the number of international diplomas issued in 1999–2014 amounted to 3558, of which IWE — 2080; IWT — 247; IWP — 197; IWS — 524; IW — 31; IWIP — 479 pcs.

The number of European diplomas issued in 1997–2014 amounted to 1620, of which EWE — 1120; EWT — 179; EWP — 158; EWS — 72; EW — 91 pcs.

Center for welding training and supervision. The Center for welding training and supervision acting at the Institute of Welding for over 25 years, was created after 1990 first of all to conduct the harmonized European education. However, the beginning of the Center activities was initiated much earlier and coincided with the moment of the Institute foundation, when the State Welding Institute established by the existing government in 1945 received the only but very urgent task of training gas and electric welders, who at that time were very much needed for restoration of Poland, seriously damaged as a result of combat actions during the Second World War.

The European education had to be carried out at the corresponding level. In this regard, the Center was projected and organized on a large scale and using the significant funds at the huge efforts of many staff members of the Institute. The rooms of the Center look attractively, and its rich technical facilities are closely connected with the equipment of the whole Institute. Due to that the Center fully meets all the theoretical and practical requirements specified for the modern welding education at the highest level.

The Center for welding training and supervision is an integral organizational link of the Institute and is directly subordinated to the Director of the

Institute. It acts on the basis of the general charter, organizational statute of the Institute and the own Charter. The activities of the Center are controlled by the Scientific Council of the Institute. The Institute is included into the lists of non-public institutions of continuing education and to the Register of educational establishments.

The Center for the first time received the authorization and status of the Polish ATB in 1996, and the validity of authorization is systematically prolonged.

The main activity of the Center is continuous education of personnel for welding production. At the Center the special training of welding personnel is organized and conducted at all the levels in accordance with the IIW and EWF programs: I/EWE, I/EWT, I/EWS, I/EWP and I/EWIP. While conducting the IWE (EWE) courses the Center uses ATB assistance at the Polish higher technical institutions conducting education, which follows from the content of the programs in the parts I, II and III. The final phase of the last part covering the laboratory studies and demonstrations of modern welding equipment is held at the Center and at the territory of the whole Institute.

The other forms of activities of the Centre in the field of education and training of the personnel is the maintenance and control of the Polish system of training of welders at the local training centers throughout the whole country, the courses in the field of non-destructive testing methods and special courses.

Maintenance and control of the Polish system of training welders at the local education centers. The Institute of Welding was involved in training welders during the first several years of its activity. Then, training of welders was mastered by numerous training centers scattered throughout the country. The quality of this training was different, there was no method for helping the weaker centers, neither a unified system of issuing documents and introduction of new principles for training welders in accordance with the requirements worked out by the European standards applied in other countries. In order to help training centers and, at the same time, to ensure the appropriate level of training welders in Poland, the Institute decided to conduct the following works:

- objective supervision of training welders all over Poland (education is conducted in accordance with the national programs);
- certification of Polish centers for training welders (in Poland there are more than 400 of such centers);
- checking of examiners conducting examinations on the basis of authority granted by the Institute of Welding (in Poland there are about 160 of such of examiners);
- issuing documents to welders on the basis of the examination protocols sent to the Institute;
- welder's qualification examination certificate according to PN-EN 287-1 or PN-EN ISO 9606 in English or German version for graduates of courses in fillet welding or welding of sheet steel and pipes;
- welder's qualification examination certificate in fillet welding or welding of sheet steel and pipes in the welded structures of the 1st, 2nd and 3rd class according to PN-M-69008, manufactured from sheet steel or pipes;
- welder's certificate.

The number of documents issued in the period from 2004 to 2014 is given in the Table. The system of supervision has proved itself also today. After several decades of improvement nobody claims against the rationality of its implementation.

Courses in non-destructive testing methods. Since 2002, the Center for welding training and supervision provides training of personnel in NDT methods. The courses are conducted at the Institute (at the special laboratories, equipped with the advanced equipment for all the testing methods) and outside it (if the customer expresses such a desire) on the basis of the own programs developed on the basis of international requirements. The examination, attestation and certification of students is conducted by the Centre for Certification of the Institute in accordance with the requirements of standard PN-EN ISO 9712:2012 (until 31.12.2012 it was standard PN-EN 473:2008) «Non-destructive testing — Aattestation and certification of NDT personnel». The graduates of the courses receive the certificates of competence and the certificates of specialists in NDT.

The courses are conducted in the following NDT methods: visual testing (VT), penetrants testing (capillary) (PT), ultrasonic testing (UT), magnetic particles testing (MT), X-ray testing/radiographic evaluation of welds (RT2 ORS) and radiographic testing/technique of performing X-ray photos/RT evaluation. Three levels of NDT personnel certification are applied. In case of the 3rd level the course covers the Basic part and the basic method.

Documents issued in the period of 2004–2014

Type of document	2004	2005	2006	2007	2008	2009	2010	2011	2012	2013	2014
Welder's qualification examination certificate	20,566	22,487	34,576	42,423	43,789	46,199	44,454	42,499	45,075	52,884	52,592
Welder's certificate	8740	10,580	15,474	21,524	17,604	14,736	13,918	13,662	17,378	18,234	18,390

The graduates of the courses RT2 ORS may gain admission to carrying out control in the industrial sector for manufacture of welded products (w), products subjected to plastic processing, except for forgings (wp) and pipes of different diameters and wall thickness (t).

Graduates of PT MT, UT and RT courses may gain admission to carrying out testing in the industrial sector on manufacture and the sector on testing before manufacture and in-process testing together with manufacture of welded products (w), castings (c), forgings (f), products subjected to plastic processing except of forgings pieces (wp), and pipes of different diameters and wall thickness (t).

The courses in NDT methods are of great concern at the Polish market, which is evidenced by the statistics on the number of participants of these courses.

A number of persons, who passed training at the courses, in 2004 was 727; 2005 — 708; 2006 — 729; 2007 — 864; 2008 — 960; 2009 — 849; 2010 — 982; 2011 — 916; 2012 — 938; 2013 —927; 2014— 1220.

Considering the numerous, often very specific requirements in the field of NDT, the Institute of Welding began cooperation with the transport technical inspection (TDT) in Warsaw, the result of which was the development of courses in NDT in the field of railway transport at the industrial sector «Maintenance of railway transport». At the Institute the specialized laboratory was founded equipped with the elements of rail cars, which in practice are subjected to NDT, as well as equipment allowing carrying out the appropriate testing method. The education is carried out according to the methods of UT, PT and MT in accordance with the requirements of standard PN-EN ISO 9712:2012 (previously PN-EN 473:2008). Education is completed with examination, conducted by TDT. The certificates of NDT personnel are issued by the certifying body, which is TDT-CERT.

Special courses. A special group of preparatory and educational courses carried out at the Institute of Welding is the special courses, including:

- course of European welder of synthetic materials (course is organized by the EWF program, examination — in accordance with PN-EN 13067 standard);
- course of welder of pipelines of synthetic materials (course is organized by the program IS, examination — in accordance with PN-EN 13067 standard);
- course for the personnel on supervision in the manufacture of pipelines of synthetic materials for water and gas supply (course is organized by the program IS, examination — in accordance with PN-EN 13067 standard).

In case of passing the examination with a positive result, the graduates will receive a certificate of competence CEPW.

For joining the modern materials and producing the critical structures the adhesion bonding is increasingly used. The Institute of Welding in cooperation with the Fraunhofer Institute in Bremen organized the courses of adhesion bonding: the European adhesion bonding technician and the European specialist in adhesion bonding (in accordance with the EWF recommendations EWF 515 and EWF 516. The course is completed with passing the written and oral exams and practical exam. After finishing the course the participants receive the European certificate. The course includes joining of metal, glass, elastomers, plastomers and synthetic materials reinforced with fibers.

In addition, at the Institute of Welding the training in the field of macroscopic and microscopic metallographic examinations of structural materials and their welded joints is carried out at three levels:

- basic — preparation of specimens for macro- and microscopic metallographic examinations;
- standard — inspection module, i.e. evaluation of quality of welded joints on the basis of the approved evaluation criteria; and
- comprehensive level.

After passing the exam with a positive result, the graduates receive the document for basic standard/comprehensive level (Record of Achievement) by the EWF, recognized in all the countries of the European Union.

Computer system for servicing the welding personnel. The activity of the Institute of Welding in the field of training and education of welding personnel requires a systematic and very clear documentation of all the actions related to this activity, both directly at the Institute (at the Centre for welding training and supervision and at the Certification Center), and in all the external education centers cooperating with the Institute. Before 2007 the documentation proceeded in the traditional way, i.e. with the participation of staff members of the Institute filling the documents manually. When the amount of incoming documents increased so dramatically that the traditional bureaucratic methods were unable to process them and it was impossible to meet the growing demands to the quality of servicing and the terms of performing the tasks, the Institute took a decision on using the modern information methods and systems.

Planning the development of the modern Institute of Welding, already in 1995 the Informatics Department was established in the organizational structure, which main objective was to create the appropriate information structure to perform three types of tasks: realization of current research and development works carried out by the Institute staff members (internal computer network), providing the development of international cooperation on a wide

scale (Internet) and the use of modern computer systems in the field of management and activity of the company (ERP — Enterprise Resource Planning, and CRM — Customer Relationship Management).

The revolutionary changes taking place at a rapid pace of the world information technologies has always found its reflection in the Institute. The first computer network was established in 1990 on the basis of already nonexistent standard ArcNet. The administrative and management programs covering finances, personnel and accounting (FK network) were introduced. The network was launched operating in the Novell environment. Over the time at the Institute the new computer devices and the modern, more complex computer programs appeared. The old technology was replaced by a new one of the Ethernet type. In connection with the requirements to security and privacy of data the FK network is autonomous. At the Institute the network equipment as well as servers and their operation system were gradually changed.

At the present time, in accordance with the international trends, at the Institute the solutions are used, the purpose of which is to provide the highest level of security and high availability, i.e. the servers are running in a cluster, they are controlled by the programs for virtualization and the data are accumulated in the redundant disc matrices. At the input of the local computer network, interconnecting about 150 devices with the port for connection to the Ethernet (servers, workstations, specialized research equipment and welding equipment operating in the network of control and monitoring), the network equipment of the highest quality is installed, which performs the Firewall, AntiVirus, Deep Inspection, WebFiltering and AntiSpam functions. All the active network devices are fully controllable, cooperate with the monitoring software and operate in the Ethernet standard 1 Gbit/s. The main framework of the network is produced using the multifiber, multimode lightguide using link aggregation.

In creation of the computer infrastructure at the Institute the Informatics Department staff members are involved. The applied information solutions were implemented without changes (software virtualization and control of the computer network), or subjected to modification in order to meet the specific aspects of the Institute activities (EPR and CRM systems). Such modification occurred in the case of informatization of the system of training the welding personnel.

The experience gained during the several decades allowed creating the computer system in Poland for servicing the welding personnel (KSOP), covering the territory of the whole country. The main objective of KSOP was its versatility and eliminating the need in installing any software on the user's computer (some institutions and systems do not permit the user's interaction to the existing software). In KSOP system the Internet technology was used, due to which the access to the system is provided by the search system at any time of the day and from any place on the Earth.

KSOP, servicing the welding personnel, comprises training, examination and certification:

- of welders at the authorized education centers;
- and supervision of the certificate of NDT personnel;
- and also supervision of the certificate according to the international requirements of IIW/EWF for all the levels realized today (IWE, IWT, IWS, IWP, IWIP, IW, EPW), and after the special EWF courses at the authorized ATB Centers (in the startup process).

The development and introduction of KSOP were facilitated by two information projects that were implemented at the Informatics Department of the Institute:

- *«The system of information and communication in the field of education of welding and NDT personnel as the element of competitiveness growth among the enterprises in the field of welding production»*, the realization of which took place from 2006 to 2008, was co-financed from the European Social Fund within the framework of the Integrated Operational Program of regional development, Action 2.6: «Regional innovation strategies and knowledge transfer», and Priority 2: «Strengthening the human resources development in the regions».

Within the frames of this project the following databases were created: the EU Directives, harmonized standards, guidelines and standards for products in the part concerning education and certification of welding and NDT personnel; institutions and forms of education in the field of training welding and NDT personnel in compliance with the European and international requirements. The system of preparation and delivery of urgent news «Newsletter» was also prepared. At present, in the system more than 400 companies and nearly 800 individual users are registered, and there is also the site in the Internet, the content of which is oriented to support the education and training of welding personnel in the broadest sense of the word. The constantly updated content of databases and the volume of knowledge provided on the website meet the constant relentless interest. In 2007–2015 the site was visited by about 25000 people;

- In the frames of the second project PO1G.02.03.00-00-003/10 *«Information welding platform of knowledge and research potential at the simultaneous expanding of the information structure of the Institute of Welding»*, the realization of which took place from 2011 to 2013, the server cluster was mounted and launched, the main task of which is to provide the reliability and productivity of the system of providing databases to the academic environment

created within the frames of the project: research works and technological solutions, technological needs of enterprises, research of potential academic institutions, structural materials, fatigue tests, issues related to environmental engineering in welding, and issues concerning education and training of welding and NDT personnel.

The process of integration of KSOP with the knowledge bases for academic environment resulted in creation of Information Platform of the Institute of Welding (IPS). IPS is subjected to continuous expanding, the next new modules are launched, the best example is the advisory system i-EkoSpawanie developed in 2015, which will be available for users at the beginning of 2016. The system i-EkoSpawanie is designed for welding technologists, employers, employees, departments of labor safety and designers of ventilation systems. This system allows optimizing the welding process in order to reduce the risks associated with evolution of dust and welding fume to minimum. System databases contain characteristics of welding processes and welding consumables from the point of view of the type and amount of evolved harmful substances.

From the very beginning of IPS creation the possibility was suggested to use it also by the users outside the Poland. For this purpose in the system the multi-lingual dictionaries (Polish-English-German and any two additional languages) are used.

Due to launching the on-line access of the education centers to KSOP, the period of time between drawing up the examination protocols and receiving the documents confirming the qualification was significantly reduced (even to one week). Thus, the inconvenience connected with errors, which significantly prolong the period of documents transfer to the interested persons, was largely eliminated. The education centers using KSOP have the opportunity to view all the qualifications, courses and students (however only and exclusively registered at the Center). The system can also help in controlling the qualifications, allows preparation of different types of reports, for example, on welding methods, validity terms, etc. The fact of reducing the costs associated with regular sending of documents by post or by courier service is also essential, which occurs in the case of centers not connected to the system.

KSOP is used by more than 400 centers for training welders, of which 103 — are on-line users. All the courses of NDT personnel end in issuing documents due to the existence of KSOP, which, moreover, allows also conducting the full supervision of certificates. Starting from 2013 the system is used by seven higher educational institutions: in Gdansk, Wroclaw, Szczecin, Czestochowa, Bydgoszcz, Warsaw and Krakow. In the system 291 users are registered (as to the end of October, 2015), which carry out serving of courses, attestation, certification and supervision of admission action. KSOP is introduced gradually in the next education centers. So far (as to the end of October, 2015) on the KSOP base 380,206 documents were accumulated for the qualifications issued to 204,210 students on the basis of 112,625 examination protocols. Each year the database is enlarged with the several tens of thousands of records.

Conclusions

Over the past 25 years in Poland a huge step forward was made in the field of training personnel for welding production, satisfying all the requirements for quantity and quality both inside the country as well as in the framework of international cooperation.

Poland (Institute of Welding) cooperates with EWF since 1992; in 1996 the Certification Center of the Institute received the status of ANB-EWF, in 1997 the Institute became a full member of EWF.

Poland (Institute of Welding) cooperates with IIW since 1958 (in the field of training personnel since 1998) and is a full member of IIW; in 1998 the Certification Center of the Institute received the ANB-IIW status.

The Center for welding training and supervision of the Institute of Welding is the first, the largest and the most active ATB in Poland (conducts education on the IWE/EWE, IWT, IWS and IWP programs).

In Poland, except of ATB at the Institute of Welding, seven ATB are functioning at the higher education institutions (conduct education on the IWE/EWE program) and two ATB at the Centers for education (conduct training on the IWS and IWP programs), which received the authorities from the Institute of Welding.

In all the ATB in Poland in the period from 1996 to 2014 more than 5,000 of welding personnel passed the education.

At the several hundred education centers, which are under supervision of the Institute of Welding, tens of thousands of welders were trained, mainly in accordance with national programs (however, the documents received by welders are recognized abroad).

The system of harmonized, European and international training, attestation and certification of personnel on welding supervision, as well as national and international system of training welders are the necessary conditions for realization of international cooperation in the field of manufacture of welded structures and products.

1. *www*.is.gliwice.pl
2. *www*.ewf.be
3. *www*.iiwelding.org

Received 17.12.2015

doi.org/10.15407/tpwj2016.02.06

MODERN COMPOSITE MATERIALS FOR SWITCHING AND WELDING EQUIPMENT
Information 2. Application of high-rate vacuum evaporation methods for manufacturing electric contacts and electrodes

N.I. GRECHANYUK[1], **V.G. GRECHANYUK**[2], **E.V. KHOMENKO**[1], **I.N. GRECHANYUK**[1] and **V.G. ZATOVSKY**[1]
[1]I.M. Frantsevich Institute of Problems of Materials Science, NASU
3 Krzhizhanovsky Str., 03680, Kiev, Ukraine. E-mail: homhelen@mail.ru
[2]Kiev National University of Construction and Architecture
31 Vozdukhoflotsky Ave., 03037, Kiev, Ukraine. E-mail: knuba@knuba.edu.ua

The paper presents the method of electron beam vacuum evaporation and condensation for the most promising technologies of manufacturing modern composite materials, used in welding and switching equipment. This method currently is one of the components of the technological process of producing thin (up to 5 μm) films for radio engineering, microelectronics, computer engineering, etc., as well as thick (more than 5 μm) films-condensates widely applied as effective protective and wear-resistant coatings. Described are the results of scientific and production activity on introduction into industry of technologies of deposition of thick films based on copper and refractory metals (molybdenum, tungsten, chromium) with additives of REM and other metals (yttrium, zirconium) on the surface of electric contacts and electrodes. Proceeding from the results of trials performed in more than 54 enterprises of Ukraine, Russia, Georgia, Rumania, Poland and PRC it was established that the developed materials are not inferior to silver-containing powder compositions in terms of serviceability, while being approximately 3 times less expensive than the latter. 57 Ref., 1 Table, 4 Figures.

Keywords: *composite materials, copper and refractory metals, welding and switching engineering, electron beam evaporation, condensate films, serviceability*

Development of physico-chemical fundamentals of creating new materials is the objective need of engineering and social advance of society. Without it, it is impossible to make significant progress in any of the important fields of science and technology. Based on estimates of US experts, in the next 20 years 90 % of modern materials will be replaced by fundamentally new ones that will lead to technological revolution in practically all the industrial sectors [1, 2]. One of progressive directions of development of principally new materials with preset properties is high-rate EB evaporation and condensation of metallic and non-metallic materials in vacuum. Evaporation and subsequent condensation of materials in vacuum is a relatively new direction in materials science [3].

At present, none of the engineering fields related to material producing and processing can do without the EB technology. This is accounted for by the highest efficiency of the electron beam, compared to other known concentrated energy flows (laser, plasma). The electron beam has the highest coefficient of energy absorption. Ranges of power and energy concentration in the beam are significant (electron beam power of 1 MW and more). In this connection, material heating up to specified melting and evaporation temperatures occurs at very high rates [4].

EB evaporation and condensation in vacuum are one of the components of the technological process of producing thin (up to 5 μm) films for radio engineering, microelectronics, computer engineering, etc. [5], as well as thick (more than 5 μm) films, applied as effective protective and wear-resistant coatings [6–10].

A promising avenue is development of multicomponent coatings designed for increasing erosion resistance of electric contacts of switching devices. Scientific and production experience gained at development of coatings from copper-based alloys alloyed with tin, chromium, aluminium, nickel and titanium is generalized in monograph [11].

Applicability of high-strength films of Cu–$0.5Al_2O_3$ system (here and furtheron — wt.%) as coatings for electrical engineering products is noted in [12]. It is established that vacuum-deposited coatings are greatly superior to the respective electroplated ones by the level of wear resistance and, particularly, temperature stability.

Despite the obvious advantages, vacuum coatings are not always economically justified, as the coeffi-

cient of vapour utilization usually does not exceed 10–15 %. At the same time, the differences in component vapour pressure lead to insurmountable difficulties at evaporation from one source of copper- or silver-based materials with additives of refractory metals (tungsten, molybdenum, tantalum, niobium, zirconium) in a particular proportion, corresponding to the composition of modern electric contact materials.

It is known that powder metallurgy methods are the traditional ones for manufacturing composite materials (CM) for electric contacts. Technological features of producing materials for electric contacts, their service characteristics and applications are described in [13–20]. The latest achievements in this field of materials science are generalized in [21].

Despite a wide selection of materials for switching and welding engineering, the problem of development of highly reliable CM still has not been fully solved, as the requirements made of contact material, depend on the type of switching device and change with its upgrading and replacement by new equipment. Similar requirements are in place also for CM applied in welding engineering. These requirements can be met by materials, characterized by optimized structure and respective set of properties, providing formation of «secondary structure» with increased electroerosion resistance, service life and reliability in the working layer.

The structural factor has a decisive influence on service properties of materials of electric contacts and electrodes. Increase of CM dispersity in Ag–Me, Ag–MeO system promotes lowering of plasma flow intensity, and increase of electroerosion resistance of contacts and electrodes from these materials [22].

Evaporation and condensation processes allow engineering materials on atomic-molecular level and, as a result, precisely controlling their dispersity. In this connection, application of high-rate EB evaporation and subsequent condensation of metals in vacuum to produce bulk condensed CM for electric contacts and electrodes is of considerable scientific and practical interest. Condensed from the vapour phase CM based on pure metals and their alloys, oxides, carbides, borides, CM which are of dispersion-strengthened, microlaminate and microporous types of 0.1 to 2.0 mm thickness, have been studied since 1970s at PWI [23], Royal Aviation Research Institute of UK Ministry of Defense [24], and a number of other research laboratories [25]. Results of these studies were generalized in [26, 27]. Until recently, however, there has been no information about industrial production of such materials as individual structural elements of assemblies, instruments and mechanisms.

Of greatest interest is development and wide introduction into different engineering sectors of CM condensed from the vapour phase for contacts and electrodes, not containing any noble metals. It should be noted that materials, produced by powder metallurgy methods without noble metals, are widely accepted in manufacture of electrodes and contacts of switching devices. Powder CM for these contacts and electrodes contain 20 to 80 % of the refractory component (as a rule, these are tungsten, molybdenum and chromium), while copper is the low-melting component. Nickel and cobalt can be the technological additives, and some oxides, boron and other elements can be the functional additives. Powder CM with 50 and 70 % content of refractory phase are mainly used in industry [15, 28].

At application of contacts and electrodes from CM of W–Cu system the oxidation products most often are WO_3 and Cu_2O_3 oxides [16, 29]. Their specific electric resistance varies in rather broad ranges: for WO_3 from 1 (at strong deviation) to $1 \cdot 10^{12}$ Ohm/cm (at stoichiometric composition), for Cu_2O — from 10^3 to 10^{10} Ohm/cm.

At current switching in air, such processes are observed also in the working layer of contacts from Mo–Cu pseudoalloys. Molybdenum and copper are mutually partially soluble [30], while their oxides interact and form resistant compounds ($CuMoO_4$, $Cu_3Mo_2O_9$) [31, 32]. At temperature above 700 °C, a low-meting eutectic forms in MoO_3–Cu_2O system. It is found that the oxide film, having the composition of eutectic of this system, spreads easily over the contact surface, filling its unevenness [31, 32]. The film has weak adhesion to the base and its delamination from the contact surface after solidification promotes the «self-cleaning» effect and lowering of the level of the contact pair transient resistance [28].

When solving the problem of producing from the vapour phase the composites for electric contacts and electrodes, a number of scientific and applied studies on development CM based on copper, molybdenum, tungsten and chromium were performed, which included:

- selection of alloying elements and development of the processes of their addition to the copper matrix to produce two- and multicomponent CM based on copper with improved physico-chemical, mechanical and corrosion characteristics;
- investigation of the influence of interphase interaction in copper–refractory component system, material, temperature and substrate roughness on CM structure and properties;
- analysis of variation of CM structure and properties, depending on chemical composition of initial (evaporated) components and their deposition rate, substantiation of separating layer material selection;
- studying the influence of alloying phases on increase of copper evaporation rate and determination of optimum composition of alloying additives;
- conducting integrated studies of the structure, physico-chemical and mechanical properties of grad-

Composition and physico-mechanical properties of Cu–Zr–Y–Mo CM

Material	Chemical composition, wt.%	Density, g/cm^3	Specific electric resistance, μOhm·m	Hardness *HV*, MPa	Mechanical properties			
					Before annealing		After annealing in vacuum (900 °C, 1 h)	
					σ_t, MPa	δ ,%	σ_t, MPa	δ ,%
DSMC-1	Cu–(0.05–0.1)(Zr, Y)–(3–5)Mo	8.9–9.0	0.021–0.022	1000–1500	300–430	10.3–7.3	295–420	17.6–9.3
DSMC-2	Cu–(0.05–0.1)(Zr, Y)–(5.1–8)Mo	9–9.05	0.022–0.024	1500–1650	440–630	7.25–3.40	425–600	9.45–4.90
DSMC-3	Cu–(0.05–0.1)Zr, Y)–(8.1–12)Mo	9.05–9.1	0.024–0.028	1650–1800	635–785	3.25–1.80	605–730	4.85–3.90

ed two- and multicomponent Cu-based CM produced on stationary and on rotating substrates;

• conducting integrated corrosion studies of CM and determination of mechanisms of corrosion processes running;

• issuing recommendations on corrosion-resistant Cu-based CM, condensed from the vapour phase, development of commercial equipment and their manufacturing technologies.

Main results of conducted fundamental, scientific and applied research are set forth in [33–35] and are generalized in [36]. Results of performance of the above-mentioned work can be described as follows. Physico-chemical principles of designing Cu-based CM condensed from the vapour phase were defined, which enabled transition from laboratory studies to their broad industrial application. Integrated studies of the structure, physico-chemical, mechanical and service properties of Cu–Mo, Cu–W, Cu–Cr, (CuZrY)–Mo CM in the range of up to 50 % concentrations of refractory components were performed; comprehensive studies of corrosion resistance of two- and multicomponent CM were conducted and their corrosion resistance points were calculated; formation of oversaturated solid solutions on submicron level in Cu–W, Cu–Mo, Cu–Cr CM was established, that leads to laminated structure formation as a result of their decomposition. It was proposed for the first time to alloy the copper matrix with zirconium and yttrium with their total content of up to 0.1 % in CM, by copper evaporation from Cu–Zr–Y alloy through intermediate pool, that provided simultaneous increase of CM corrosion resistance and copper evaporation rate 2 to 3 times, and it was experimentally shown that Cu–0.1(Zr, Y)–(8–12)Mo and Cu–0.1(Zr, Y)–(0.3–0.34)Cr–(8–12) Mo CM condensed from the vapour phase are bulk nanocrystalline systems.

Cu–Z–Y–Mo CM condensed from the vapour phase. Cu–Zr–Y–Mo systems have become the most widely applied [33, 36, 37].

The Table gives chemical composition and main physico-chemical properties of the above materials.

New composites, called dispersion-strengthened materials for electric contacts (DSMC), are certified in keeping with Ukrainian standards [38, 39]. Chemical composition and technology of their manufacturing are protected by patents of Ukraine and Russian Federation [40–42].

Cu-, Mo- and W-based CM, condensed from the vapour phase, are characterized by a laminated structure with layer hierarchy on macro-, micro- and submicron levels (Figure 1).

Lamination is weakly pronounced at small concentration of molybdenum (up to 7–8 %) and tungsten (up to 4 %). With increase of refractory component content, the image contrast is enhanced that points to their greater lamination due to various factors. Presence of lamination on the macrolevel is due, most probably, to development of electric microbreakdowns, arising at high-rate evaporation of initial commercially pure components (rate of copper deposition on a rotating steel substrate of 1000 mm diameter reaches 60–70 μm/min, that of molybdenum — 6–8 μm/min). Lamination on the microlevel is due to impurities,

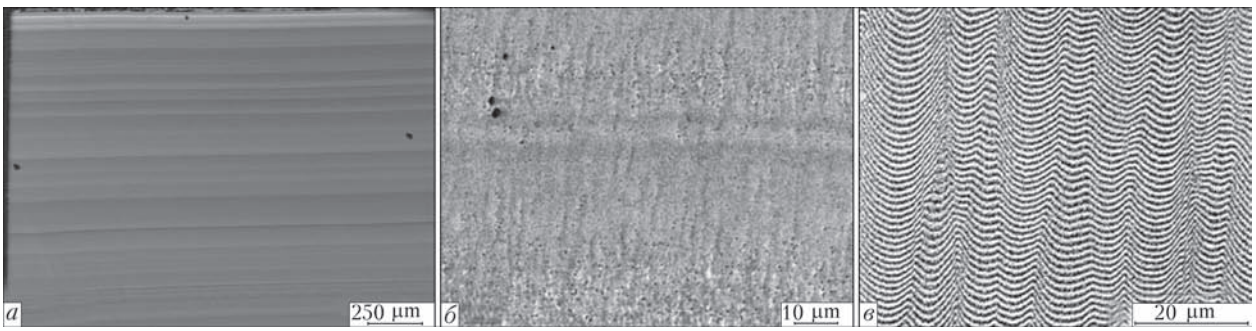

Figure 1. Laminated structure of Cu- and Mo-based CM on macro- (*a*), micro- (*b*) and submicron (*c*) level

present in the initial (evaporation) materials. Layer formation at submicron level is associated with formation of oversaturated solid solutions, which, while decomposing, form the respective microlayers [36]. Switching testing showed that in such a graded laminated nanomaterial changes of layer chemical composition essentially limit the zone of discharge thermal impact. In a number of types of switching devices and instruments, smaller changes of working layer of contacts and electrodes and increase of erosion resistance are observed, compared to analogs produced by powder metallurgy.

The most effective fields of DSMC application are city transport (contacts, used in city trams, trolleybuses, metro trains; intercity electric transport, diesel locomotives, electric trains; lift facilities (passenger and cargo lifts); port, ship cranes and other hoisting mechanisms; electric trolleys of all types; mining equipment; industrial and household electric appliances, containing relays, starters, contactors, knife switches, etc.).

General view of breaking contacts, made with application of DSMC, is shown in Figure 2.

DSMC-3 have become applied by industry as electrodes for welding brass strip to copper wire in capacitor spot welding machines of TKM 15 and TKM 17 type. Results of electrode testing in «Shostka Kazenny Zavod «Impuls» enterprise are given below.

Actual operating life of electrodes made from DSMC-3 (scheduled life of 100000 cycles) is as follows:

- 1 (upper electrode in TKM 15) — 105,000;
- 2 (lower electrode in TKM 15) — 120,000;
- 3 (upper electrode in TKM 17) — 110,000;
- 4 (lower electrode in TKM 15) — 125,000.

Electrodes manufactured from DSMC-3 meet all the requirements made of electrodes used in capacitor spot welding machines of TMK 15 and TKM 17 type.

A fundamentally new application of DSMC-3 was their use as electrodes for live tissue welding [43]. Manufacture of nozzles from these materials for supersonic electric arc spraying was mastered. Replacement of beryllium bronze by DSMC is promising. Unlike bronze, CM of DSMC grade do not lose their strength right up to heating temperature of 900 °C. Above-mentioned CM can also be used as spring alloys with high electric conductivity, alloys resistant to radiation swelling, and as coatings for mirrors in power metal optics [36].

Composite materials condensed from the vapour phase. *Cu–Cr–Zr–Y–Mo CM*. Cu–(0.2–0.41)Cr–(0.05–0.1)(Zr, Y)–(8–12)Mo CM (MDK3Kh grade) are an optimized variant of DSMC-3. It was experimentally confirmed that Cu–(0.05–0.1)(Zr, Y)–(8–12)Mo CM are bulk nanocrystalline materials with average grain dimensions of 80 nm for copper and 10 nm for molybdenum. Owing to additional alloying with chromium, MDK3Kh feature 1.5 to 2 times higher corrosion resistance,

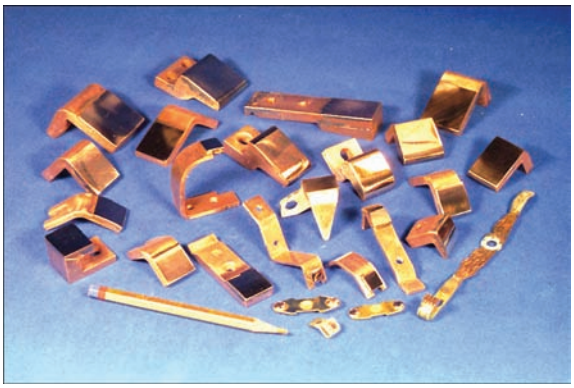

Figure 2. General view of typical breaking contacts made with application of DSMC

compared to DSMC-3 with preservation of the level of physico-mechanical properties of the latter [44]. They are, mainly, used for manufacturing breaking contacts of mining equipment, where humidity reaches more than 80 % and CO_2 and SO_3 aggressive gases are present, in particular, in Smolinskaya and Ingulskaya uranium mines (Ukraine).

Cu–Zr–Y–C CM. Cu–(0.05–0.1)(Zr, Y)–(0.3–0.6) C CM (MDK3S grade) are used on industrial scale for manufacturing sliding contacts [45, 46]. Pantographs from these materials (Figure 3) have become applied in locomotives, pulling trolleys with copper ore at Copper-Ore Works (Lublin, Poland).

Cu–(0.05–0.1)(Zr, Y)–W CM. Structure, physico-chemical, mechanical and service properties of composites with up to 50 % W content are described in detail in [47–50]. Cu- and W-based composite materials are traditionally used as high-current electric contacts in oil circuit-breakers. Recently they are also becoming applied in some types of vacuum devices. In particular, Cu–(0.05–0.1)(Zr, Y)–(32–36)W CM, condensed from the vapour phase, have become applied in industry for manufacturing contacts of oil circuit-breakers of RNO and RNT-17 type. The above materials have successfully passed pilot industrial testing in vacuum arc chutes MVK-440, used, mainly, in coal mines [51].

Cu–(0.05–0.1)(Zr, Y)–Cr CM. Influence of technological factors on the structure and mechanical properties of Cu–Zr–Y–Cr CM condensed from the vapour phase with up to 60 % Cr content is described in [52]. Cu–Cr CM with 35–50 % Cr are widely applied for manufacturing contacts of vacuum arc chutes.

Possibility of applying condensed CM of this system is due to the features of chemical composition and morphology of «secondary» structure formed on contact working surface. Under non-equilibrium conditions of the arc discharge, mutual solubility of copper and chromium in the working layer rises, and solid solution decomposition with dispersed structure formation takes place. Cu–Zr–Y–Cr condensates at this chromium content have a laminated structure on

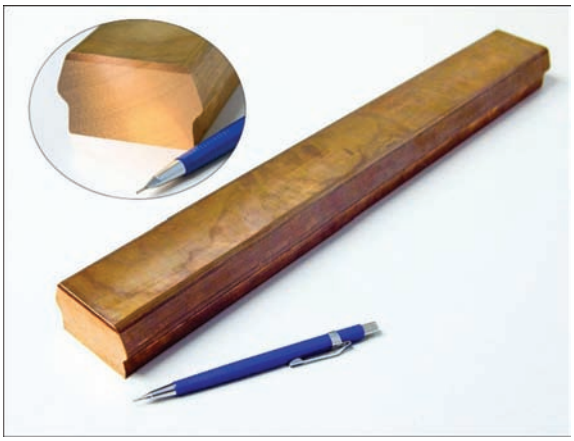

Figure 3. General view of sliding contacts made from MDK3S material

macro-, micro- and submicrolevels. Lamination of the latter two levels is attributable to anisotropy of normal grain growth, promoting formation of «columnar» structure within several layers of the condensate, in which a structure with polygonal grain shape (Figure 4, *a*) and indications of solid solution delamination (Figure 4, *b*) forms in the section of the layer, normal to the columns, under the impact of temperature and time.

Change of Vickers hardness, depending on chromium content, is of a linear nature; in the concentrational range of 35–50 % Cr, hardness varies in the range of 2069 to 2503 MPa. At tensile testing, ultimate strength rises to 550 MPa, the CM, however, has zero ductility. Cu–Zr–Y–Cr CM are becoming accepted for manufacturing arc chute contacts [53, 54].

CM condensed from the vapour phase feature several advantages: they are produced in one process cycle, they are less expensive than their analogs produced by powder metallurgy methods (1.5 to 1.7 times) and essentially (4 times) less expensive than the materials of silver-containing contacts. In terms of their serviceability, condensed CM are not inferior to materials based on silver-containing compositions. They are readily treatable by cutting, grinding, drilling; are easily soldered by any of the known soldering processes, with application of standard silver-containing and non-silver solders. Industrial certified EB equipment has been developed for manufacturing CM condensed from the vapour phase [55, 56], which allows manufacturing up to 12 tons per year of composites of various composition. During the period of 1995 to 2015, more than 15 tons of CM have been manufactured, from which about 1.6 mln contacts and electrodes of 386 typesizes have been produced [57].

Conclusions

Industrial EB equipment has been developed for producing copper-, molybdenum-, tungsten- and chromium-based CM, condensed from the vapour phase,

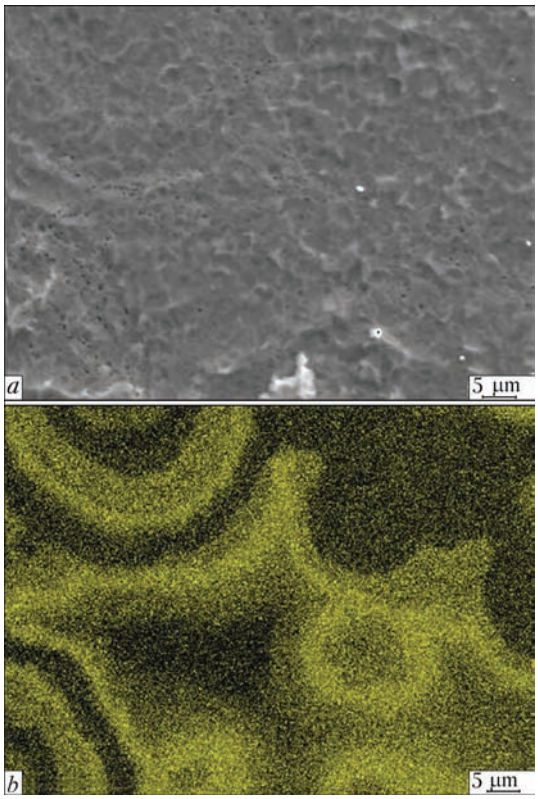

Figure 4. Microstructure of Cu–Zr–Y–Cr CM with 35–50 % Cr in secondary electrons (*a*) and in copper X-rays (*b*)

which are used in manufacture of electric contacts and electrodes.

Testing conducted in more than 54 enterprises of Ukraine, Russia, Georgia, Rumania, Poland and PRC showed that, in terms of serviceability, the developed materials are not inferior to silver-containing powder compositions, while being approximately 3 times less expensive than the latter.

1. (2002) *New materials*. Ed. by Yu.S. Korobasov. Moscow: MISIS.
2. (2008) *Materials science. Technology of structural materials*. Ed. by V.S. Cherednichenko. Moscow: Omego-L.
3. Bunshah, R.F. (1984) Vacuum evaporation — History. Recent developments and application. *Zeitschrift fuer Metallkunde*, 75(**11**), 840–846.
4. Zuev, I.V. (1998) *Treatment of materials by concentrated energy flows*. Moscow: MEI.
5. (1997) *Technology of thin films*: Refer. Book. Ed. by L. Majsell et al. Moscow: Sov. Radio.
6. Samsonov, G.V., Epik, A.P. (1973) *Refractory coatings*. Moscow: Metallurgiya.
7. Schiller, S., Heisig, U., Panzer, S. (1980) *Electron beam technology*. Moscow: Energiya.
8. Movchan, B.A., Malashenko, I.S. (1983) *Vacuum deposited heat-resistant coatings*. Kiev: Naukova Dumka.
9. (1984) *Improvement of surface quality and cladding of metals*: Refer. Book. Ed. by A. Knaunirs. Moscow: Metallurgiya.
10. Eliseev, Yu.S., Abramov, N.V., Krimov, V.V. (1999) *Chemical heat treatment and protective coatings in aircraft building*. Moscow: Vysshaya Shkola.
11. Kostorzhitsky, A.I., Lebedinsky, O.V. (1987) *Multicomponent vacuum coatings*. Moscow: Mashinostroenie.
12. Iliinsky, A.I. (1986) *Structure and strength of laminated and dispersion-strengthened films*. Moscow: Metallurgiya.
13. Frantsevich, I.N. (1980) Electric contacts made by powder metallurgy method. *Poroshk. Metallurgiya*, **8**, 36–47.

14. Rakhovsky, V.I., Levchenko, G.V., Teodorovich, O.K. (1966) *Interrupting contacts of electric apparatuses*. Moscow: Metallurgiya.
15. (1981) *Sintered materials for electrical engineering and electronics*: Refer. Book. Ed. by G.G. Gnesin. Moscow: Metallurgiya.
16. (1982) *Materials in instrument-making and automatics*: Refer. Book. Ed. by Yu.M. Pyatin. Moscow: Mashinostroenie.
17. (1985) *Composite materials*: Refer. Book. Ed. by D.M. Karpinos. Kiev: Naukova Dumka.
18. Tuchinsky, L.I. (1998) *Composite materials produced by impregnation method*. Moscow: Metallurgiya.
19. Minakova, R.V., Grekova, M.L., Kresanova, A.P. et al. (1995) Composite materials for contacts and electrodes. *Poroshk. Metallurgiya*, **7/8**, 32–52.
20. Slade, P.G. (2008) *The vacuum interrupter. Theory, design and application*. CRC Press.
21. Khomenko, E.V., Grechanyuk, N.I., Zatovsky, V.Z. (2015) Modern composite materials for switching and welding equipment. Inf. 1. Powdered composite materials. *The Paton Welding J*., **10**, 36–42.
22. Leis, P., Schuster, K.K. (1979) Der Einfluss des Kontaktmaterials auf die Austilgung von Plasmastrahlen. *Elektrik*, 33(**10**), 541–516, 559.
23. Movchan, B.A., Grechanyuk, N.I. (1988) New materials and coatings manufactured by electron beam technologies. In: *Proc. of Int. Conf. on EBT* (31 May–4 June 1988, Varna, Bulgaria), 1005–1023.
24. Fatkullin, O.Kh. (1991) New structural powder materials and their application. In: *Results of science and technology*. Powder metallurgy, Vol. 5, 140–177. Moscow: VINITI.
25. Singh, I., Wolfe, D.E. (2005) Review: Nano- and macrostructured component fabrication by EB-PVD. *J. Materials Sci.*, **40**, 1–26.
26. Demchishin, A.V. (1981) *Structure and properties of thick vacuum condensates of metallic and nonmetallic materials and scientific bases of their fabrication*: Syn. of Thesis for Dr. of Techn. Sci. Degree. Kiev: PWI.
27. Grechanyuk, N.I. (1988) *New structural materials manufactured by vacuum vapor phase condensation for products of new technology*: Syn. of Thesis for Dr. of Techn. Sci. Degree. Kiev: PWI.
28. Minakova, R.V., Kresanova, A.P., Grechanyuk, N.I. (1996) Composite materials for contacts and electrodes. Materials on molybdenum base. In: *Electric contacts and electrodes*, 95–105. Kiev: IPM.
29. Slade, P.E. (1986) Arc erosion of tungsten based contact materials: A review. *Int. J. Refractory and Hard Metals*, 5(**4**), 208–214.
30. (1979) *Binary and multicomponent systems on copper base*. Ed. by M.E. Drits et al. Moscow: Nauka.
31. Mackey, T., Ziolkowski, I. (1980) Subsolidas phase diagram of Cu_2O–CuO–MoO system. *J. Solid Stat. Chem*., **31**, 135–143.
32. Mackey, T., Ziolkowski, I. (1980) Phase relation in the cupric molibdates–cuprous molibdates system. *Ibid*., 145–151.
33. Grechanyuk, I.N. (2007) *Structure, properties and electron beam technology in manufacturing of Cu–Zr–Y–Mo composite materials for electric contacts*: Syn. of Thesis for Cand. of Techn. Sci. Degree. Kiev: IPM.
34. Chornovol, V.O. (2011) *Structure and corrosion resistance of Cu–Mo, Cu–W composite materials produced by electron beam evaporation-condensation method*: Syn. of Thesis for Cand. of Techn. Sci. Degree. Kiev: IPM.
35. Artyukh, A.Yu. (2011) *Development of materials for electric contacts based on copper and molybdenum alloyed with Al, Cr, Zn, produced by electron beam evaporation-condensation method*: Syn. of Thesis for Cand. of Techn. Sci. Degree. Kiev: IPM.
36. Grechanyuk, V.G. (2013) *Physical-chemical principles of formation of copper-based composite materials condensed from vapor phase*: Syn. of Thesis for Cand. of Techn. Sci. Degree. Kiev: IPM.
37. Grechanyuk, N.I., Osokin, V.A., Grechanyuk, I.N. et al. (2006) Composite materials on base of copper and molybdenum, condensed from vapor phase, for electric contacts. Structure, properties, technology. Pt 2: Fundamentals of electron beam technology for producing materials for electric contacts. *Advances in Electrometallurgy*, **2**, 8–17.
38. *TUU 20113410.001–98*: Dispersion-strengthened materials for electric contacts. Introd. 02.06.98.
39. *TU U24.4-33966101-001:2014*: Dispersion-strengthened materials for electric contacts. Introd. 17.11.14.
40. Grechanyuk, M.I., Osokin, V.O., Afanasiev, I.B. et al. (2002) *Composite material for electric contacts and method for its manufacturing*. Pat. 34875 Ukraine. Publ. 16.12.2002.
41. Grechanyuk, M.I. (2005) *Method of manufacturing microlayer thermally stable materials*. Pat. 74155 Ukraine. Publ. 15.11.2005.
42. Grechanyuk, N.I. (2006) *Method of manufacturing of microlayer thermally stable materials*. Pat. 2271404 RF. Publ. 03.10.2006.
43. *www*.weldinglivetissues.com
44. Grechanyuk, M.I., Grechanyuk, V.G., Bukhanovsky, V.V. (2014) *Composite material for electric contacts and method for its manufacturing*. Pat. 104673 Ukraine. Publ. 25.02.2014.
45. Miedzinski, B., Okraszewski, Z., Grechanyuk, N. et al. (2008) Performance of sliding contacts with Cu–Mo layers for transportation in mining industry. In: *Electric contacts and electrodes*, 150–155. Kiew: IPM.
46. Grechanyuk, N., Minakova, R., Bukhanovsky, V. et al. (2014) Manufacturing technique and properties of condensed copper–carbon composite materials for sliding electrical contacts. *Open Access Library J*., Vol. 1, 1–9.
47. Grechanyuk, M.I., Grechanyuk, I.M., Grechanyuk, V.G. (2009) *Composite material for electric contacts and electrodes and method for its manufacturing*. Pat. 86434 Ukraine. Publ. 27.04.2009.
48. Bukhanovsky, V.V., Rudnitsky, M.P., Kharchenko, V.V. et al. (2011) Relation between composition, structure and mechanical properties of condensed composite material of copper–tungsten system. *Problemy Prochnosti*, **4**, 87–102.
49. Bukhanovskyi, V.V., Grechanyuk, N.I., Minakova, R.V., et al. (2001) Production technology, structure and properties of Cu–W layered composite condensed materials for electrical contacts. *Refractory Metals and Hard Mater.*, **29** (Issue 5), 573–581.
50. Denisenko, V.O., Minakova, R.V., Grechanyuk, V.G. et al. (2008) Structure and physical-chemical properties of composite copper and tungsten base materials manufactured by electron beam evaporation. *Nauk. Visnyk ChernivetsDU*, Chemistry, Issue 422, 26–33.
51. Miedzinski, B., Okrasczewski, Z., Grechanyuk, M. et al. (2010) Performance of LV vacuum contactors with condensed composite multicomponent contacts. In: *Electric contacts and electrodes*, 139–144. Kiew: IPM.
52. Bukhanovsky, V.V., Grechanyuk, N.I., Rudnitsky, N.P. et al. (2009) Influence of technological factors on structure, mechanical properties and nature of fracture of composite material of copper-chrome system. *Metallovedenie i Term. Obrab. Metallov*, **8**, 26–31.
53. Grechanyuk, M.I., Plashchenko, M.M., Osokin, V.O. et al. (2000) *Contact material for extinguishing chambers and method of its manufacturing*. Pat. 32368A Ukraine. Publ. 15.12.2000.
54. Grechanyuk, M.I., Plashchenko, M.M., Zvarych, A.V. et al. (2006) *Contact system of vacuum extinguishing chamber*. Pat. 76737 Ukraine. Publ. 15.09.2006.
55. Grechanyuk, V.G. (2013) Corrosion-resistant composite materials on copper base and electron beam equipment for their manufacturing. *Nauk. Visnyk ChernivetsDU*, Issue 640, 43–51.
56. *DSTU GOST 15.005:2009*: Producing of items of single-part and small-bath productions assembled in operation site. Introd. 02.01.09.
57. *TU U 31.20113410-003–2002*: Electric contacts based on dispersion-strengthened materials (MDK). Introd. 30.10.02.

Received 21.07.2015

doi.org/10.15407/tpwj2016.02.07

ANALYSIS OF APPLICABILITY OF SLAG CRUST IN PRODUCTION OF AGGLOMERATED FLUXES

I.A. GONCHAROV[1], **L.I. FAJNBERG**[1], **A.A. RYBAKOV**[1] and **A.V. NETYAGA**[2]
[1]E.O. Paton Electric Welding Institute, NASU
11 Kazimir Malevich Str., 03680, Kiev, Ukraine. E-mail: office@paton.kiev.ua
[2]NTUU «Kiev Polytechnic Institute»
37 Pobeda Ave., 03056, Kiev, Ukraine

The use of wastes of fused and agglomerated fluxes is an urgent task. But as-applied to agglomerated fluxes the data on the effective use of slag crust are absent in the literature. In this work the analysis of possibility of using a slag crust of agglomerated fluxes for production of fluxes, providing the quality formation and high mechanical properties of weld metal at high-speed multi-arc welding of cold-resistant low-alloy steels was carried out. The comparative investigation of welding and technological properties of original flux OK 10.74 and experimental fluxes based on the crushed slag crust in single- and four-arc welding was carried out. Using the method of spectral analysis the chemical composition of weld metal was studied. The method of optical metallography was used to investigate the distribution of nonmetallic inclusions in them and characteristics of microstructure. The impact toughness of weld metal was determined by tests on impact bending. It was established that the flux, produced by the method of agglomeration with addition of 5 wt.% of metallic manganese into the composition of charge, was close to original flux OK 10.74 according to all the investigated indicators, and as to the level of impact toughness met the requirements for welded joints of cold-resistant gas-pipeline steel up to strength category X80 inclusive. The results represent interest to the consumers of flux from the point of view of improving the efficiency of its use in multi-arc welding of large-diameter pipes. 10 Ref., 4 Tables, 3 Figures.

Keywords: *submerged arc welding, agglomeration, regeneration, nonmetallic inclusions, microstructure, impact toughness of weld metal*

In submerged arc welding the wastes are formed, including the non-fused part of flux and slag crust (SC), which is characterized by a low content of hydrogen dissolved in the form of OH^- [1], sulfur and phosphorus. These wastes related to the III class of hazard, and should be stored in the closed containers. The volumes of SC at a number of enterprises, for example, pipe plants, are estimated in thousands tons, therefore, the works on their recovery are very relevant.

The issue of using wastes of fused fluxes (of the molten flux and SC) has been long time standing before the researchers [2]. The known technology of regeneration of a part of non-fused flux [3], which is at advanced pipe mills is realized directly in the process of welding. SC is used in melting of fluxes [4], or by adding it in a powdered form to the original flux. The investigations showed that during welding a significant change in the structure and composition of slag excluding the possibility of its application directly in the form of flux does not occur [5]. Therefore, its application as the charge component for melting flux is irrational in cases when there is no need in obtaining fluxes with bulk mass of <1.1 kg/dm^3, being commonly used in multi-arc welding at high speed. The technology of production of regenerated welding fluxes was offered, consisting in SC crushing followed by magnetic separation and sieving into fractions [6]. Such fluxes provide the increased resistance of welds to the pore formation [7].

All the investigations described above concerned the fused welding fluxes. To agglomerated fluxes considering their high cost the increased requirements are specified for strength of the granules in order to increase the fraction of the wastes of non-fused flux in welding after separation.

There are not many works in the literature devoted to application of SC of agglomerated flux. In work [8] it was established that the agglomerated flux produced of SC reduces the weld alloying and, respectively, the strength properties, while its impact toughness depends on the specific conditions. Therefore, its application requires carrying out the control of quality of welded joints and technology of production of regenerated flux [9].

Our investigations [10] showed the possibility of using SC formed during multi-arc welding under the mixture of agglomerated aluminate-basic flux OR-132 and fused manganese-silicate flux AN-60 taken in ratio 1:4 in production of regenerated flux. Such flux had good forming properties in single-arc welding of low-carbon and low-alloy steels at speed up to 40 m/h. The mechanical properties of weld metal in welding using wire Sv-08G1NMA of 4 mm diameter were as follows: σ_y = 530.7 MPa; σ_t = 649.4 MPa; δ = 25.3 %;

Table 1. Chemical composition (wt.%) of weld metal in welding of steel 10G2FB under different fluxes using welding wire Sv-08G1NMA

Flux	Number of arcs	Number of weld	C	Si	Mn	Ni	Mo	Al	Nb	V	Ti	S	P
OK 10.74	1	401	0.084	0.50	1.71	0.25	0.28	0.028	N/D	0.060	0.010	N/D	N/D
OK 10.74	4	386	0.085	0.43	1.64	0.20	0.20	0.025	0.021	0.059	0.012	0.009	0.019
A	1	400	0.090	0.34	1.57	0.20	0.23	0.026	N/D	0.064	0.006	N/D	N/D
B	4	405	0.088	0.30	1.68	0.19	0.22	0.024	0.024	0.059	0.007	N/D	N/D
BM: 10G2FB steel			0.103	0.25	1.57	0.20	<0.01	0.030	0.030	0.081	0.013	0.005	0.013

Table 2. Physical properties of fluxes used

Flux	Flux granular size, mm	Bulk mass, kg/dm^3	Note
A	0.315–4.0	1.72	Predominance fraction 0.315–1.6 mm
B	0.2–4.0	1.26	Predominance fraction 0.2–1.6 mm
OK 10.74	0.2–1.6	1.02	–

ψ = 63.7 %; KCV_{-20} = 35.3–40.3/37.7, KCV_0 = 41.2–47.1/44.9 and KCV_{20} = 54.9–82.4/71.8 J/cm^2.

However, this flux was not suitable for high-speed multi-arc welding because of high bulk weight, which is the cause of weld defects formation. In addition, the level of impact toughness of weld metal does not satisfy the requirements for welded joints of cold-resistant steels.

The aim of this work is the analysis of possibility of using SC of agglomerated fluxes for production of fluxes, providing the quality formation of high mechanical properties of weld metal at high-speed multi-arc welding of cold-resistant low-alloyed steels.

Nowadays the pipe plants use agglomerated imported fluxes predominantly of aluminate-basic type according to the classification EN 760 of grades OR 132 (Oerlikon), OK 10.74 (ESAB), 995N, 998 (Lincoln) and others. Considering the high cost of these fluxes, the practical interest was represented by evaluation of possibility of producing the fluxes of SC formed during welding. As the object of investigations the SC of flux OK 10.74 was taken, formed in multi-arc welding of pipe steels using wire Sv-08G1NM A.

Below the procedure of work on production of regenerated flux is described. From the crushed SC of flux OK 10.74 two factions of 0.315–4 and ≤0.315 mm were selected.

Then, the thorough magnetic separation was carried out, as a result of which the drops of electrode metal and scale were removed from SC fractions of 0.315–4 mm. As a result the product was made corresponding to granulometric composition of fused flux of AN-60 grade. The similar technology was used in works [6, 7] in production of regenerated flux. Therefore, the material mentioned above we designated conditionally as a regenerated flux according to variant «A». Its bulk mass amounted to 1.72 kg/dm^3, which significantly exceeds recommended values of 0.9–1.2 kg/dm^3 in multi-arc welding. The grain of flux had size of 0.315–4 mm with a predominance of fraction of 0.315–1.6 mm size. It should be noted that this fraction is the most typical for a number of agglomerated and fused fluxes. Before welding the fluxes were calcinated at 400 °C for 2 h.

From the data on chemical composition of weld metal, produced under flux OK 10.74 (welds 386 and 401) and under regenerated flux according to and variant A (weld 400), it is seen that when using the regenerated flux the alloying of weld metal as to the number of elements is significantly reduced (Table 1),

Table 3. Modes of welding modes using wire Sv-08G1NMA of 4 mm diameter

Flux	Number of arcs	Number of weld	I/U, A/V	v_w, m/h	q/v_w, kJ/mm	B, mm
A	1	400	720–750/39–40	23.5	4.4	21
B	1	403	850–880/36–37	24.0	4.7	25
	1	402	820–850/38–39	24.0	4.8	27–28
B	1	405	1150/35–36	99.2	4.5	25
	2		800–850/35			
	3		650–700/38			
	4		700/38–40			
OK 10.74	1	401	820–830/37	23.5	4.7	30
OK 10.74	1	386	1150/33	98.0	4.5	25
	2		900/35			
	3		700/40			
	4		600/43			

Notes. Inter-electrode distance in four-arc welding amounted to 15–21 mm; q/v_w — energy input of welding process; B — weld width.

Figure 1. Appearance of welds produced using single- (*a*) and four-arc (*b*) process under flux B of the flux OK 10.74 SC (×1.5)

the most significant is the decrease in manganese content.

Considering the data obtained after magnetic separation and calcination, 5 % of metallic manganese of grade Mn-98 (fraction of 0.2–0.4 mm) was added to the milled SC of <0.315 mm fraction obtaining a uniform dry mixture in the intensive mixer. Then, based on Na–K liquid glass binder according to the known technology the batch of agglomerated flux was produced. Bulk mass of the produced flux, hereinafter designated as B, amounted to 1.26 kg/dm^3 (Table 2).

The fluxes were evaluated according to formation of deposits, as well as to the chemical composition and impact toughness of control welds produced on one-sided butt joints of steel 10G2FBYu of 19 mm thickness with V-shaped edge preparation of 5 mm×90°. The modes of single- and twin-arc welding using wire Sv-08G1NMA of 4 mm diameter are given in Table 3.

The process of welding under flux A was unstable with splashes and formation of high narrow ridge of SC. Produced weld 400 had a high reinforcement with non-smooth transition to the base metal and small undercuts. Such a weld formation is connected apparently with increased bulk mass of the flux (1.72 kg/dm^3).

In welding under flux B the process stability and quality of the formation of welds, produced using single- and four-arc welding, were satisfactory. The photos of welds are shown in Figure 1.

Weld 400 produced using single-arc process under regenerated flux A showed a rather high impact

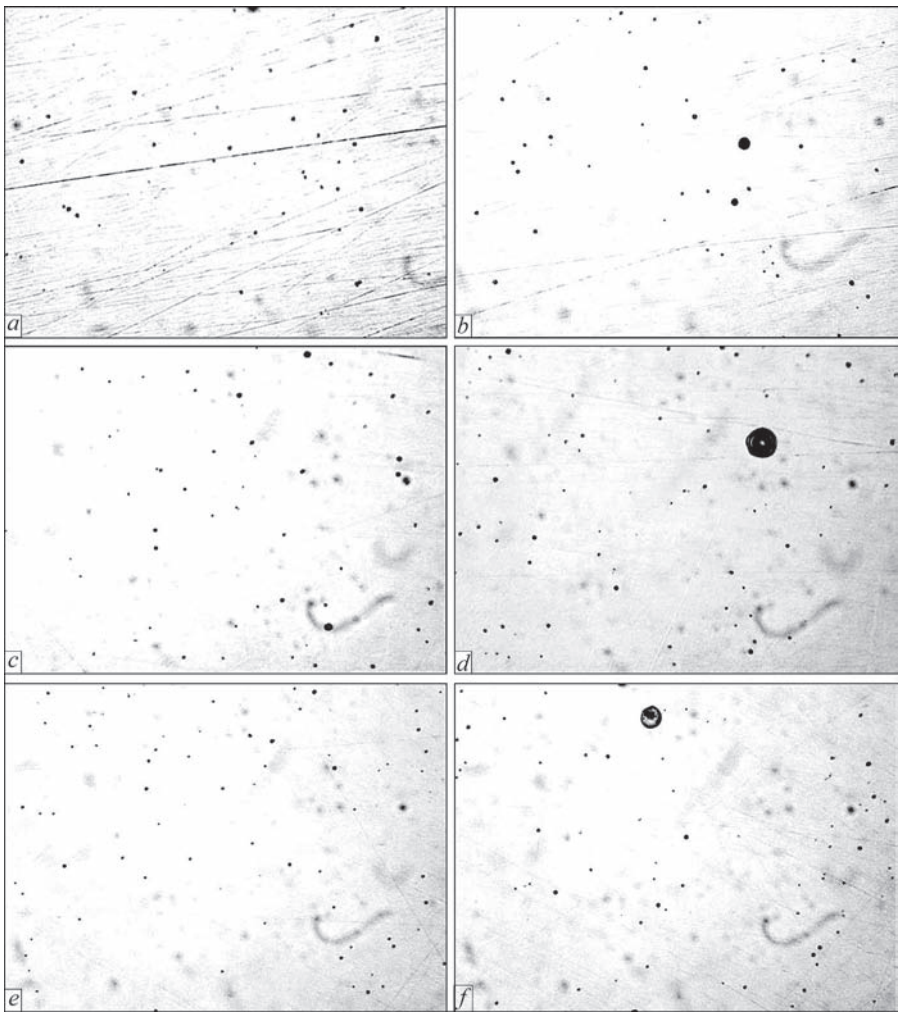

Figure 2. Microstructure (×800) of NMI in metal of investigated welds 386 (*a*, *b*), 400 (*c*, *d*) and 405 (*e*, *f*)

Table 4. Impact toughness of weld metal in welding of steel 10G2FB

Flux	Number of arcs	Number of weld	*KCV*, J/cm², at		
			–20 °C	–40 °C	–60 °C
OK 10.74	4	386	106.2–203.7 162.9	77.1–101.2 92.9	43.5–77.3 60.6
A	1	400	95.2–109.1 100.7	53.7–69.5 62.6	33.4–55.5 44.0
B	4	405	85.1–162.0 115.7	60.8–96.8 81.8	30.3–71.1 54.6

strength (KCV_{-40} = 62.6 J/cm²), but, as was mentioned, the weld had drawbacks as to its appearance.

Weld 405, produced using four-arc welding under agglomerated flux B, had satisfactory properties. According to chemical composition except of silicon it is close to weld 386, produced using four-arc welding with original flux OK 10.74 (see Table 1), and impact toughness (Table 4) is only slightly inferior to it. Average value for weld according to variant B (KCV_{-40} = 81.8 J/cm²) is quite acceptable. The possible reserve to provide higher impact toughness of welds at –40 °C, and lower is Ti–B alloying.

The morphology and features of distribution of nonmetallic inclusions (NMI) in the welds were investigated for not etched sections with the polished surface at magnification of 800. It was established that the NMI basic mass is located relatively uniform and represents small globular oxides of complex composition consisting of Mn, Al, Si, Ti, Ca, Fe in different ratios.

In weld 386, made under flux OK 10.74, size of the greater part of NMI is 1.0–1.2 μm (Figure 2, *a*). In some fields of view 1–2 larger inclusions of about 1.5 μm size are observed (Figure 2, *b*). In welding under the regenerated flux according to variant A (weld 400) the total number of NMI is slightly increased. Their size amounts mostly to 1.0–1.6 μm (Figure 2, *c*). At the same time, the number and size of large (more than 1.5 μm) inclusions with higher content of silicon (Figure 2, *d*) also increases.

In weld 405 produced under the agglomerated flux according to variant B, the number, distribution and sizes of NMI are close to weld 386 produced under original flux OK 10.74, while silicate inclusions observed in weld 400 are absent (Figure 2, *e*, *f*).

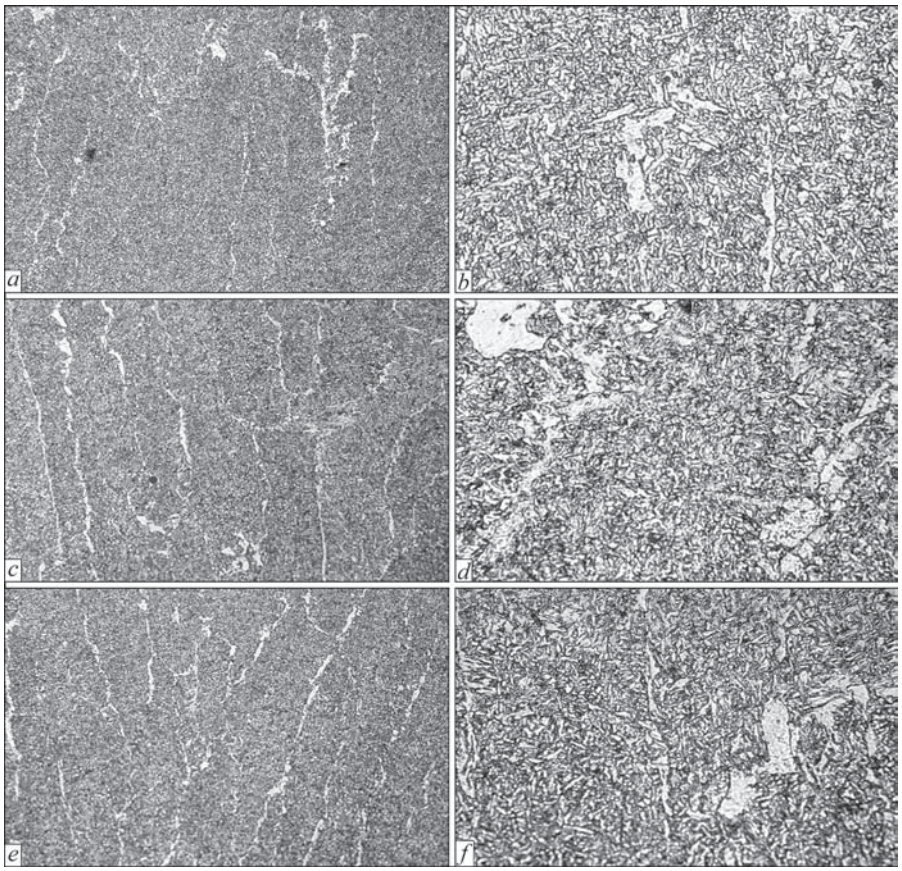

Figure 3. Microstructure of metal of investigated weld 386 (*a*, *b*), 400 (*c*, *d*) and 405 (*e*, *f*) (*a*, *c*, *e* — ×100; *b*, *d*, *f* — ×500)

The features of composition and morphology of structural components of welds were investigated on the sections after their etching in 4 % alcoholic solution of nitric acid at magnification of 100 and 500. The microstructure of welds consists of a mixture of different forms of ferrite in their different proportions. Thus, in weld 386 (flux OK 10.74) the main structural component is acicular ferrite. The share of grain boundary polygonal ferrite, evolved in the form of layers of width from 6 to 16 μm, or chains of separate grains does, not exceed 6 % (Figure 3, *a*, *b*). The single sections of intragranular polygonal ferrite are also observed, including the relatively large formations of massive ferrite with disordered MAC-phase (Figure 3, *b*), which is evolved also along the boundaries of the larger formations of grain boundary and intragranular polygonal ferrite.

In weld 400, produced under the regenerated flux according to variant A, the fraction of grain boundary polygonal ferrite is increased to 12 % (Figure 3, *c*). The sizes of formations of intragranular massive polygonal ferrite are also increased, and the width of layers of intergranular polygonal ferrite increases to 18–20 μm (Figure 3, *d*), due to which the number of MAC-phase clusters on their boundaries increases.

The microstructure of weld 405, produced under the agglomerated flux according to variant B, is close to the microstructure of weld 386 (flux OK 10.74). The fraction of grain boundary polygonal ferrite is slightly higher and amounts to 7–9 %, and the width of its layers does not exceed 18 μm (Figure 3, *e*, *f*). The dimensions of formations of massive intragranular ferrite with precipitation of MAC-phase slightly exceed the dimensions of this structural component in weld 386 (Figure 3, *f*).

The microhardness of investigated welds 386, 400 and 405 was approximately at the same level and amounted to *HV*5-227–230, *HV*5-219–221 and *HV*5-221–227, respectively.

Thus, the metallographic examination showed that the use of regenerated flux according to variant A produced of SC, as compared to the original flux, leads to deterioration of weld structure. At the same time, the weld structure, produced under agglomerated flux of the flux OK 10.74 SC with additional charging with 5 % of metallic manganese (variant B), is close to the structure of weld produced under the original flux according to all the investigated parameters.

Conclusions

The investigation of the possibility of using SC, formed in multi-arc welding under the agglomerated aluminate-basic flux, for production of welding fluxes was carried out. On the basis of the flux OK 10.74 SC the experimental fluxes were prepared according to the technology of regeneration (SC crushing followed by sieving and magnetic separation) and technology of agglomeration with additional charging with 5 % of metallic manganese.

A comparative investigation of welding and technological properties of original flux OK 10.74 and experimental fluxes in single- and four-arc welding was made. The chemical composition of weld metal, distribution of NMI in them, especially microstructure and indicators of impact toughness of weld metal were determined.

It was established that the flux, produced according to the method of agglomeration with addition of 5 wt.% of metallic manganese into the charge according to all of these indicators including the impact strength of weld metal, is close to original flux OK 10.74 and meets the requirements for welded joints of cold-resistant gas-pipeline steel up to strength category of X80 inclusively.

Application of flux produced from SC according to regeneration technology is accompanied by a certain reduction in the level of impact toughness of weld metal and some deterioration of the weld appearance original as compared to welding under flux OK 10.74. Therefore, a decision on the possibility of using regenerated flux in welding should be taken in each case taking into account the requirements for the quality of welded joints.

1. Goncharov, I.A., Paltsevich, A.P., Tokarev, V.S. et al. (2001) About the form of hydrogen existence in welding fused fluxes. *The Paton Welding J.*, **4**, 27–30.
2. Podgaetsky, V.V. (1961) How to use slag crust. *Avtomatich. Svarka*, **6**, 93–94.
3. Kolisnyk, V.N., Galinich, V.I., Kuzmenko, V.G. et al. (1969) Slag waste recovery in pipe welding production. *Ibid*., **8**, 66–67.
4. Galinich, V.I., Kolisnyk, V.N., Kotenzhi, V.Yu. et al. (1964) Application of slag crust for melting of flux AN-60. *Ibid*., **11**, 86–91.
5. Kuzmenko, V.G., Goncharov, I.A. (1997) Peculiarities of slag crust formation in arc welding. *Ibid*., **12**, 7–13.
6. Goncharov, I.A., Tokarev, V.S., Kuzmenko, V.G. (1998) Development of flux of general purpose based on slag crust of flux AN-60. In: *Advanced technique and technology of machine-building, instrument engineering and welding fabrication*, Vol. 4, 227–231. Kyiv: KPI.
7. Goncharov, I.A., Paltsevich, A.P., Tokarev, V.S. (2002) Low hydrogen welding flux providing higher resistance of welds to pore formation. *Svarshchik*, **1**, 12–13.
8. Murlin, D. (2010) The use of crushed slag as submerged arc welding flux. *Welding J*., **8**, 41–44.
9. Beck, H.P., Jackson, A.R. (1996) Recycling SAW slag proves reliable and repeatable. *Ibid*., **6**, 51–54.
10. Goncharov, I.A., Tokarev, V.S. (2005) Development of recovered welding flux on the base of slag crust of flux OR-132. In: *Proc. of Int. Sci.-Techn. Seminar on Modern Welding Fluxes and Experience of Their Application in Industry* (Zaporozhie, 29–31 Aug. 2005), 9, 10. Kiev: PWI.

Received 28.12.2015

REPORTING CONFERENCE ON PROGRAM «RESOURCE»

On January 22, 2016 at the E.O. Paton Electric Welding Institute the reporting conference on the results of fulfillment of the fourth stage of the target integrated Program of the NAS of Ukraine «Problems of Life and Safe Operation of Structures, Constructions and Machines» («Resource») in 2013–2015 was held. In the work of the Conference more than 100 scientists and experts from different institutions and organizations of Ukraine participated.

The Conference was opened by L.M. Lobanov, the Academician of the NASU. He reported that to fulfill this Program, which consisted of 9 sections and included 126 projects, 25 institutes of 8 Departments of the NASU were involved. The part of the works was devoted to implementation of results of the previous stages of the Program to the corresponding industrial branches of Ukraine and the further improvement of monitoring of technical state of critical objects.

The following review papers of the scientific supervisors of the sections on the main results of Program «Resource» were delivered:

- V.V. Kharchenko, the Corr. Member of the NASU, Chief of Section «Development of methodological fundamentals of evaluation and life extension of structural elements of objects of increased danger and aerospace engineering»;
- Z.T. Nazarchuk, the Academician of the NASU, Chief of Section «Development of methods and new technical means of nondestructive testing and diagnostics of state of materials and products of long-term service»;
- Prof. M.S. Khoma, the Deputy Chief of Section «Development of methods of protection of structural elements of the objects of long-term service against corrosion»;
- V.N. Voevodin, the Corr. Member of the NASU, Chief of Section «Development of effective methods for evaluation and service life extension of objects of nuclear power engineering»;
- A.A. Dolinsky, the Academician of the NASU, Chief of Section «Improvement of reliability and service life extension of power equipment and systems»;

Speech of Prof. V.V. Panasyuk

- A.Ya. Krasovsky, the Corr. Member of the NASU, Chief of Section «Creating of systems for monitoring of technical state of pipelines and objects of gas and oil industry»;
- L.M. Lobanov, Chief of Section «Improvement of reliability and service life extension of bridges, building, industrial and transport structures»;
- K.A. Yushchenko, the Academician of the NASU, Chief of Section «Development of technology of repair and restoration of structural elements of the objects of increased danger for their service life extension»;
- V.V. Panasyuk, the Academician of the NASU, Chief of Section «Preparation and issue of standard documents and scientific-and-technical manuals on the problems of life evaluation of objects of long-term service».

In the process of projects fulfillment of the Program the important scientific, technical and practical results were obtained. Let us represent some of them.

For the branch of railway transport within the frames of the integrated Project, fulfilled by the Institute of Ferrous Metallurgy, Physical-and-Technological Institute of Metals and Alloys and H.V. Karpenka Physico-Mechanical Institute, the new wear-resistant steel for railway wheels and the methods for determination of their service life at the presence of the damaged rolling surface defects of dent type were developed. The laboratory metallurgical complex was created, which allows manufacturing the experimental specimens being constant by chemical composition, nonmetallic inclusions and harmful impurities. The parameters of hot deformation meet the requirements of industrial production of wheels and are different from the base steel by the reduced carbon content and the use of technologies of dispersion nitride and solid solution strengthening by manganese and silicon. A significant increase in the service life and reliability of the wheels is predicted.

The specialists of Physical-and-Technological Institute of Metals and Alloys proved that the increase in life of high-current sliding contact is based on the application of inserts based on copper with alloying additions of iron, chromium and carbon, which provide the increased tribological properties at lower wear of the contact wire. The technological equipment was created, experimental specimens and inserts were manufactured, investigations of their properties according to the needs of Company «Ukrzaliznytsya» were carried out. In cooperation with the enterprise, which manufactures the contact plates of pantographs, the technological recommendations for industrial mastering of production of the proposed contact parts were developed used in the railway transport.

I.M. Frantsevich Institute of Problems of Materials Science developed the technologies for manufacture of elements of friction pairs of powder composite materials with the increased service life for braking devices of the rolling stock of railway transport. The complex of laboratory and bench tests of physical-mechanical and tribotechnical characteristics of the produced materials of metal–glass system and the pilot-industrial approbation of the developed technology in the plant conditions was carried out, the preparations for their serial production began.

The system for control of process of flash-butt welding of rails under stationary and field conditions was created, which increases the service life and reliability of railway tracks. It allows also detecting the deviation of parameters and preventing their exceeding of the normative tolerances, that stabilizes the welding process and improves the quality and longevity of welds. The system passed testing under the industrial conditions, and is implemented in the rail-welding enterprises of «Ukrzaliznytsya».

The complex of technical means for automated ultrasonic flaw detection of railroad tracks was created using the updated information technologies. The mathematical software of microprocessor units and means of interactive interaction of operator with control organs of the ultrasonic rail flaw detector was developed. The comprehensive investigation of the designed mechanical and electronic units of the detector on the specimens with different types of defects was carried out. The pilot model of the automated ultrasonic flaw detector was created for application in railway economy of Ukraine for detecting defects in the rails of track.

For the branch of pipeline transport the causes for fracture of circumferential welded joints of main gas-and-oil pipelines were investigated. It was established that they are caused by the presence of technological defects, mainly corrosion due to a low quality of assembly-welding and maintenance works. The level of mechanical properties of welded joint metal, considering the long operation of oil-and-gas pipelines, is sufficient and can not be considered as the causes for their fracture. The recommendations regarding elimination of the causes of defects and prevention of fracture of circumferential joints during service were provided.

The first domestic equipment for low-frequency ultrasonic testing of state of technological pipelines and other long objects without scanning their surfaces was created. Its essential advantage is a long-range action and efficiency of diagnostics of long objects in the places, where other methods are unsuitable, as, for example, underground where pipelines cross roads

and railway tracks, as well as pass across the rivers and other obstacles. The testing and adaptation of the equipment was carried out as applied to the industrial conditions. It was established that it provides an increased sensitivity to corrosion-erosion damages, and as to accuracy of determination of distance to the defects it corresponds to the best foreign analogues.

PWI developed the system of continuous acoustic-emission monitoring of technical state of high-temperature components of the power equipment. It allows determining the preliminary fracture load of material under the real operating conditions of structural elements on the basis of acoustic emission data at any time irrespective of operation period and variations in temperature. The system was put into industrial operation for monitoring of steam pipelines of hot steam overheat of power unit No. 1 of Kiev Central Heating Plant-6. The works are also conducted regarding its application for the continuous monitoring of the boiler drum at Kiev Central Heating Plant-5.

The complex of technical measures for high-frequency and optical-acoustic diagnostics of composite structural elements of aerospace engineering was created. The complex includes ultrahigh-frequency reflectometer of millimeter range of wave lengths, optical-acoustic interference correlator and software for detection of delaminations and other inner defects in the composites in real time. The investigation of defects detection in the composite specimens of multi-layered and cellular structure was carried out. The testing of the developed complex of technical means of ultrahigh-frequency and optical-acoustic diagnostics is planned in the industrial conditions at State Enterprise «Antonov» and Design Bureau «Yuzhnoe».

The technology of diagnostics using the method of electronic shearography of aircraft structural elements of metallic and composite materials was developed. Its effectiveness is confirmed by research works both on test specimens, as well as on full-scale elements of fuselage lining of the aircraft wing. It can be used in manufacture of structures, as well as during their operation and maintenance. Nowadays, the technology is introduced for diagnostics of aircraft equipment components at Company «Antonov».

The hybrid technology was developed, which combines EBW and FSW for restoration of life of aerospace engineering structures made of aluminum and magnesium alloys. The standard series of tools and methodology of preliminary treatment with friction and stirring of the surface layers were developed, which allow obtaining a fine-grained structure of alloys, and significantly improving the strength of joints after EBW. The hybrid technology is implemented at Company «Motor-Sich».

The total expected economic effect from implementation of the results of the projects of Program «Resource» amounts to tens of millions UAH per year. In general, many other useful results were obtained from the projects. These results are challenging and give grounds about the practicability of the further work of the Program at the next stage.

The materials of Program «Resource» can be found in the open access on the link: *http*://patonpublishinghouse.com/ compilations/ Resource2015.pdf.

Dr. A.T. Zelnichenko, PWI

PATON PUBLISHING HOUSE

www.patonpublishinghouse.com

SUBSCRIPTION

«The Paton Welding Journal» is Published Monthly Since 2000 in English, ISSN 0957-798X.

«Avtomaticheskaya Svarka» Journal (Automatic Welding) is Published Monthly Since 1948 in Russian, ISSN 005-111X.

«The Paton Welding Journal» is Cover-to-Cover Translation of Avtomaticheskaya Svarka» Journal into English.

If You are interested in making subscription directly via Editorial Board, fill, please, the coupon and send application by Fax or E-mail.

The cost of annual subscription via Editorial Board is $348 for «The Paton Welding Journal» and $180 for «Avtomaticheskaya Svarka» Journal.

«The Paton Welding Journal» can be also subscribed worldwide from catalogues subscription agency EBSO.

SUBSCRIPTION COUPON

Address for journal delivery _____

Term of subscription since _____ **20** **till** **20** _____

Name, initials _____

Affiliation _____

Position _____

Tel., Fax, E-mail _____

We offer the subscription all issues of the Journal in pdf format, starting from 2009.

The archives for 2009–2014 are free of charge on *www.patonpublishinghouse.com* site.

ADVERTISEMENT

in «Avtomaticheskaya Svarka» and «The Paton Welding Journal»

External cover, fully-colored:
First page of cover (190×190 mm) — $700
Second page of cover (200×290 mm) — $550
Third page of cover (200×290 mm) — $500
Fourth page of cover (200×290 mm) — $600

Internal cover, fully-colored:
First/second/third/fourth page of cover (200×290 mm) — $400

Internal insert:
Fully-colored (200×290 mm) — $340
Fully-colored (double page A3) (400×290 mm) — $500

- Article in the form of advertising is 50 % of the cost of advertising area
- When the sum of advertising contracts exceeds $1001, a flexible system of discounts is envisaged

Size of journal after cutting is 200×290 mm

Editorial Board of Journal «Avtomaticheskaya Svarka» and «The Paton Welding Journal»
E.O. Paton Electric Welding Institute of the NAS of Ukraine
International Association «Welding»
11 Kazimir Malevich Str. (former Bozhenko Str.), 03680, Kiev, Ukraine
Tel.: (38044) 200 60 16, 200 82 77; Fax: (38044) 200 82 77, 200 81 45
E-mail: journal@paton.kiev.ua; www.patonpublishinghouse.com